Behavior of the Elements at High Pressures

John Francis Cannon

High Pressure Data Center, 574 Lee Library, Brigham Young University, Provo, Utah 84602

Data on polymorphic phase changes and variation of melting temperature of the elements with pressure have been compiled and critically evaluated. Emphasis has been placed on work done at pressures exceeding 1 kbar. Pressure-temperature phase diagrams showing first-order solid-solid phase boundaries and/or melting curves derived from the best available data are given for 58 elements. Information on the crystal structures of high-pressure polymorphs is also reviewed. Those elements that exist in the gaseous state at room temperature and pressure are not included.

Key words: Critically evaluated data; crystal structures; elements; high pressure; melting curves; phase diagrams; polymorphism.

Contents

List of Tables and Figures

1. Introduction

For this review an attempt has been made to cover all the literature relating directly or indirectly to the pressure-temperature phase diagrams[1] of the elements. All the elements have been considered excepting those that exist in the gaseous state at room temperature and pressure. The elements Ac, At, Co, Cr, Fr, Ir, Nb, Os, Pa, Pd, Pm, Po, Ra, Re, Ru, Sc, Tc, and Y have no reported high-pressure phase transitions and no reported data on the variation of melting temperature with pressure. Information on each of the remaining elements is reviewed in the body of the paper.

The literature was covered in the following manner. Bridgman's work was examined through the index to *Collected Experimental Papers of P. W. Bridgman* [80][2]. The subject indexes compiled at the NSRDS High Pressure Data Center at Brigham Young University [111, 286] were searched under each element name and under common generic names (halogen, lanthanide, alkali metal, and so forth). Also the latest (as yet unindexed) issues of "Bibliography on High Pressure Research" [287] were scanned cover-to-cover. This gave a nucleus of papers which included most of the important works. As these papers were read additional references were obtained from their individual bibliographies. Finally, letters were written from time to time to persons who are or were active in research involving high-pressure phases of the elements. It is felt that this coverage is quite complete although some sources have undoubtedly been inadvertently missed.

---

[1] Emphasis was placed on work involving pressures above 1 kbar (1 bar= 10^5 N/m^2).

[2] Figures in brackets indicate literature references at the end of this paper.

During the writing of this paper it became apparent that a few descriptive phrases were used frequently. Consequently, these were assigned the following abbreviations:

RT	room temperature (about 25 °C)
RP	room pressure (about 1 bar)
RTP	room temperature and pressure
R(p)	variation of resistance with pressure
V(p)	variation of volume with pressure

The following abbreviations for common crystal structures have also been used:

bcc	body-centered cubic
bct	body-centered tetragonal
dhcp	double hexagonal close-packed
fcc	face-centered cubic
fct	face-centered tetragonal
hcp	hexagonal close-packed
sc	simple cubic

One of the most difficult problems encountered in preparing this review was the standardization of reported pressures and temperatures. There are several methods for determining the pressure applied to a sample in a high-pressure device. Usually the pressure calibration procedure depends on the type of high-pressure equipment used. Some types of equipment are well suited to direct determination of pressure by a force-per-unit area calculation, others (equipped for X-ray measurements at pressure) may use the NaCl semiempirical equation of state, and still others require the use of secondary standards. The particular problems involved with each of these methods are discussed in the following paragraphs.

For the determination of pressure by force-per-unit-area calculation the most serious problem involves the correction for "friction". The "friction" correction usually refers to all effects which cause pressure on the sample to be different from the calculated pressure. These effects include the actual friction of the piston against the cylinder wall plus pressure gradients that exist in solid cell components. Apparently the latter effect sometimes causes pressure intensification and other times pressure reduction on the sample being studied [228]. Unfortunately the method of correcting for these effects is not always mentioned in the literature reports, and when it is mentioned, often only the comment "corrections applied for friction" is made. Because of this it is frequently impossible to know whether the investigator fully appreciated and accounted for each of the possible sources of error.

Another potential source of error arises in the determination of the force applied to the piston and in the determination of the area of the piston face. These measurements are almost never discussed in the literature, so again it is impossible to determine the magnitude of potential error from this source.

The use of the NaCl semiempirical equation of state for determining pressure in high-pressure X-ray devices is fairly straight forward. Investigators using this method have usually been careful to cite the source of the particular equation used, and the minor differences are conveniently taken into consideration. The one difficulty involves determination of the lattice parameters used in pressure calculation. There is seldom any indication given of the accuracy of the lattice parameter determination from which the pressure is obtained. Thus it is difficult to evaluate the error from this source.

The use of secondary standards is very widespread and finds particular value in the calibration of Bridgman anvils, belt, girdle, supported tapes (Drickamer), and multianvil devices. The most common secondary standards involve the variation of resistance with pressure in manganin wire and the so-called pressure fixed-points—volume and/or resistance discontinuities encountered when a pressure induced phase change occurs. Less common standards include the compressibility of certain well-characterized substances (NaCl or Ag for example) and the variation of superconductivity with pressure of Pb.

Investigators who use manganin wire for pressure determination seldom state what values were accepted as correct in calibrating the wire or the method used in obtaining the calibration. Such specifications are particularly important when manganin is used to determine the higher pressures (above 50–60 kbar) and/or when it is used in a nonhydrostatic medium. Under these rather severe conditions the R(p) for manganin frequently deviates from linearity. If the method of calibration is not stated it is impossible to know whether such factors were understood and compensated.

The pressure fixed-points most often used involve the following transitions: Bi(I–II), Bi(III–V), Tl(I–III) and Ba(I–II) for pressures below 80 kbar and Sn(I–III), Fe(I–IV), Ba(III–IV) and Pb(I–II) for pressures above 80 kbar. The accepted pressures for these transitions at RT have varied considerably over the years. In order to correlate the pressures from different studies it is necessary to know what transitions were used for calibration purposes, what values were accepted as "correct" for the transition pressures, and what interpolation and extrapolation procedures were employed. Investigators almost without exception presented information regarding the former two requirements, but the latter was sometimes not specified. The values for these pressure fixed points considered correct for the purposes of this review are given in table 1.

Often secondary standards were used to calibrate equipment at RT, and then data were taken at other temperatures. Most investigators did not correct their pressures for the effect of temperature change. There

TABLE 1. Pressure fixed points

Transition	Pressure at RT (unless otherwise noted) (kbar)	Source
Hg(L–I)	7.57 (0 °C)	128
Bi(I–II)	25.5	128
Tl(I–III)	36.7	128
Cs(II–IV)	41.7	128
Ba(I–II)	55.3	128
Bi(III–V)	76.7	128
Sn(I–III)	[a] 94	211
Fe(I–IV)	110–115	131
Ba(III–IV)	118–122	131
Pb(I–II)	128–132	131

[a] Corrected to Decker's revised values [127].

is no universally accepted method for making such a correction, so the effect is usually assumed to be small and generally ignored. Decker, et al. [128] have discussed this problem at length, and it appears that the error (on the order of 1 kbar per 100 °C rise in temperature) may not be negligible. The problem may be complicated at temperatures above 500–600 °C because of phase changes and/or chemical reactions in pyrophyllite, a common pressure cell component.

Temperatures are most frequently determined by thermocouple measurements. It is therefore important to know what, if any, effect pressure has on thermocouple emf. Several studies of this effect have been published. A critical review on this subject is beyond the scope of this paper, so the interested reader is referred to the papers presented at the Symposium on the Accurate Characterization of the High Pressure Environment [34, 148, 156, 175, 416] and to four papers that have appeared since the Symposium [155, 243, 246, 367]. One of the Symposium papers [175] is a review which covers all of the important earlier works.

There is still considerable controversy on this subject. Corrections advocated by Hanneman and Strong [172–174] are nearly twice those suggested by Getting and Kennedy [155] at the higher temperatures. It has been suggested [175] that the best corrections probably lie somewhere between the two. This attitude is reflected in a small section of the recent paper by Strong, et al. [367] in which they report some revised thermocouple correction data. Thermocouple corrections usually cannot be applied to literature data (except qualitatively) because pressure cell seal temperatures are not known.

The policy outlined below was used in an effort to obtain standardization of reported pressures and temperatures. Pressures calculated from force-per-unit-area and determined from R(p) of manganin were accepted as published unless data were presented for one or more of the fixed-point transitions. In the latter case, pressures were corrected as for data based on secondary standards. In cases where details of correction and/or calibration procedures were omitted, it was arbitrarily (and not necessarily correctly) assumed that errors are probably greater than those stated by the investigator. All NaCl semiempirical-equation-of-state pressures were standardized to Decker's [127] revised values. Fixed point pressures were standardized to the values shown in table 1. Where interpolation and extrapolation procedures were not given, corrections were based on the assumption that error varied on a percentage basis according to a smooth curve through percent error versus pressure values determined from the fixed points used. Figure 1 shows the curve used to correct pressures for Bridgman's resistance experiments [75]. Other methods of pressure calibration could generally be related back to one or more fixed points and were thus corrected on that basis. *In the body of the review, pressures that have been corrected as outlined above are given in italics.* The above correction procedure has been applied to all data presented graphically.

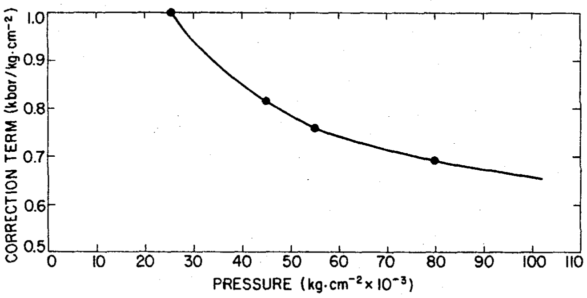

FIGURE 1. Pressure correction for Bridgman's resistance scale.

Temperature data have generally been accepted as given. No attempts have been made by the reviewer to correct data for the effect of pressure on thermocouple emf. In cases where some data are corrected and some are not, preference is given to those which have been corrected if the raw (before temperature correction) data appear to be in close agreement. In cases where no thermocouple corrections are made, the temperature error estimated by the investigator is revised upward according to the effect (roughly estimated assuming a 20 °C seal temperature) pressure has on the type of thermocouple used. The data of Getting and Kennedy [155] have arbitrarily been chosen for making these rough estimates. Had the data of Hanneman and Strong been chosen the error flags would be slightly larger.

In a few cases investigators have used shock pressure methods to determine phase boundaries or search for polymorphic transitions. Shock pressures exist for such a brief time that it is difficult to know whether equilibrium could be established during such experiments. Because of this problem, data taken by shock methods have generally not been used in this review. If a polymorphic change has been reported on the basis of shock data, the change is noted, but the pressure at which the change occurred is not considered to be on the equilibrium phase boundary.

As emphasized above, there are several possible uncertainties involved in evaluating data from high pressure literature. The potential errors are not always subject to quantization, so limits of accuracy are usually termed "estimated uncertainty". This very name implies a certain amount of subjectivity which cannot be avoided. The following criteria were used as a base for estimating the probable uncertainty for a given best phase boundary: (1) The estimated error of each individual investigator; (2) the additional error assigned to individual reports as a result of uncertainties such as lack of thermocouple correction for pressure and/or lack of details concerning pressure calibration; (3) additional possible errors introduced by taking data from graphs rather than tables and correcting pressures to the currently accepted scale; and (4) scatter among data from different reports.

In the course of this review agreement between data sets from different sources is often referred to as "good", "fair" or "poor". These usually vague terms have been applied roughly as outlined in table 2.

Each of the phase diagrams published with this review has been prepared from the best available data. To give the reader a "feel" for the agreement among different investigators, representative points from individual reports are included in each diagram. The points shown do not necessarily represent actual data collected by the primary investigator, but rather reflect the average (or best) values represented in the published diagrams. The size of the figures used to designate the points does *not* represent limits of error. The estimated uncertainty for selected points on each best phase boundary is illustrated by error bars imposed on individual diagrams.

TABLE 2. Definition of agreement terms

Agreement	Condition
Good..................	Within the estimated error of the weighted average [a]
Fair.....................	Within twice the estimated error of the weighted average [a]
Poor....................	Outside twice the estimated error of the weighted average [a]

[a] Weighted average = average of the data when weighted proportionately to the inverse of the estimated error.

The phase designations have been made as follows. The phase stable at RTP is designated phase I. Phases appearing at RP upon increasing temperature are numbered consecutively beginning with II; those appearing at RP upon decreasing temperature follow; and finally those appearing with increasing pressure are specified. In a few cases alternative phase designations (such as those employing Greek symbols) are already well established in the literature. In these cases the alternative designations are specified in parentheses on the phase diagrams.

In many cases the crystal structures of high-pressure phases have been reported. Every effort has been made to determine the best values of the lattice parameters of these phases. Crystallographic data for high-pressure polymorphs are shown in table 3. For convenience, crystallographic data of RP phases of those elements discussed in this review are also given. These latter data have been taken from Pearson [310] or from Wyckoff [425].

TABLE 3. Crystallographic data

Element	Pressure (kbar)	Temperature (°C)	Crystal system	Structure type	*a* Å	*b* Å	*c* Å	Angle (degrees)	*Z*	Space group	Ref.
Li	R	25	cubic	bcc	3.5100				2	*Im*3*m*	310
Na	R	20	cubic	bcc	4.2906				2	*Im*3*m*	310
K	R	−195	cubic	bcc	5.247				2	*Im*3*m*	310
Rb	R	20	cubic	bcc	5.70				2	*Im*3*m*	310
Cs(I)	R	R	cubic	bcc	6.141				2	*Im*3*m*	413
Cs(II)	≈ 25	R	cubic	fcc	6.465				4	*Fm*3*m*	413
	40	27	cubic	fcc	5.984				4	*Fm*3*m*	170
Cs(III)	*41.7*	27	cubic	fcc	5.800				4	*Fm*3*m*	170
Be(I)	R	R	hexagonal	hcp	2.286		3.584		2	$P6_3/mmc$	310
Be(II)	R	1255	cubic	bcc	2.551				2	*Im*3*m*	310
Mg	R	25	hexagonal	hcp	3.2094		5.2105		2	$P6_3/mmc$	310
Ca(I)	R	26	cubic	fcc	5.5884				4	*Fm*3*m*	310
Ca(II)	R	467	cubic	bcc	4.480				2	*Im*3*m*	310
Sr(I)	R	25	cubic	fcc	6.0849				4	*Fm*3*m*	310
Sr(II)	R	614	cubic	bcc	4.85				2	*Im*3*m*	310
	42	R	cubic	bcc	4.43				2	*Im*3*m*	278

TABLE 3. Crystallographic data—Continued

Element	Pressure (kbar)	Temperature (°C)	Crystal system	Structure type	*a* Å	*b* Å	*c* Å	Angle (degrees)	*Z*	Space group	Ref.
Ba(I)	R	25	cubic	bcc	5.013				2	$Im3m$	310
Ba(II)	*58*	R	hexagonal	hcp	3.901		6.154		2	$P6_3/mmc$	23, 25
Ba(IV)	> 120	R	cubic (?)	fcc (?)							130
Al	R	25	cubic	fcc	4.0496				4	$Fm3m$	310
Ga(I)	R	24	orthorhombic		4.5197	4.5260	7.6633		8	$Cmca$	310
Ga(II)	> 20	R	tetragonal	bct	2.808		4.458		2	$I4/mmm$	413
In	R	R	tetragonal	bct^a	3.2512		4.9467		2	$I4/mmm$	310
Tl(I)	R	18	hexagonal	hcp	3.4566		5.5248		2	$P6_3/mmc$	310
Tl(II)	R	*262*	cubic	bcc	3.882				2	$Im3m$	*310*
Tl(III)	≈ 60	R	cubic	fcc	4.778				4	$Fm3m$	312
C(I)	R	R	hexagonal	graphite	2.456		6.696		4	$P6_3mc$	425
C(II)	R	20	cubic	diamond	3.56679				8	$Fd3m$	425
Si(I)	R	25	cubic	diamond	5.4307				8	$Fd3m$	310
Si (II or III)	> *134*	R	tetragonal	white-Sn	4.686		2.585		4	$I4_1/amd$	194
Si (III or II)	R	R	cubic		6.636				16	$Ia3$	218
Ge(I)	R	25	cubic	diamond	5.6575				8	$Fd3m$	310
Ge(II)	R	R	tetragonal		5.93		6.98		12	$P4_32_12$	218
Ge(III)	> *100*	R	tetragonal	white-Sn	4.884		2.692		4	$I4_1/amd$	194
Sn(I)	R	25	tetragonal	white-Sn	5.8315		3.1814		4	$I4_1/amd$	310
Sn(III)	39	314	tetragonal	bct	3.81		3.48		2	$I4/mmm$	24
Pb(I)	R	25	cubic	fcc	4.9502				4	$Fm3m$	310
Pb(II)	139	R	hexagonal	hcp	3.265		5.387		2	$P6_3/mmc$	377
P(Black I)	R	22	orthorhombic		3.3136	10.478	4.3763		8	$Cmca$	310
P(Black II)	*86*	R	rhombohedral	As	3.524			57.25	2	$R\bar{3}m$	195
			hexagonal		3.377		8.806		6		195
P(Black III)	*101*	R	cubic	sc	2.377				1		195
As(I)	R	23	rhombohedral	As	4.1318			54.13	2	$R\bar{3}m$	310
			hexagonal		3.7598		10.547		6		310
As(II)	R	R	tetragonal		8.691		6.363				133
Sb(I)	R	25	rhombohedral	As	4.5067			57.107	2	$R\bar{3}m$	310
			hexagonal		4.3084		^{b}11.274		6		310
Sb(II)	*64*	R	cubic	sc	2.986				1		395
Sb(III)?	*115*	R	monoclinic		5.56	4.04	4.22	86	4	$P2_1/m$	217
Sb(III)?	*115*	R	tetragonal		8.04		5.95				133
Bi(I)	R	25	rhombohedral	As	^{b}4.746			57.23	2	$R\bar{3}m$	310
			hexagonal		4.546		11.862		6		310
Bi(II)	26	R	monoclinic		6.674	6.117	3.304	110.33	4	$C2/m$	82
Bi(V)	90	R	cubic	bcc	3.800				2	$Im3m$	331
Se	R	25	hexagonal		4.3656		4.9590		3	$P3_121$	310
Te(I)	R	25	hexagonal		4.4566		5.9268		3	$P3_121$	310
Te(III)	≈ *115*	*R*	*rhombohedral*	*β-Po*	*3.002*			*103.3*	*1*	$R\bar{3}m$	198
			hexagonal		^{b}4.709		3.822		3		198
I	R	26	orthorhombic		7.27007	9.79344	4.79004		4	$Bmab$	425
Ti(I)	R	25	hexagonal	hcp	2.9511		4.6843		2	$P6_3/mmc$	310
Ti(II)	R	900	cubic	bcc	3.3065				2	$Im3m$	310
Ti(III)	R	R	hexagonal		4.625		2.813		3		196
Ti(IV)?	R	R	cubic	bcc	3.276				2	$Im3m$	310
Zr(I)	R	25	hexagonal	hcp	3.2312		5.1477		2	$P6_3/mmc$	154
Zr(II)	R	862	cubic	bcc	3.6090				2	$Im3m$	310
Zr(III)	R	R	hexagonal		5.036		3.109		3		196
Zr(IV)?	R	R	cubic	bcc	3.568				2	$Im3m$	154
Fe(I)	R	20	cubic	bcc	2.8664				2	$Im3m$	310
Fe(II)	R	916	cubic	fcc	3.6468				4	$Fm3m$	310
Fe(III)	R	1394	cubic	bcc	2.9322				2	$Im3m$	310
Fe(IV)	*151*	R	hexagonal	hcp	2.461		3.952		2	$P6_3/mmc$	192, 376
Rh	R	20	cubic	fcc	3.8044				4	$Fm3m$	310
Ni	R		cubic	fcc	3.5238				4	$Fm3m$	310
Pt	R	20	cubic	fcc	3.9239				4	$Fm3m$	310
Cu	R	20	cubic	fcc	3.6147				4	$Fm3m$	310
Ag	R	25	cubic	fcc	4.0862				4	$Fm3m$	310
Au	R	25	cubic	fcc	4.0785				4	$Fm3m$	310
Zn	R	25	hexagonal	hcp	2.6649		4.9468		2	$P6_3/mmc$	310
Cd	R	21	hexagonal	hcp	2.9788		5.6167		2	$P6_3/mmc$	310
Hg(I)	R	−46	rhombohedral	Hg	3.005			70.53	1	$R\bar{3}m$	310
			hexagonal		3.467		^{b}6.724		3		310

TABLE 3. Crystallographic data—Continued

Element	Pressure (kbar)	Temperature (°C)	Crystal system	Structure type	a Å	b Å	c Å	Angle (degrees)	Z	Space group	Ref.
Hg(II)	R	−196	tetragonal	bct	3.995		2.825		2	*I4/mmm*	13
La(I)	R	R	hexagonal	dhcp	3.770		12.159		4	$P6_3/mmc$	310
La(II)	R	R	cubic	fcc	5.296				4	*Fm3m*	310
	64	R	cubic	fcc	4.958				4	*Fm3m*	279
La(III)	R	887	cubic	bcc	4.26				2	*Im3m*	310
Ce(I)	R	23	cubic	fcc	5.1601				4	*Fm3m*	310
Ce(II)	R	25	hexagonal	dhcp	3.673		11.802		4	$P6_3/mmc$	310
Ce(III)	R	−196	cubic	fcc	4.85				4	*Fm3m*	310
	15	R	cubic	fcc	4.82				4	*Fm3m*	146
Ce(IV)	R	757	cubic	bcc (?)	4.12				2	*Im3m*	310
Ce(V)?	49.5	R	cubic	fcc	4.66				4	*Fm3m*	146
Ce(V)?	≈ 65	R	hexagonal		3.16		5.20				285
Pr(I)	R	R	hexagonal	dhcp	3.6725		11.8354		4	$P6_3/mmc$	310
Pr(II)	R	821	cubic	bcc	4.13				2	*Im3m*	310
Pr(III)	≈ 40	R	cubic	fcc	4.88				4	*Fm3m*	313
Nd(I)	R	R	hexagonal	dhcp	3.6579		11.7992		4	$P6_3/mmc$	310
Nd(II)	R	883	cubic	bcc	4.13				2	*Im3m*	310
Nd(III)	≈ 50	R	cubic	fcc	4.80				4	*Fm3m*	313
Sm(I)	R		rhombohedral	Sm	8.996			23.22	3	$R\bar{3}m$	310
			hexagonal		3.621		26.25		9		310
Sm(II)?	R	> 920	cubic	bcc							209
Sm(III)	R	R	hexagonal	dhcp	3.618		11.66		4	$P6_3/mmc$	205
Eu	R	25	cubic	bcc	4.5820				2	*Im3m*	310
Gd(I)	R	20	hexagonal	hcp	3.6360		5.7826		2	$P6_3/mmc$	310
Gd(II)	R		cubic	bcc	4.06				2	*Im3m*	310
Gd(III)	R	R	rhombohedral	Sm	8.92			23.3	3	$R\bar{3}m$	206
			hexagonal		3.61		26.03		9		206
Gd(III)	≈ 35	R	rhombohedral	Sm	8.76			23.0	3	$R\bar{3}m$	280
			hexagonal		3.49		25.6		9		280
Tb(I)	R	R	hexagonal	hcp	3.6010		5.6936		2	$P6_3/mmc$	310
Tb(II)	R		cubic	bcc					2	*Im3m*	310
Tb(III)	R	R	rhombohedral	Sm	8.83			23.42	3	$R\bar{3}m$	353
			hexagonal		3.58		25.76		9		353
Tb(III)	≈ 60	R	rhombohedral	Sm	8.40			23.4	3	$R\bar{3}m$	280
			hexagonal		3.41		24.5		9		280
Dy(I)	R	R	hexagonal	hcp	3.5903		5.6475		2	$P6_3/mmc$	310
Dy(II)	R		cubic	bcc					2	*Im3m*	310
Dy(III)	≈ 75	R	rhombohedral	Sm	8.39			23.0	3	$R\bar{3}m$	280
			hexagonal		3.34		24.5		9		280
Ho(I)	R	R	hexagonal	hcp	3.5773		5.6158		2	$P6_3/mmc$	310
Ho(II)	R		cubic	bcc					2	*Im3m*	310
Ho(III)	≈ 85	R	rhombohedral	Sm	8.26			23.3	3	$R\bar{3}m$	280
			hexagonal		3.34		24.1		9		280
Er(I)	R	R	hexagonal	hcp	3.5588		5.5874		2	$P6_3/mmc$	310
Er(II)	R		cubic	bcc					2	*Im3m*	310
Tm(I)	R	R	hexagonal	hcp	3.5375		5.5546		2	$P6_3/mmc$	310
Yb(I)	R	R	cubic	fcc	5.4862				4	*Fm3m*	310
Yb(II)	R	23	hexagonal	hcp	3.8799		6.3859		2	$P6_3/mmc$	223
Yb(III)	39.5	R	cubic	bcc	4.02				2	*Im3m*	168
Lu	R	R	hexagonal	hcp	3.5031		5.5509		2	$P6_3/mmc$	310
Th(I)	R	R	cubic	fcc	5.0845				4	*Fm3m*	310
Th(II)	R	1450	cubic	bcc	4.11				2	*Im3m*	310
U(I)	R	25	orthorhombic	U	2.8537	5.8695	4.9548		4	*Cmcm*	310
U(II)	R	720	tetragonal		10.759		5.656		30	$P4_2/mnm$	310
U(III)	R	805	cubic	bcc	3.524				2	*Im3m*	310
Np(I)	R	20	orthorhombic		6.663	4.723	4.887		8	*Pnma*	310
Np(II)	R	313	tetragonal		4.897		3.388		4	$P42_12$	310
Np(III)	R	600	cubic	bcc	3.52				2	*Im3m*	310
Pu(I)	R	21	monoclinic		6.183	4.822	10.963	101.79	16	$P2_1/m$	310
Pu(II)	R	190	monoclinic		9.284	10.463	7.859	92.13	34	*I2/m*	310
Pu(III)	R	235	orthorhombic		3.1587	5.7682	10.162		8	*Fddd*	310
Pu(IV)	R	320	cubic	fcc	4.6370				4	*Fm3m*	310

TABLE 3. Crystallographic data—Continued

Element	Pressure (kbar)	Temperature (°C)	Crystal system	Structure type	*a* Å	*b* Å	*c* Å	Angle (degrees)	Z	Space group	Ref.
Pu(V)	R	500	cubic	bcc	3.638				2	*Im3m*	310
Am(I)		20	hexagonal	dhcp	3,4680		11.240		4	*P6₃/mmc*	310
Am(II)	R	22	cubic	fcc	4.894				4	*Fm3m*	310

[a] Values given in the reference were for the fct cell. These were converted to bct by $a_{bct} = a_{fct}/(2)^{1/2}$ and $c_{bct} = c_{fct}$.
[b] Corrected for apparent calculation error or misprint in source.

2. Group I A (The Alkali Metals)

2.1. Lithium

Stager and Drickamer [344] have reported a large drop in the resistance of Li at RT and about *63* kbar. They suggest that this phenomenon is caused by a first order phase transition. If Stager and Drickamer encountered a solid-solid phase line it must have a positive slope with a triple point beyond 80 kbar, because the melting curve to 80 kbar [261] does not show behavior characteristic of a triple point. Bridgman [75] detected a drop in the resistance of Li at about *60–65* kbar (the limit of his experiments on resistance) which he attributed to a transition in AgCl. We now know that the maximum pressure attained in Bridgman's resistance measurements was about 65 kbar, so the AgCl transition (80 kbar) could not have been responsible for the resistance drop in Bridgman's experiments with Li. It is possible that what Bridgman observed was the beginning of the same transition reported by Stager and Drickamer. The fact that Bridgman also observed the same phenomenon in K diminishes the validity of this argument somewhat. Volume measurements by Bridgman [70, 73] to about *85* kbar revealed no indication of a phase transition.

The melting curve of Li has been reported six times [54, 57, 227, 261, 299, 318] from three different laboratories. Of the three melting curves from Kennedy's laboratory [227, 261, 299], the most recent [261] appears to be superior in terms of sample purity, pressure determination, and method of determining the melting point. For these reasons, data from the earlier works [227, 299] have not been used in determining the best melting curves for any of the alkali metals. Bridgman's [54, 57] data were taken only to about 8 kbar on a sample that was "evidently somewhat impure". Consequently, his data have been discarded also. Ponyatovskii [318] performed his experiments in a hydrostatic medium to about 30 kbar. Unfortunately he did not report his data in tabular form so accuracy was probably lost in taking values from his graph. The melting curve shown in figure 2 is the best curve resulting from the average of data from Ludemann and Kennedy [261] and Ponyatovskii [318] with the latter data given a weight of one-half.

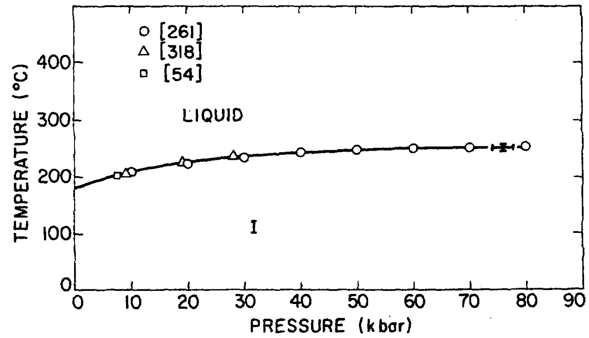

FIGURE 2. Phase diagram for lithium.

2.2. Sodium

Resistance measurements by Stager and Drickamer [344] to about *450* kbar and both resistance [75] and volume [70, 73] measurements by Bridgman to about *65* kbar and *85* kbar respectively show no indication of a first order phase transition.

The melting curve has been reported seven times [9, 50, 57, 227, 261, 299, 318] from four different laboratories. Reasons enumerated in the section on Li lead to the elimination of data from two of these reports [227, 299] and to the assignment of a weight of one-half to the data of another report [318] . Anderson, et al. [9] based the pressure calibration for their tetrahedral press on the Hg melting curve reported by Klement, et al. [235]. The temperature of the Na melting curve lies on the order of 100 °C above the Hg melting curve. This means that the pressure calibration used by Anderson, et al. is probably a little low. Decker, et al. have indicated that for the tetrahedral press there is roughly 1 kbar rise in pressure per 100 °C rise in temperature for temperatures up to 400–500 °C. If this criterion is applied to the data of Anderson, et al., the correction is about the same magnitude as their estimated error in pressure. The effect of using this correction is therefore minimal but is considered sufficient to warrant application. The melting curve shown in figure 3 is a combination of the data from Luedemann and Kennedy [261], Bridgman [50, 57], the corrected data of Anderson, et al. [9] and the weighted data of Ponyatovskii [318].

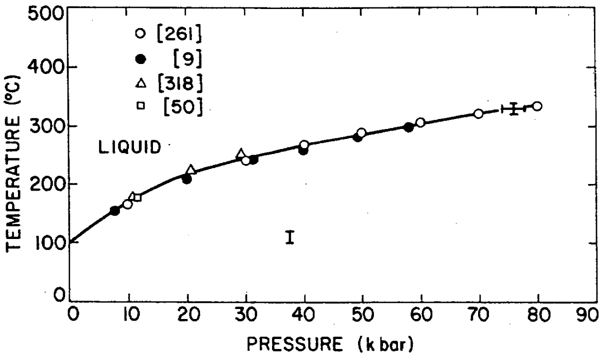

FIGURE 3. Phase diagram for sodium.

2.3. Potassium

Resistance [75] and volume [70, 73] measurements by Bridgman to *65* kbar and *85* kbar respectively give no indication of a phase transition. At − 196 °C Stager and Drickamer [344] observed resistance changes in K at *190* kbar and *240* kbar which they attribute to first order phase transitions. For unknown reasons these transitions were not detected in resistance measurements at 23 °C.

Data for the melting temperature versus pressure have been published in seven reports [9, 50, 57, 261, 299, 314, 318] from four laboratories. These data have been treated as outlined in the section on Na to give the melting curve shown in figure 4.

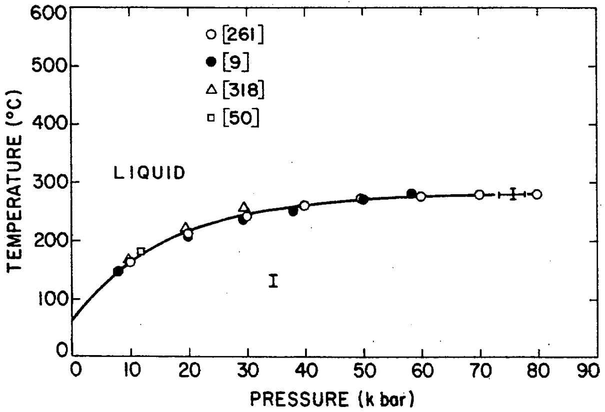

FIGURE 4. Phase diagram for potassium.

2.4. Rubidium

Several studies have been made on the pressure induced variation of resistance and/or volume of Rb. Bridgman [75] detected no resistance discontinuities up to *65* kbar and no volume discontinuities to *85* kbar. Bundy [87] and Vereshchagin, et al. [397] both detected sharp resistance increases at about *67–68* kbar with the latter investigator going on to find another, much larger, jump at 110–114 kbar. In Drickamer's laboratory a break in the slope at about *60* kbar was discovered [344] as well as a large increase in resistance [20, 344] at about *142–153* kbar. The 60 kbar disturbance is presumably the same transition reported by Bundy and by Vereshchagin (the 7–8 kbar difference in pressure may be attributed to the fact that Drickamer's press does not allow reliable determination of pressure in the region of the break). The large resistance increases reported from Drickamer's and Vereshchagin's laboratories are similar in character and are probably caused by the same physical change. The large difference in transition pressures could possibly be attributed to different impurity levels, but this is difficult to determine since Drickamer reported purity only as "c.p.". At − 196 °C, Drickamer [344] reported the higher pressure transition at about *167* kbar.

Bundy [87] has reported transition pressures of about *69* kbar and *70* kbar at temperatures of about 70° and 118 °C respectively for Rb(I–II). Upon extrapolation (over about 160°) the Rb(I–II) boundary thus determined intersects Luedemann and Kennedy's melting curve [261] at about 73 kbar. Since this melting curve (to 80 kbar) shows no evidence of a triple point, the actual Rb(I–II) boundary probably has a slope somewhat less steep than is indicated in Bundy's report (see discussion below regarding reliability of Bundy's data). There seems little doubt that Rb(I–II) does exist, although (for reasons stated above) the position of the Rb(I–II) phase boundary above RT is uncertain. The existence of a Rb(II–III) transition is regarded as tentative and its possible position on the *P–T* diagram has certainly not been established.

The melting curve for Rb has been investigated in four laboratories and reported in seven papers [7, 8, 56, 57, 87, 261, 299]. Data from Kennedy's laboratory [261, 299] and by Anderson, et al. [7, 8] have been treated as mentioned above under sections on Li and Na, respectively. For undetermined reasons Bundy's [87] data, even after pressure calibration correction, deviate drastically from the melting curve data of others. The Bundy melting curve shows a maximum near *35–38* kbar, at which point it is roughly 30 °C *above* the other determinations, and descends from that point until at about *55* kbar it is roughly 25 °C *below* the other

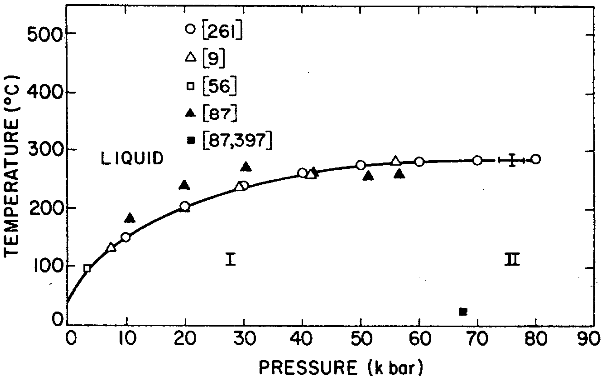

FIGURE 5. Phase diagram for rubidium.

determinations. Because of this lack of agreement, Bundy's data have not been considered in determining the best melting curve. For the same reason, considerable doubt is cast on the reliability of Bundy's solid-solid transition pressures discussed in the previous paragraph. The melting curve shown in figure 5 has been determined from the data of Luedemann and Kennedy [261], Bridgman [56, 57] and the corrected data of Anderson, et al. [7, 8].

2.5. Cesium

The Cs(I–II) transition has been studied by resistance, volume, and X-ray methods [10, 63, 64, 72, 170, 225, 226]. The reported RT transition pressures vary from 21.6 kbar (Bridgman's [64] resistance work) to 23.7 kbar (X-ray work of Hall, et al. [170]). Studies at higher [64, 226] and lower [10] temperatures show that the Cs(I–II) boundary has a very steep positive slope. The line representing this boundary in figure 6 was determined by consideration of the position of the L–I–II triple point (see discussion on melting below) and an equal weighting of the data mentioned above.

At one time the Cs(II–III) and Cs(III–IV) transitions were not resolved (less than 1 kbar separate the two at RT) and only one transition was thought to take place [75, 167, 225, 226, 397]. During this time Kennedy, et al. [226] examined the phase boundary by volume methods and reported that it has a positive slope of 11.8°/kbar with a triple points at 47.2 kbar and 90 °C. Determinations of the RT transition varied from *40* kbar (Bridgman's [75] resistance data) to 43 kbar (Halls [167] resistance work).

In 1964, Hall, et al. [170] published data which revealed the resolution of the Cs(II–III) and Cs(III–IV) transitions. Since that time, Jayaraman, et al. [210] have determined some points on the Cs(II–III) and Cs(III–IV) phase boundaries. Their work, and arguments advanced by McWhan and Stevens [284], indicate that these phase boundaries have very steep slopes and are nearly parallel. The II–III–IV triple point is difficult to determine because the phase boundaries are so nearly parallel and because low temperature experiments give poor pressure resolution of two first order transitions so close together (see also the section on Bi). The work of McWhan and Stevens indicates a II–III–IV triple point at about *41* kbar and 7 °C. The RT value for the Cs(II–IV) transitions has been reviewed carefully elsewhere [128] and will not be discussed further in this report. The II–III, III–IV and II–IV boundaries in figure 6 were determined by consideration of the data of Jayaraman, et al. [210] and McWhan and Stevens [284], modified appropriately to reflect the value for the RT transition suggested in the above-mentioned review [128]. The positions of these boundaries may require modification after further experiments have been done (see discussion on melting below).

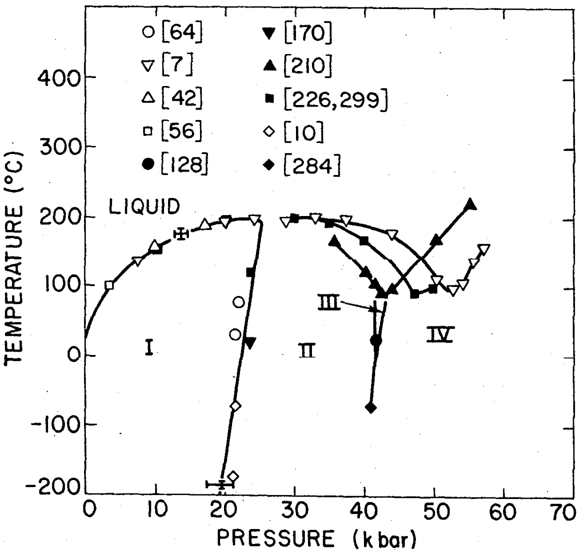

FIGURE 6. Phase diagram for cesium.

The Cs(IV–V) transition has been observed as a discontinuity in the resistance curve [346, 397, 424] and by the onset of superconductivity in Cs(V) [422]. Stager and Drickamer have observed that this transition occurs at about the same pressure (*133–142* kbar) at RT as at −196 °C. Wittig [422, 424] and Vereshchagin, et al. [397] report somewhat lower pressures (*98–102* kbar and about *105* kbar, respectively) for this transition. Wittig [424] has emphasized that in experiments where Pb is placed in series with Cs in the pressure cell, the Cs(IV–V) transition occurs *before* the Pb(I–II) transition, whereas Stager and Drickamer's work places Cs(IV–V) slightly *above* Pb(I–II). The Cs used by Stager and Drickamer was 99.95 percent pure, whereas Vereshchagin's Cs was less than 98.4 percent pure (Wittig did not report sample purity). The increased impurities in the Cs used by Vereshchagin could have caused the lower transition pressure. It is also possible that the Pb used as a pressure calibrant by Vereshchagin and by Wittig differed in impurity level from that used by Stager and Drickamer. The problem cannot be resolved without further information, so the position of Cs(IV–V) must be considered highly uncertain.

The melting curve has been investigated several times [7, 8, 42, 56, 57, 210, 226, 299, 358]. Good agreement exists among the different investigators up to the L–I–II triple point, but the data diverge considerably thereafter. The portion of the melting curve to the first triple point has been determined by giving equal weight to all data considered [7, 8, 42, 56, 57, 226, 299] with Anderson's [7, 8] data corrected as discussed in the section on Na. The data of Stishov and Makarenko [358] were not used because values were not reported in tabular form and the published graph was considered too small to read properly. The L–I–II triple point is the average of the three reported values [7, 8, 226, 358].

Three investigations of the melting curve above the first triple point [7, 8, 210, 226, 299] have been reported. In the vicinity of the L–II–III triple point these sources vary by about 10 kbar pressure but show good agreement in temperature. Apparently, the difficulty lies in the techniques of pressure determination. Jayaraman, et al. [210] believe that "the discrepancy (from the data of Kennedy, et al. [226, 299]) is most likely due to underestimation of the frictional loss in the earlier work." It is interesting to note, however, that the value of Cs(II–IV) at RT reported by Kennedy, et al. is within 1 kbar of the value used by Jayaraman, et al. (note also that Jayaraman is a co-author of the Kennedy paper). Furthermore, the pressure calibration used by Anderson [7, 8] is based on the Hg melting curve reported by Klement, Jayaraman, and Kennedy [235] in 1963. This is within a year of the report (from the same laboratory) on Cs for which frictional losses were supposed to have been underestimated, yet Anderson's melting curve for Cs lies at *higher* pressures than that of Kennedy (the reader should recall at this point that Anderson's data for Na, K, and Rb are in good agreement with data from other workers—see the corresponding sections for discussion).

Since the issue appears confusing at best, no definite conclusions have been drawn concerning the position of the melting curve above the L–I–II triple point. Data from each of the three investigations are shown in figure 6. As the phase diagram emphasizes, the Cs solid-solid boundaries appear to agree best with the melting curve of Jayaraman, et al.

The crystal structures of Cs(II) and Cs(III) were determined to be fcc by Hall, et al. [170]. That Cs(II) is fcc has been confirmed by the single crystal work of Weir, et al. [413]. Crystal structures of Cs(IV) and Cs(V) have yet to be determined. Crystallographic data are given in table 3.

3. Group II A (The Alkaline Earths)

3.1. Beryllium

The change in resistance of Be with pressure has been investigated [75, 122, 145, 268, 361] as has the change in volume with pressure [73]. In 1963 Marder [268] reported a large drop in resistance at *81* kbar and RT which he tentatively attributed to the hcp–bcc phase transition. Subsequent X-ray work by Jamieson [199] at pressures exceeding 81 kbar revealed no trace of a bcc structure. X-ray spectra taken after pressure release were the same as those taken above 81 kbar (hcp with the 002 line missing) and are attributable to a reorientation of the sample. Other investigators [75, 122, 145, 361] have observed no resistance discontinuities at RT even to pressures of 150 kbar [122]. Francois and Contre have studied [145] the variation of the hcp–bcc phase line with pressure to about *56* kbar. An extrapolation of their work shows that the RT hcp–bcc transition will probably occur at pressures in excess of 150 kbar. Bridgman's volume work [73] revealed no evidence for a phase transition at RT to about *85* kbar.

The melting curve has been investigated by Francois and Contre [145] to about *56* kbar. They encountered serious contamination difficulties when the Be was melted and have estimated their melting temperature uncertainty at about ± 100 °C. The phase diagram shown in figure 7 is entirely attributable to Francois and Contre.

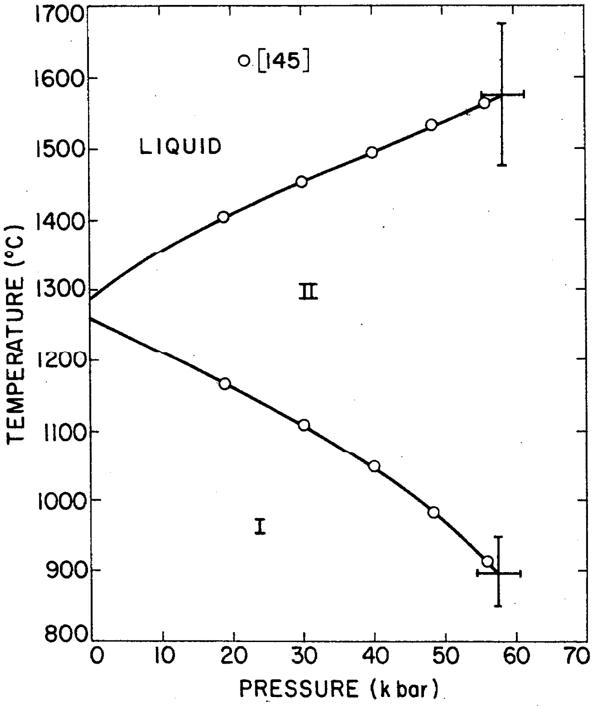

FIGURE 7. Phase diagram for beryllium.

3.2. Magnesium

Investigations of the resistance [75, 343] and volume [73, 117, 311] variations with pressure show no definite discontinuities. However, Perez-Albuerne, et al. [311] believe their X-ray data and earlier resistance data [343] indicate a subtle hcp–dhcp transition beginning in the vicinity of 50 kbar. The transition was reported on the basis of an examination of the $(c/a)/(c/a_0)$ versus V/V_0 plot which shows a large increase in the former parameter beginning at a V/V_0 of about 0.88.

The melting curve has been reported only once [227] and is shown in figure 8.

3.3. Calcium

Bridgman's early work [63, 70] on compressibilities indicated two possible RT phase transitions at 25–30 kbar and *59* kbar, but these possibilities were not confirmed by Bridgman's own resistance measurements [75]. Jayaraman, et al. [200] could not confirm the 25–30 kbar transition by volume methods (they did not investi-

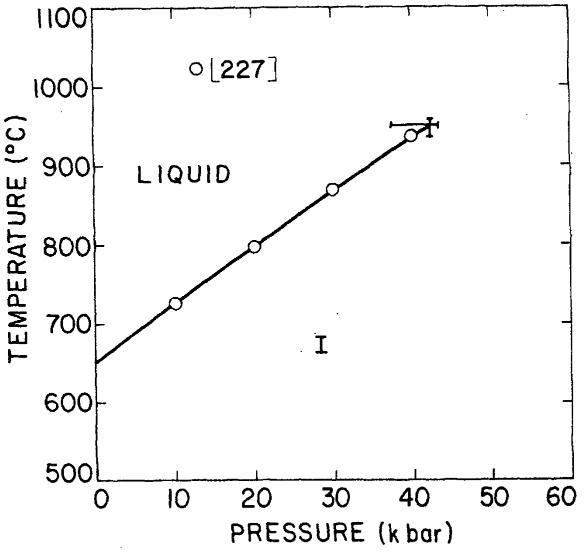

FIGURE 8. Phase diagram for magnesium.

gate the 59 kbar transition). Investigations from Drickamer's laboratory [20, 131, 343] show R(p) anomalies that indicate RT transitions at about *116* kbar and *235–255* kbar. Vereshchagin's resistance work [390, 397] tends to verify the qualitative features reported by Drickamer, but Vereshchagin does not comment on the possibility that phase transitions were the cause of the R(p) features (apparently he had not seen the paper from Drickamer's group [343] which dealt with those matters). More work must be done before the position or even the existence of these proposed transitions can be decided.

The melting curve and Ca(I–II) phase boundary were determined by Jayaraman, et al. [200] to pressures of about 40 kbar. The phase diagram shown in figure 9 is entirely attributable to this source.

3.4. Strontium

Bridgman [63, 69, 70, 75] found both resistance and volume transitions with pressure for Sr. With increasing pressure at RT he reported a volume transition at 37.2 kbar [63] and a resistance transition at 44.1 kbar [75]. At the time, Bridgman did not recognize a difference in his volume and resistance pressure measurements and so did not believe the volume and resistance transitions mentioned above were attributable to the same physical change in Sr. Correcting Bridgman's pressures to today's scale shows both volume and resistance transitions at about *36* kbar, thus indicating that the two phenomena are both caused by the Sr(I–II) transition. Bridgman also reported a volume anomaly at *60* kbar [69, 70] but found no corresponding resistance transition to *65* kbar [75].

The Sr(I–II) transition has been confirmed by both resistance [200, 343] and volume [200, 386] methods. No transitions were found beyond Sr(I–II) to *380* kbar by Stager and Drickamer's [343] R(p) measurements. McWhan and Jayaraman [278] used X-ray methods to show that Sr(I–II) is an fcc–bcc transition and that Sr retains the bcc structure to about 80 kbar, thus indicating that Bridgman's 60 kbar volume anomaly was not caused by a first order phase change.

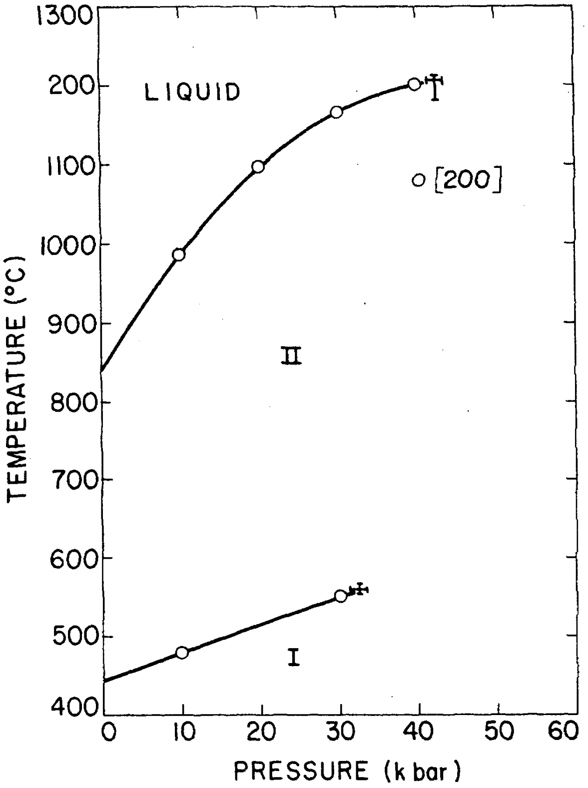

FIGURE 9. Phase diagram for calcium.

Jayaraman, et al. [200] have determined the Sr(I–II) phase boundary and the melting curve to about 40 kbar. The strong curvature shown by the solid-solid boundary (see figure 10) was thought at first to indicate two different phase transitions. This has been discounted, however, by McWhan and Jayaraman's [278] X-ray work showing that the RT transition at 35–36 kbar is fcc–bcc, analogous to the RP transition of 550–60 °C. The diagram in figure 10 is entirely attributable to Jayaraman, et al. [200].

3.5. Barium

Barium has been studied extensively (particularly at RT) because of its widespread use as a pressure calibrant and because of the interesting features of the *P–T* diagram. A critical analysis of the Ba(I–II) transition pressure at RT has been published elsewhere [128] and will not be repeated here.

Bridgman discovered small discontinuities in volume [63, 64] and resistance [64, 75] versus pressure measurements at about 17 kbar which he attributed to a first-

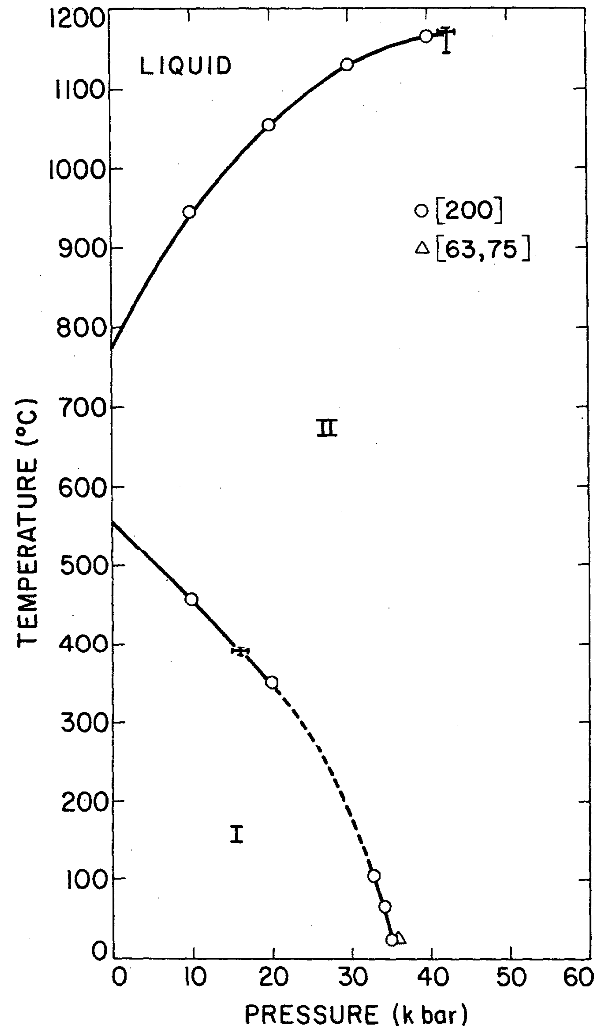

FIGURE 10. Phase diagram for strontium.

order phase transition. His resistance measurements gave very erratic results with large differences in the transition pressure [75], and the volume discontinuity was not seen in his earlier work with a higher purity sample [61]. Subsequent work employing ultrasonic pulse and volume methods [409] has revealed the transition at 17.2 kbar, but other workers using volume [203], DTA [203], X-ray [23, 25], and resistance [124] techniques have failed to confirm the transition. Because the volume and resistance discontinuities cannot be reproduced by others, because no discontinuity in *d*-values or change in crystal structure is detectable by X-ray investigations, and because no discontinuity exists in the melting curve to indicate a triple point, it appears that there is no first-order phase change in Ba in the vicinity of 17 kbar.

The pressure of Ba(I–II) at 25 °C has been determined many times. The review [128] mentioned earlier places this pressure at 55.3±1.2 kbar. The Ba(I–II) phase boundary has been investigated at temperatures above 25 °C in three laboratories [27, 28, 124, 203]. Data from two of these investigations [27, 28, 203] are in good agreement, but that of the third [124] differs drastically. In the former the slope of the phase line is positive, whereas in the latter, it is negative. Using thermodynamic arguments Susse and Epain [373] have shown that the slope must be positive, so the data showing negative slope have been discarded. The Ba(I–II) boundary shown in figure 11 is a combination of data from the two remaining investigations corrected to reflect the indicated RT transition pressure.

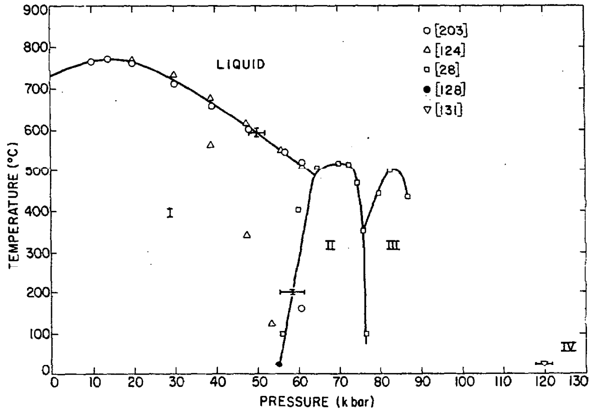

FIGURE 11. Phase diagram for barium.

Bastide, et al. [27, 28] have recently reported at Ba solid-solid transition in the neighborhood of 73–76 kbar (at 100 °C). Evidence for this transition includes the DTA event that revealed the transition at 100 °C and a sharp cusp in the melting curve indicative of a triple point. Bastide, et al. also show resistance data by Stromberg and Stevens and by Contre which show slight discontinuities near 80 kbar which they attribute to the proposed Ba(II–III) transition. Stromberg and Stevens [362] attribute that discontinuity in their data to a transition in the AgCl surrounding the Ba sample (similar discontinuities were seen by them during resistance measurements on elements other than Ba). Contre, on the other hand, used Teflon as a pressure transmitting medium, so the discontinuity of his resistance work cannot be attributed to AgCl.

Resistance measurements by others [20, 130, 343, 360, 421] have not revealed any discontinuity in the vicinity of the Ba(II–III) transition. Bridgman's volume work [70] also fails to show a transition in the 70–85 kbar region. Experiments by Il'ina and Itskevich [184] show a jump in the superconducting transition temperature of Ba at 75–78 kbar which indicates the presence of a new phase. However, superconductivity data taken at the University of California in San Diego [295, 421] show a smooth increase in T_c from 55 to 100 kbar with no indication of a phase change.

The definite indication by the melting curve of a L–II–III triple point is strong evidence for the existence of a Ba(II–III) transition, but lack of concrete confirmation by other indicators does cause some doubt. Isothermal enthalpic detection and X-ray studies now underway in Bastide's laboratory [29] will perhaps offer evidence to conclusively confirm the existence of Ba(II–III).

Resistance versus pressure experiments in Drickamer's laboratory [20, 130, 131, 343] have indicated two more possible phase transitions for Ba. The first of these, at about *118–122* kbar, has been confirmed by the resistance measurements of others [360, Contre's data in 28] and is sometimes used as a pressure calibration point. Superconductivity measurements [295, 421] also indicate the presence of this phase change. At one time this was thought to be a solid-liquid transition [343] but later X-ray work [130] showed it to be solid-solid [Ba (III–IV)]. The second transition has been detected only at −196 °C [130, 343] at about *190* kbar.

The melting curve has been investigated in three laboratories [27, 28, 124, 203]. The region below the first triple point (to about *60* kbar) has been investigated twice [124, 203] with good agreement. Data above 60 kbar have been reported only by Bastide, et al. [27, 28]. The melting curve shown in figure 11 is averaged data to about 60 kbar and Bastide's data thereafter.

The crystal structure of Ba(II) has been determined as hcp [23, 25] by X-ray measurements. Preliminary investigations [130] indicate that Ba(IV) is probably fcc, but this must be regarded as tentative. The crystal structures of Ba(III) and Ba(V) have not been determined.

4. Group III A

4.1. Boron

There are several different polymorphic forms of B known at RTP. Very little is known about the thermodynamic stabilities of these different forms or about their behavior under pressure. The variation of resistance at RT with pressure has been determined for B (polymorphic form unspecified) to 40 kbar [171] and to about *200* kbar [393] with no indication of a phase transition. Tetragonal and β-rhombohedral B have been studied (resistance versus pressure) to 60 kbar and 300 °C with the same result [11].

Wentorf [415] has prepared a new form of B at high pressure (*85–120* kbar) and temperature (1500–2000 °C) from both "amorphous" and β-rhombohedral B. The new form is retained when temperature and pressure are returned to 25 °C and 1 atmosphere. Wentorf reports the X-ray powder pattern but was unable to index it. If heated to 1500 °C at 30 kbar, the new polymorph reverts to the β-rhombohedral form. There have been no reported studies of the melting curve or of any solid-solid phase boundaries.

4.2. Aluminum

While making compressibility measurements by high-pressure X-ray methods, Roy and Steward [330] found evidence for a fcc to hcp transition in Al. The existence of the hcp polymorph was suggested by the appearance of three additional lines in the X-ray spectrum at RT and 205 kbar. The lines were indexed as $10\bar{1}0$, $10\bar{1}1$, and $10\bar{1}2$, but no data concerning the *d*-values or hcp cell parameters were given. No information was given on the purity of the Al or on the method used for pressure calibration. In view of the scarcity of data, the transition pressure and even the existence of the transition must be regarded as highly tentative. Resistance [75] and volume [73] measurements by Bridgman to *65* kbar and *85* kbar respectively gave no indication of any first order transitions.

The melting curve has been determined by Gonikberg, et al. [159], Jayaraman, et al. [204] and Lees [247]. The data of Gonikberg and Lees are in good agreement whereas those of Jayaraman are about 50° lower at 45 kbar. It is interesting to note that Jayaraman used Mo to contain the Al sample and reported that Ta containers appeared to contaminate the Al. On the other hand, Lees found that Mo contaminated his Al samples and eventually used Ta containers. Lees employed microprobe analysis to determine the existence of contamination. Jayaraman did not report this method of determining contamination.

Each of the investigators used DTA methods for determination of the melting point. Lees' method allowed only a few seconds contact between molten Al and its container (thus reducing the chances for contamination), whereas Jayaraman's method involved repeated contacts on the order of 30 seconds duration. Gonikberg's report did not give many experimental details, so an assessment of possible contamination is difficult to make. His samples were contained in graphite and heated by passing an electric current through surrounding coils of Nichrome wire. The maximum

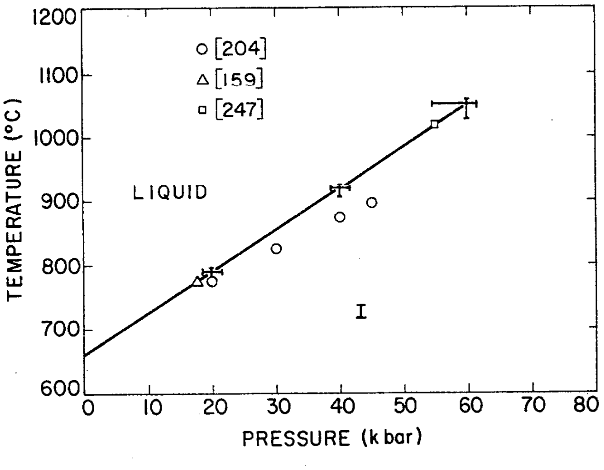

FIGURE 12. Phase diagram for aluminum.

pressure he used was 17.6 kbar so temperatures in his work never exceeded 775 °C. Since the melting points reported by Jayaraman appear to be low as a result of contamination, only the data of Gonikberg and Lees are combined to give the melting curve shown in figure 12.

4.3. Gallium

The Ga(I–II) transition has been investigated several times [44, 45, 61, 85, 204]. The agreement among the various reports is good, so the Ga(I–II) boundary shown in figure 13 is an average of all available data.

The Ga(II–III) transition has been determined in two laboratories [45, 204] with only fair agreement. The L–II–III triple point temperatures agree within 0.5 °C, but the pressure spread is 3.1 kbar. It appears, therefore, that the problem lies in pressure calibration. The Ga(II–III) boundary in figure 13 is an average of the data from the two sources cited above.

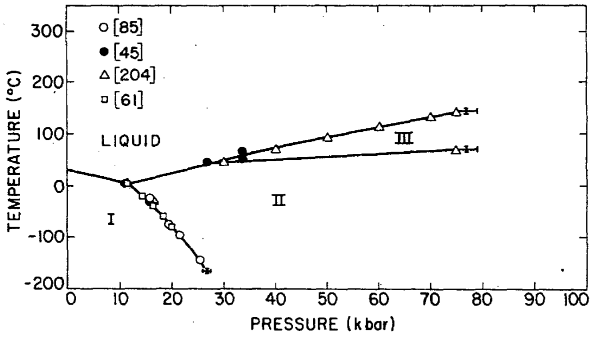

FIGURE 13. Phase diagram for gallium.

The melting curve has been reported in four instances [44, 45, 61, 204] with good agreement to about 20 kbar and only fair agreement thereafter. The melting curve shown in figure 13 is an average of all available data.

The crystal structure of Ga(II) was determined by Vereshchagin, et al. [394] to be body-centered tetragonal (In-type). Weir, et al. [413] have confirmed this structure and pointed out a slight error in the calculation of the lattice parameters in Vereshchagin's paper. Weir's apparatus allowed for the collection of more than twice as much data as Vereshchagin's and is correspondingly more accurate. The crystallographic data reported in table 3 is entirely attributable to Weir, et al. [413]. The crystal structure of Ga(III) is as yet unknown, although Jayaraman, et al. [204] have suggested that it is probably bcc.

4.4. Indium

X-ray [387, 394], resistance [75], and volume [70] measurements up to 345 kbar, *65* kbar and *85* kbar respectively at RT show no evidence for a first order phase transition. Fadeev [138] has reported a slight (0.2–0.3 °C) dip in the melting curve at about 3 kbar which he interprets as evidence of a triple point. He gives almost no experimental details in his paper, so his work is difficult to evaluate. In addition, it should be emphasized that he did not mention having observed the solid-solid transition associated with the proposed triple point. Other persons, while investigating the melting curve by DTA [106, 204, 272] and by resistance [132, 291] methods, have also failed to report any trace of a solid-solid transition. Further evidence is necessary before the proposed triple point can be accepted.

The melting curve has been investigated several times [106, 132, 138, 204, 272, 291]. The data are in good agreement to about 30 kbar, but the three reports on work above that pressure [132, 204, 291] are in poor agreement (total spread at 70 kbar is about 40 °C). Dudley's work [132] has a high (±20 °C) uncertainty in the temperature measurement. Jayaraman, et al. [204] underestimated the frictional losses in their piston-cylinder apparatus [234], and the data of Millett [291] suffer from the difficulty of correcting for the effect of temperature on pressure in a tetrahedral-anvil apparatus. It is impossible to know the quantitative effect of these difficulties, so corrections have not been made (except to change Dudley's room temperature fixed points to reflect currently accepted values). The melting curve in figure 14 is an average of all available data to 30 kbar. Above 30 kbar, the data from the individual reports are shown.

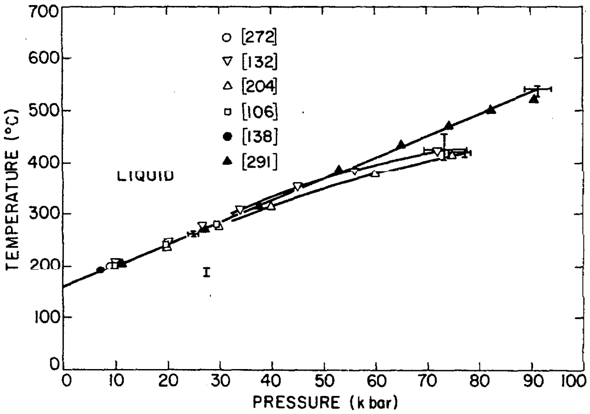

FIGURE 14. Phase diagram for indium.

4.5. Thallium

The Tl(I–II) transition has been investigated by resistance [2, 204], volume [61], and DTA [204, 272, 316] methods. Bridgman [61] took only one data point, Adler and Margolin [2], only five (in the 30–35 kbar region), and McDaniel, et al. [272] reported that their DTA signals were too weak to allow measurement. Ponyatovskii [316] did not state how much data he recorded, but his *P–T* diagram (which shows only a smooth curve) implies that data were taken at invervals up to about 33 kbar. Jayaraman, et al. [204] took 12 data points distributed evenly over the region 8–38 kbar. Conclusions concerning the shape of the Tl(I–II) phase boundary vary considerably, depending on the data being analyzed. Conclusions drawn by Bridgman and by Adler and Margolin suffer from lack of data. Particularly does the large curvature near the triple point suggested by Adler and Margolin seem unjustified on the basis of their scant data. Since Ponyatovskii did not show his data points, only Jayaraman's conclusions appear entirely justified on the basis of the data shown. The phase boundary shown in figure 15 for Tl(I–II) is due to Jayaraman, et al. [204].

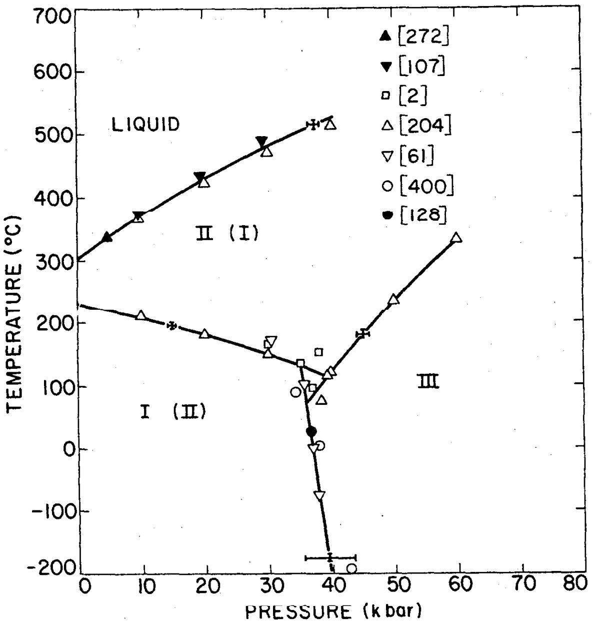

FIGURE 15. Phase diagram for thallium.

The Tl(I–III) transition[3] is widely used as a pressure calibration point at RT. An analysis of the reported data on the RT transition pressure has been made elsewhere [128] and will not be repeated here. Data at temperatures other than 25 °C have been reported from four sources [2, 61, 204, 400]. Jayaraman, et al. [204], and Adler and Margolin [2] each recorded data at and above RT. Data above RT were grouped around points at 85 °C and 95 °C respectively, thus giving only two effective points in each study. They both reported a positive slope for the phase boundary. Bridgman [61] and Vereshchagin, et al. [400] on the other hand, took data both above and below RT and at four or more different temperatures. They both reported a negative slope for the phase boundary. Further evidence that the Tl(I–III) boundary has a negative slope was obtained from superconductivity studies [186]. It is difficult to know why there is such a difference in the data for Tl(I–III). It seems reasonable to place more weight on the studies with more data, and this was done in deciding on the phase boundary shown in figure 15.

The Tl(II–III) boundary has been determined by Jayaraman, et al. [204] and by Adler and Margolin [2]. The latter workers reported only 2 or 3 points (depending on how their data are interpreted) on this boundary. The Tl(II–III) boundary in figure 15 is essentially that of Jayaraman, et al.

The I–II–III triple point has been determined in 3 instances [2, 61, 204]. Bridgman's point [61] is not considered here since it is based to a large extent on his single data point for the Tl(I–II) boundary. The point suggested by Adler and Margolin [2] has also been discarded because of insufficient data [see discussion above on the Tl(I–II) boundary]. The triple point region shown in figure 15 is defined by extensions of the solid-solid boundaries discussed above.

The melting curve has been determined in three laboratories [107, 204, 272, 316] with fair agreement. The curve shown in figure 15 is an average of the available data.

Using a diamond anvil high pressure cell, Piermarini and Weir [312] have determined that the crystal structure of Tl(III) is fcc. Crystallographic data are presented in table 3.

5. Group IV A

5.1. Carbon

Carbon is probably best known for its very hard, very beautiful allotropic form called diamond. The C(I–II) boundary (graphite-diamond) has been extensively studied because of the attraction of converting 35¢/pound graphite into $4000/pound diamond. The only work in this area to find its way into the open literature is attributed to Bundy, et al. [88]. They determined the C(I–II) boundary in the 45–75 kbar region, using a catalyst in an effort to avoid over pressurization. The rate of noncatalyzed C(I–II) conversion is so low that it is beyond detection unless pressures well into the C(II)-stable region are used [90, 95].

Forms of carbon other than hexagonal graphite and cubic diamond have been reported. Ergun and Alexander [136] have discussed the possibility that diamond exists in a hexagonal form, and Bundy and Kasper [99] have reported the synthesis of a new hexagonal form at high pressure and temperature (different from that proposed by Ergun and Alexander). El Goresy and Donnay [135] have discovered a new form of C in the Ries Crater in Bavaria. This same form has recently been synthesized under low-pressure, high-temperature conditions by Whittaker and Kinter [417]. A new cubic form reported by Aust and Drickamer [14] was later found to be AgCl from the medium surrounding the C sample. There are numerous other uncharacterized types of C under the names "carbon", "graphite", "amorphous carbon", "paracrystalline carbon", "carbon black", and so forth. At present, the thermodynamic

---

[3] The nomenclature in many reports designates the RT modification as Tl(II) and the high temperature form as Tl(I).

regions of stability for these various other forms are not known. It is probable that many, if not all, of them exist only metastably and have no stable region of existence.

The melting curve has been investigated to 1 kbar by Schoessow [333] and to much higher pressures at General Electric [89, 94] and in Moscow [139–141, 399]. The agreement is rather poor but this is understandable in view of the experimental difficulties involved. Schoessow found that melting temperatures varied by more than 100 °C depending on the grade of graphite used. This difference pales to insignificance alongside the scatter in the data from the high pressure experiments, so difference in source graphite cannot account for difference in the reported melting curves. The melting curves are sufficiently different that an average would have little meaning. Consequently, both are shown in figure 16.

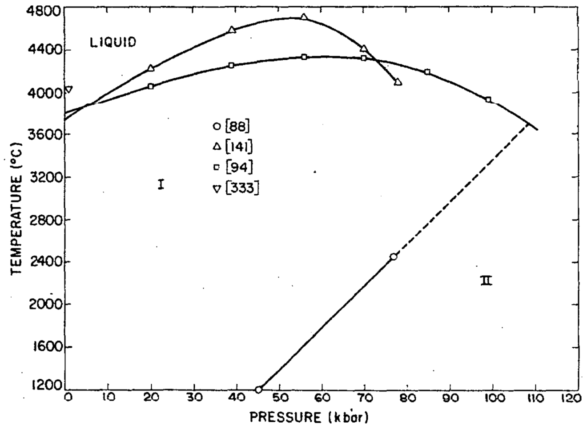

FIGURE 16. Phase diagram for carbon.

Bundy [97, 100, 101] and others [238, 359] have extensively reviewed the C phase diagram. Bundy is undoubtedly the most knowledgable in view of his close association with the General Electric diamond synthesis group. He has made some interesting extrapolations based on shock experiments and on analogies with other IV–A elements. Although his predictions are highly speculative and thus beyond the scope of this review, they nevertheless give the best insight now available into the C phase diagram. His reviews do have the disadvantage of not being corrected to the currently accepted pressure scale. Thus the predicted L–I–II triple point shown at about 125–130 kbar and 3750–3950 °C should be placed nearer 109 kbar and 3700 °C. Also Bundy did not recognize the melting curve data of Fateeva, et al. [139–141, 399]. If their melting curve was accepted, rather than Bundy's, the triple point position would be about 96 kbar and 3200 °C.

5.2. Silicon

Minomura and Drickamer [293] were the first to report a first order phase change in Si. They detected a large drop in sample resistance in the region *120–160* kbar (depending on the amount of shear on the sample). This transition has since been confirmed several times by resistance [96, 414], shock [165, 309] and X-ray [194, 396] methods, but the nature of the transition has been difficult to determine. Jamieson [194] used his high pressure X-ray apparatus to show that the high pressure phase is a mixture of two phases, a tetragonal Sn-type and a complex bcc structure (the bcc structure was first determined by Wentorf and Kasper [218, 414]). The Sn-type phase disappears upon release of pressure, whereas the bcc phase is retained metastably. When heated at atmospheric pressure the bcc phase changes to a mixture of ordinary Si (diamond-cubic) and hexagonal form, the relative amounts depending on the intensity and duration of the heat treatment.

The transition from diamond-cubic Si at high pressure is very sluggish and apparently quite sensitive to shear. Consequently, the transition pressure is not known with any degree of certainty. Long term (up to 6 days duration) experiments by Bates [31] indicate that the transition occurs at pressures above 125 kbar at 100 °C and above 105 kbar at 200 °C. It is not certain which phase—Sn-type or bcc—is the thermodynamically stable form at high pressure, or, for that matter, whether both phases have a thermodynamically stable region. Because of these difficulties the position of the Si[I–(II–III)] phase boundary is very uncertain. Crystallographic data are given in table 3.

The melting curve has been investigated in three laboratories [96, 202, 247]. The work of Lees and Williamson [247] and of Jayaraman, et al. [202] agree well with each other and with the uncorrected data of Bundy [96]. The latter worker had corrected his raw pressure values upward in an effort to account for increased pressure in the belt apparatus caused by heating. Apparently, the actual pressure rise attributable to increased temperature is small [247] or is offset by other factors (perhaps polymorphic and/or chemical changes in pyrophyllite parts). Because Bundy's raw data (corrected to the current pressure scale) correspond well with that of other workers, it will be used here in favor of his corrected values. The melting curve shown in figure 17 is an average of available data to 60 kbar. Above 60 kbar the melting curve is entirely attributable to Bundy.

5.3. Germanium

In 1962, the first reports [275, 293] of a RT first-order phase transition in Ge were published. Shortly thereafter Jamieson [194] verified that a transition occurred and determined the crystal structure of a phase stable only at high pressure, and Bundy and Kasper [92, 218] identified and determined the structure of a different phase that was metastable at RTP. The existence of this metastable phase has been confirmed by Vereshchagin,

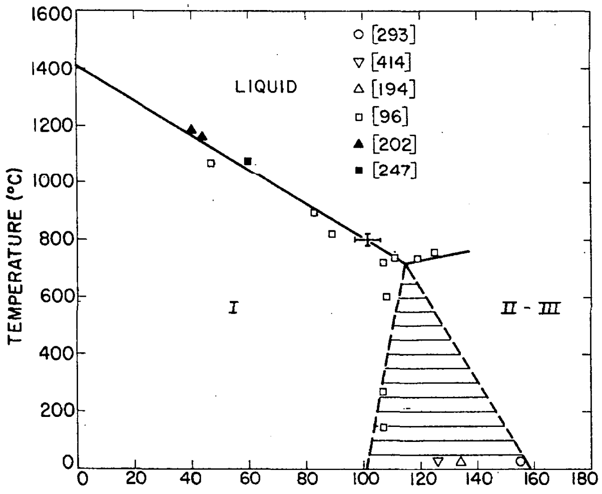

FIGURE 17. Phase diagram for silicon.

et al. [396]. The phase diagram was then determined independently at General Electric [96] and at Penn State [30, 31] with dramatically different results. By employing an experimental method considerably different than the one used at General Electric, the Penn State group identified at least one, and possibly two, further pressure induced phases of Ge. Finally, Bundy, using a more refined version of the General Electric experimental technique [102], has redetermined the R(p) data and found evidence for two phase transitions at RT (rather than just one as reported earlier).

High pressure work on Ge is plagued with the problems of sluggish phase transitions and possible metastable phases. It is not known with a great degree of certainty where the solid-solid phase boundaries lie or for sure which of the pressure induced phases have thermodynamically stable regions of existence. In 1966, Bundy, Jamieson, and Rustum Roy (of Penn State) discussed the conflicting conclusions concerning the Ge phase diagram [103] and tentatively agreed upon the solid-solid boundaries shown in figure 18. There are still many unanswered questions, however, and final conclusions must await further experiments (perhaps *in situ* X-ray work involving long term pressure runs).

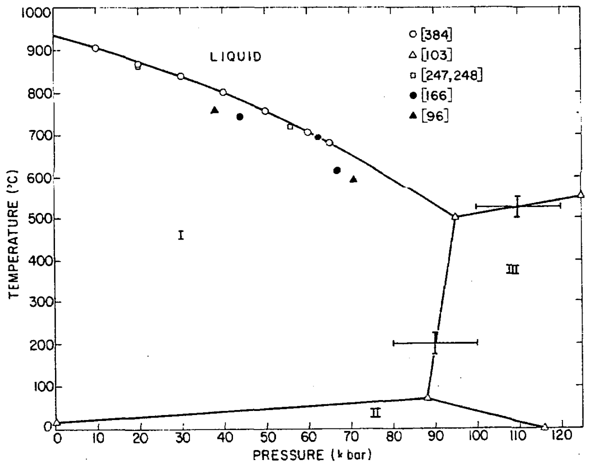

FIGURE 18. Phase diagram for germanium.

The melting curve has been determined several times [96, 166, 202, 247, 248, 384]. The most recent determination [384] appears to be the most accurate for the following reasons: (1) pressure was determined directly using methods which lead to the accepted best values for pressure fixed points, (2) a large number of data were taken (about 70 points to 65 kbar) and (3) reasonable corrections were made for the effect of pressure on thermocouple readings. Appropriate corrections to the other melting curve data tend to move them toward the Vaidya [384] curve. Because of this and because of the difficulty of making good quantitative corrections to the earlier data, the Vaidya curve is accepted as it stands. Unfortunately, Vaidya, et al. [384] made measurements only to 65 kbar. To give an idea of the melting curve beyond that point, Bundy's [96] data (corrected to coincide with Vaidya, et al. [384] up to 65 kbar) were used. This melting curve is shown in figure 18.

5.4. Tin

The Sn(I–III) transition[4] has been investigated several times [24, 25, 26, 121, 202, 211, 227, 269, 289, 291, 341, 347, 360]. The RT transition pressure is often used as a pressure fixed point and this accounts for the amount of study done on this transition. Transition pressures as determined vary from 113–115 kbar [341] to 92 ± 3 kbar [26, 211]. Correcting the pressures to correspond with the currently accepted fixed point values for Bi, Tl, Cs and Ba [128] and with Drickamer's [131] new value for Fe(I–IV), the Sn(I–III) transition pressures all [26, 121, 211, 289, 341, 347, 360] fall in the range 93–95 kbar. If Sn(I–III) is to be employed as a fixed point for pressure calibration purposes, the value 94 ± 4 kbar should be used.

Solid-solid transitions above RT have been investigated three times in two laboratories [24–26, 202, 227, 291]. The data of two of these investigations [202, 227, 291] do not extrapolate to the 94 kbar RT value and so have been discarded. The phase boundary shown in figure 19 is from the latest report by Barnett, et al. [26].

Below 13 °C at RP, Sn(I) transforms slowly to Sn(II). This transformation has been studied twice at high pressures [221, 303] with good agreement. The transition exhibits large hysteresis, so the determined position of the equilibrium phase boundary is somewhat uncertain.

The melting curve has been reported on a number of occasions [16, 24–26, 105, 110, 132, 202, 212, 227, 272, 291, 379]. Data from different sources agree fairly well

---

[4] Note that Sn(III) in this report is frequently designated Sn(II) in other literature.

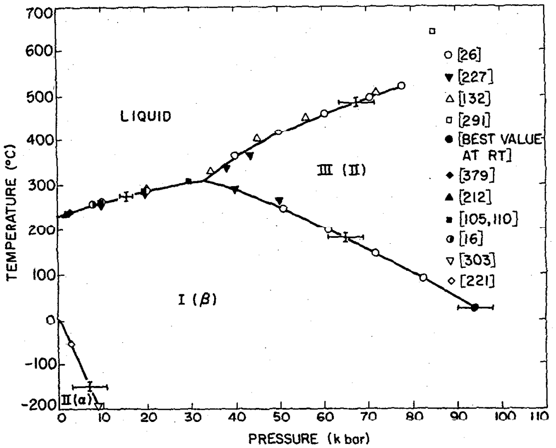

FIGURE 19. Phase diagram for tin.

on the triple point. In determining the Sn(I) melting curve shown in figure 19 only the data of McDaniel, et al. [272] have been discarded (because of an apparent error in their graph) but other data from the same laboratory [16] are used. The triple point was determined by averaging the four reported values [26, 132, 227, 291], after corrections to the current pressure scale were made. Data on the melting of Sn(III) are in fair agreement (after corrections to the average triple point) except for that of Millett [291]. His Sn(III) melting data are unreliable (the melting curve is a straight line with temperatures about 90 °C above other data at 80 kbar) because of the method of pressure calibration used. The remaining data [26, 132, 227] are somewhat uncertain because of large standard deviations in the temperature [132], uncertainty in the effect of temperature on pressure [26, 132], and underestimation of friction losses [227]. The average melting curve shown in figure 19 is therefore assigned a high degree of uncertainty.

The crystal structure of Sn(III) has been determined by Barnett, et al. [24–26] to be bct. This structure has been confirmed by Martin and Smith [269]. Crystallographic data are shown in table 3.

5.5. Lead

The Pb(I–II) transition was first reported by Balchan and Drickamer [20] to occur at 161 kbar at RT. This figure was used for several years as a pressure calibration point. Subsequent work with X-ray methods [131, 265, 377] has indicated that this transition occurs nearer 130 ± 10 kbar. Recent, more carefully executed, experiments on R(p) have also led to the conclusion that the 161 kbar figure is high [290, 398, 401]. An average of the latest R(p) and X-ray data on Pb(I–II) gives a value of 134 ± 4 kbar for the transition at RT. It appears that this transition can be very easily overshot by increasing the pressure too rapidly. Indications are that rates of pressure increase exceeding 1 kbar/hour may result in overpressurization [265, 290].

The melting curve has been determined several times [4, 22, 105, 114, 180, 212, 227, 272, 291] with good agreement to about 25 kbar. Above 25 kbar there is considerable scatter, the total spread at 55 kbar being about 80 °C. Corrections for pressure effect on thermocouples and temperature effect on pressure calibration would tend to bring the extreme sets of data into better agreement. The very recent work of Akella, et al. [4] employed these corrections and has resulted in a set of data between the extremes mentioned above. For this reason the melting curve shown in figure 20 is drawn according to the data of Akella, et al. [4]. Representative data from the other sources are also shown.

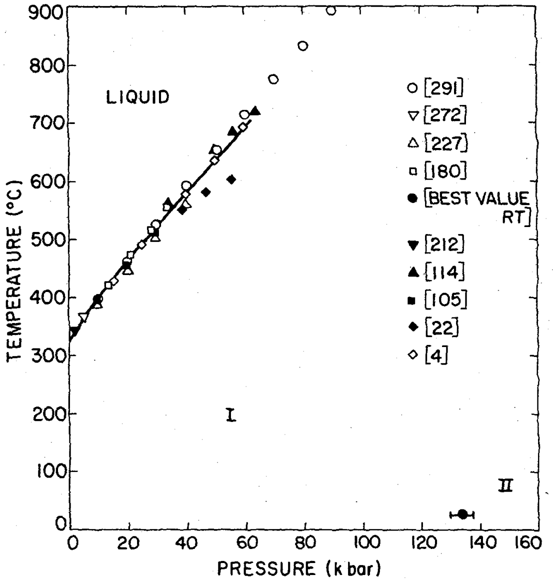

FIGURE 20. Phase diagram for lead.

In 1963 Klement [233] suggested that Pb(II) has the hcp structure. This prediction was later confirmed by the X-ray data of Takahashi, et al. [377]. Crystallographic information is contained in table 3.

6. Group V A

6.1. Phosphorus

This element exhibits some very interesting properties that make it impossible at present to arrive at a meaningful phase diagram. There are three modifications of P indentifiable by differences in color—white (or yellow), red (or violet) and black. There are two types of white P, several red modifications (depending on method of preparation), and four types of black P (two observable only at high pressure).

Phosphorus was first extensively investigated at high pressure by Bridgman [50, 51, 53, 59–62, 73]. He determined the white (I)-white (II) boundary to about 12 kbar [50, 51] and performed the first synthesis [50] of black P [from white (I) at about 12 kbar and 200 °C]. He later prepared black P at RT from white (II) at about *34* kbar [59] and from red at *38–47* kbar [60, 62] with shear and at *70–80* kbar [73] without shear.

The white (I)-white (II) transition has also been investigated by Gabrysh, et al. [150]. They reported the transition pressure only at 21 °C. Their value is in fair agreement with the data of Bridgman.

The white-black transition has been investigated by two other workers [189, 306] besides Bridgman. Jacobs [189] discovered that an amorphous black P could be prepared by stopping the white-black reaction before it had gone to completion. Patz [306] investigated the variation in white-black transition temperature with pressure and reported a transition temperature of about 125 °C at 34 kbar—the same pressure where Bridgman obtained white-black at RT. The initial sluggishness of this transition could account for the discrepancy, i.e. Patz may have heated to the point where white-black occurs relatively rapidly before the RT transition could occur. It is important to note, however, that the transition does not always occur at the same pressure at RT. Suchan, et al. [368] were able to measure the effect of pressure on the absorption edge of white P to about 50 kbar on one run (other runs terminated with the formation of black P at about 30 kbar). There has been no report of a white-red transition at high pressure.

Reports of the red-black transition at RT show remarkable differences in the transition pressure. Harris, et al. [176] show R(p) data indicating the transition at 60 kbar, and they comment that it can be made to occur at pressures as low as 20 kbar. Vereshchagin and Zubova [391] place the transition pressure at about 44 kbar, and Wittig and Matthias [419] place it in the vicinity of 110 kbar. Bridgman's studies [60, 62, 73] mentioned above show the transition at *37–80* kbar depending on the amount of shear. The facts that the properties of red P vary with the method of preparation and that the red-black transition is very sensitive to the conditions of pressure application (particularly the presence of shearing forces) probably account for the wide (20–110 kbar) variation in transition pressure.

Papers by Long, et al. [260] and by Sorgato, et al. [338] (both from the same laboratory) report the variation of the red-black transition with temperature. They report temperature and pressure conditions for which the transition occurs in about 10 minutes. An extrapolation of their data (maximum pressure, about 60 kbar) meets satisfactorily with Bridgman's *70–80* kbar RT transition. They collected data for this transition at pressures as low as 3 kbar (value read from their graph) at which point the transition temperature was about 540 °C. Butuzov, et al. [108, 110], on the other hand, report a reversible red-red transition at about 4 kbar[5] and 600 °C, indicating that the irreversible red-black transition had not occurred under those conditions. Bridgman [52] reports that at pressures certainly below 1 kbar (actual pressure unknown) red P melts without conversion to black P at a temperature below the melting point of black P.

Experiments with black P indicate reversible transitions at about *53* kbar [73] and about *95* kbar [195]. Superconductivity measurements by Berman and Brandt [36] indicate that there may be further high pressure modifications in the 170–260 kbar region, but the evidence is very sketchy and inconclusive at present. Jamieson [195] has reported the crystal structures of the two high pressures phases of black P. Data are shown in table 3.

The melting curve of black P has been determined to about 17 kbar [260, 267]. Butuzov, et al. [108, 110] have also determined the melting curve, but they report only one point. It is about 25 °C below (at about 17 kbar) the melting curve mentioned above. The melting curve may not represent a solid-liquid *equilibrium* boundary. Bridgman [51] has reported that red and black P both melt to the same type liquid but that solidification of the melt results in a glassy mass with a chocolate-brown color. The density of this material is considerably less than that of black P, indicating that some sort of rearrangement occurred upon melting or upon refreezing.

The information shown in figures 21 and 22 is a summary of the reported data discussed in the preceed-

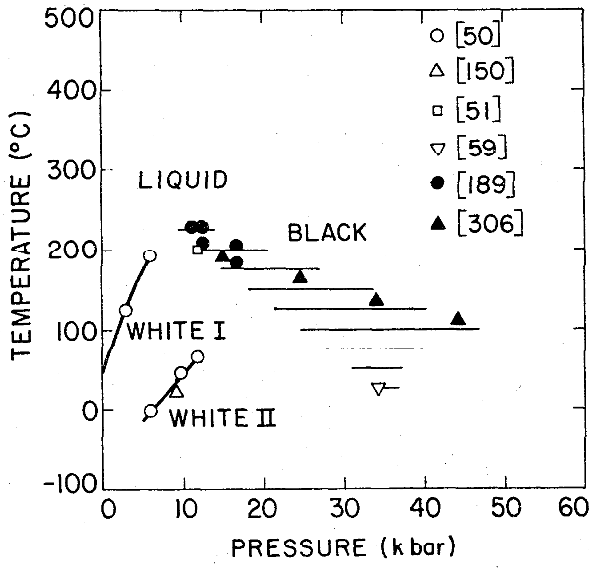

FIGURE 21. Partial phase diagram for phosphorus.

---

[5] The English translation of Butuzov's work [110] incorrectly gives this pressure as about 39 kbar (40,000 kg/cm²).

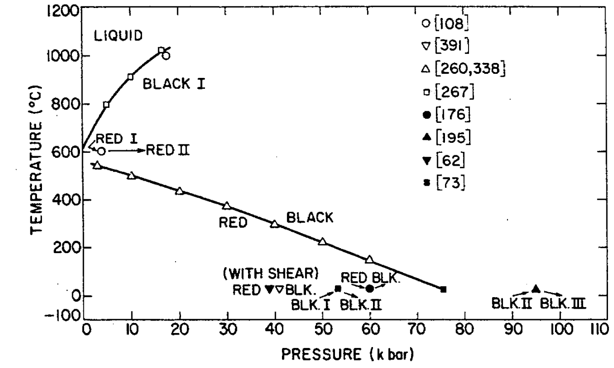

FIGURE 22. Partial phase diagram for phosphorus.

ing paragraphs. These figures should not be considered as phase diagrams, and no claim is made that any of the lines shown are equilibrium phase boundaries.

6.2. Arsenic

Investigations of the RT variation of volume [73] and resistance [75, 390, 420] of As with pressure to *85* kbar and *160* kbar respectively have failed to reveal any suggestion of a first order phase transition. Superconductivity measurements at pressures to *160* kbar [420] failed to reveal superconductivity at temperatures down to 1.3 K, but superconductivity was found [37] at 0.2 K for pressures as low as 85–125 kbar. These superconductivity measurements indicated that the phase transition was not complete until pressures of 120–160 kbar were reached at which point $T_c = 0.5$ K. As pressure was increased beyond 120–160 kbar, T_c decreased smoothly to a value of 0.31 K at 200–240 kbar. Duggin [133] reported that a single crystal of As compressed to 150 kbar (presumably at RT) was partially converted to a new tetragonal polymorph that was retained at RP. This is apparently the same phase that was responsible for the superconducting transitions mentioned above. Crystallographic data are given in table 3.

The melting curve has been investigated in two instances [113, 234] with fair agreement. Data from the the two reports do not overlap but appear to join satisfactorily.

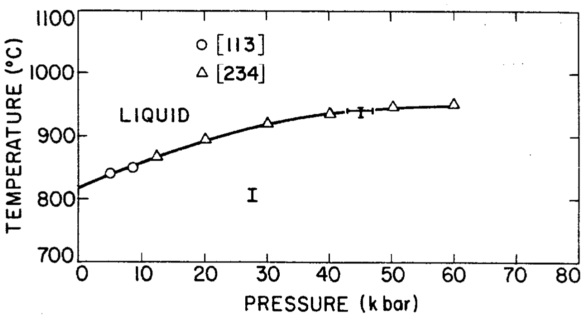

FIGURE 23. Phase diagram for arsenic.

6.3. Antimony

Two RT phase transitions have been induced in Sb by the application of pressure [60, 69, 70, 214, 217, 219, 239, 240, 390, 395, 412]. X-ray measurements taken at high pressure [240] show that these transitions occur over a wide pressure range. This probably accounts (in part at least) for the variation in reported transition pressures (*47–64* kbar and *71–82* kbar). Vereshchagin and Kabalkina [395] have suggested that Sb(I–II) is a continuous transition from hcp to sc, but further analysis [217, 239, 320] indicates that the transition is first order with a very small discontinuity. These transitions have not been studied at temperatures other than 25 °C.

Kabalkina, et al. [214] first reported the structure of Sb(II) as sc. Later reports by the same group [239, 240, 395] confirm this structure. X-ray data taken at 75 kbar and above have been variously interpreted to indicate hexagonal [214, 295], monoclinic [217, 240], and tetragonal [133] symmetry for Sb(III). The hexagonal symmetry can definitely be eliminated because it does not account for all the lines in the X-ray spectrum [217, 273]. The monoclinic interpretation results in serious differences between observed and calculated line intensities (tentative explanations for these differences have been advanced [217, 240]). The interpretation leading to tetragonal symmetry does not include any suggestion for the structure, so no comparison of intensities is possible. There is not sufficient evidence to accept either of these proposed structures without reservation. Crystallographic data are shown in table 3.

The melting curve has been reported on four occasions [107, 227, 234, 355]. The data of Butuzov, et al. [107] falls below the other's with increasing pressure and is about 20 °C low at 30 kbar. The L–I–II triple point reported by Stishov and Tikhomirova [355] was not observed by the others. This is reasonable since the estimated error in temperature reported by the others is sufficiently high (± 2–3 °C) that the slight dip in the melting curve resulting from L–I–II would have been smoothed over. Since the data of Butuzov, et al. [107] may be low because of sample contamination (they did not report sample purity), it has been discarded. The earlier work from Kennedy's laboratory [227] has been passed over in favor of the more recent results [234]. The melting curve shown in figure 24 is thus a combination of data from two sources [234, 355].

6.4. Bismuth

The phase changes of bismuth have been examined by a large number of investigators. This is due in part to the fact that the Bi(I–II) and Bi(III–V) transitions are widely used as pressure calibration points. A critical analysis of the literature values for these transition pressures at RT has been published elsewhere [128] and will not be dealt with further here.

For the purposes of analysis the Bi phase diagram will be divided into three regions. The first region includes that part above 0 °C and below 30 kbar, the second, the part above 0 °C and above 30 kbar and the third, the part below 0 °C.

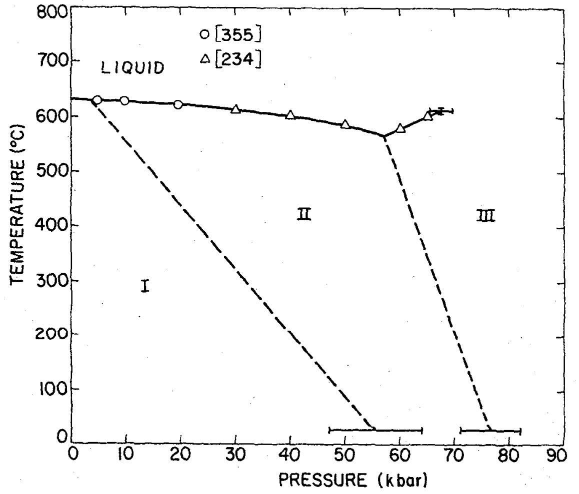

FIGURE 24. Phase diagram for antimony.

The triple points in the first region (L–I–II, L–II–IV, II–III–IV) have been specified by seven different investigators [61, 86, 104, 109, 110, 234, 305, 317, 382]. Of these seven only the data of Bundy [86] were discarded due to the fact that four features of his phase diagram appear to be incorrect in comparison with other work [Bi(I) melting curve concave up; Bi(II) melting curve has substantial negative slope; Bi(III–IV) phase line terminates on the liquidus; Bi(III–IV) phase line shows a cusp]. The remaining data have been averaged and are shown in figure 25.

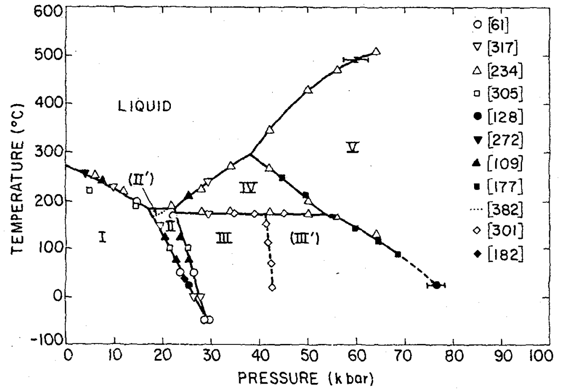

FIGURE 25. Phase diagram for bismuth.

Tikhomirova, et al. [382] have reported a phase boundary not observed by other workers. The heat change associated with the transition of this boundary is reported as roughly equivalent to that of the Bi(III–IV) transition. It would be interesting to know why the other workers have not reported this new transition even though Bi(III–IV) was apparently detected without difficulty. Acceptance of this new boundary must be tentative until more evidence has been collected. Consequently, the boundary is shown as a dotted line in figure 25. The data of Tikhomirova, et al. have been adjusted such that their triple points coincide with the average values of the triple points discussed in the previous paragraph.

Data analysis for the second region is complicated by the fact that early determinations of pressures above 25–30 kbar have now been shown to be incorrect [128]. Because of the difficulty encountered in accurately correcting the pressures of earlier work and because of the fine work recently done by Haygarth [177] and by Klement [234], work done before 1963 on the second region has not been considered. The second region triple points taken from the data of Haygarth [177] and Klement [234] are shown in figure 25.

Considerable controversy has arisen over the existence of a RT phase transformation at 41–44 kbar. This transition has been observed by some investigators [60, 185, 241, 300–302, 428], and specifically stated as unobserved by others [75, 86, 112, 157, 234, 244]. The recent work on the variation of resistance [300, 301] and volume [302] with pressure by Nichols and the superconductivity studies [185] reported by Il'ina and Itskevich lend strong support to the existence of this transition. One must wonder, however, why the 1 percent volume change [302] reported to be associated with this transition was not detected by the very recent work of Cedergren and Backstrom [112], who diligently searched (with equipment capable of detecting 0.1% volume change) for this specific transition and found nothing from Bi(II–III) to 55 kbar.

It appears fairly certain that something occurs in Bi in the 41–44 kbar region under certain circumstances, but the lack of reproducibility from laboratory to laboratory leads one to suspect that whatever occurs may not be a first order phase transition (see discussion in [244]). Further evidence is necessary (perhaps X-ray or neutron diffraction data) before this transition can be accepted unequivocally. For this reason the proposed Bi(III–III') phase boundary [301] is shown as a broken line in figure 25.

Another possible transition first reported by Bridgman [70] at about 60 kbar has recently been reported again on the strength of the superconductivity measurements of Il'ina and Itskevich [185]. In the interum period this transition was observed by Kossowsky [241] and by Zeitlin and Brayman [428], but other reports [75, 86, 157, 234, 305] indicate that the transition was not found. As with the reported transition discussed in the previous paragraph, this transition must be regarded with a critical eye until further evidence is in.

Work in the third region is complicated by a lengthening transition time attributable to low temperatures and by the convergence of the Bi(I–II) and Bi(II–III) phase boundaries. Because of these difficulties, resolution of the Bi(I–II) and Bi(II–III) transitions is often not observed. Of the six studies [47, 48, 120, 183, 297, 328, 388, 426] on Bi phase transitions at low temperatures, only one [297, 426] gives an indication that the Bi(II–III) transition occurs below −110 °C. Those who have not observed this transition believe that the Bi(II–III) solidus meets the Bi(I–II) solidus at about −110 °C [47, 48, 120, 183], or that the Bi(II–III) solidus ends in a critical point [328]. A new low temperature polymorph reported by Il'ina, et al. [183] has not been observed by subsequent investigators [120, 181, 297, 328, 388, 426] and is therefore assumed not to exist.

Bridgman [61] reports a I–II–III triple point by extrapolation from higher temperatures at about 32 kbar and −110 °C. Extrapolation of the data of Roux, et al. [328] shows no I–II–III triple point above 0 K. Extrapolation of the Bi(I–II) and Bi(II–III) phase lines in figure 25 gives a triple point of 29 kbar and −43 °C. By varying the L–I–II and L–II–III triple points within the limits of two standard deviations and considering a probable error of about 0.2 kbar [225] in the RT value for the Bi(II–III) transition, one can vary the extrapolated I–II–III triple point from finite values (such as quoted above) to below 0 K. For this reason and because of the large uncertainty in transition pressures at temperatures in the third region, this portion of the phase diagram is considered too uncertain for any definite conclusions about the positions of the phase lines, the value of the I–II–III triple point (if it exists), or the existence of a critical point. Certainly the existence of the triple point is called seriously into question by the work of Mori, et al., [297, 426] and the possibility of a critical point is far from proved by Roux, et al. [328].

The crystal structures of the high pressure phases of Bi have been very difficult to investigate. The structures appear to be fairly complex [with the exception of Bi(V)] and X-ray data are generally poor because of experimental difficulties, particularly high sample absorption. The structure of Bi(II) has been determined from neutron diffraction data [82, 83] to be monoclinic with 4 atoms per unit cell. Neutron diffraction [83] and X-ray [217] data have been taken on Bi(III), but the X-ray spectrum (only 4 lines were recorded) does not agree with the much more detailed neutron spectrum and is probably in error. The neutron spectrum could not be satisfactorily indexed by its originators, but recently Duggin [133] has reported indexing their data on the basis of a tetragonal unit cell. In view of the lack of specific structural data (so that observed and calculated neutron intensities could be compared) and the lack of good agreement between calculated and observed *d*-values [Duggin's suggested unit cell results in deviation of $\geqslant 1\%$ for about 10% of the lines with maximum deviations of 1.6% whereas the correct indexing of Bi(II) results in a maximum deviation of $\leqslant 0.5\%$] it seems unlikely that this tetragonal unit cell could be correct. Consequently, the structure and symmetry of Bi(III) are still unknown. X-ray data recently taken [331] on Bi(V) indicate that it is bcc. Crystallographic data are shown in table 3.

7. Group VI A (The Chalcogens)

7.1. Sulfur

This element, like P, is characterized by sluggish phase transformations and an apparent profusion of polymorphic forms with complex structures. In addition, liquid S may exist in at least four different states (distinguished by the degree of polymerization) depending on pressure and temperature conditions [402]. Because of these interesting properties it has been very difficult for those investigating the *P T* behavior of S to interpret their data properly or, for that matter, to even obtain data that can realiably be duplicated in other laboratories. The result is a body of literature that is spectacular in its lack of agreement.

Bridgman reported the variation in volume [63, 65, 66, 71] and shear strength [60] with pressure. Although in two instances [60, 63] there was some indication that a phase change had occurred, in no case was the evidence great enough for Bridgman to report the existence of a new phase. In addition, optical studies in Drickamer's laboratory [19, 336] on the pressure variation of the absorption edge gave no indication of a phase transition to pressures exceeding 100 kbar. Later reports from other laboratories [307, 308, 403] interpret at least one definite anomally in the compression curve as a first order phase transition with lesser indications [403] of three more.

X-ray spectra taken of S after it had been exposed to high pressure and temperature indicate the existence of five pressure-induced forms of S. The first of these was reported by Bridgman [68] from RT runs to over 300 kbar. The X-ray spectrum of the pressurized sample consisted only of a few broad lines which did not agree with the spectrum of the original material. A later run resulted in material with no observable X-ray spectrum. Data from the post-pressure X-ray were not published, and this work has apparently not been duplicated since.

The next report of a pressure-induced phase of S was made by Baak [15] in 1965. He reported the preparation of a cubic form with 104 atoms in the unit cell. Later investigators were unable to duplicate his work [151, 335], although Vezzoli and Dachille [405] did manage to obtain some product that had an X-ray pattern similar to that reported by Baak. A comparison of the *d*-spacings reported by Baak with those calculated from the lattice constant indicates that the X-ray spectrum has been improperly indexed and that a cubic phase does not exist.

The final three phases were first reported by Geller [151] and (one of them) by Sclar, et al. [335]. Geller's phases I and III are apparently closely related, but little is known about either. Geller has suggested that phase I may be the same as the ω-S prepared by hydrolysis of S_2Cl_2 at 1 bar. Roof [325], on the basis of a computer analysis of Geller's data, has suggested that phase I and III each have monoclinic symmetry, but he could not assign a unique space group. Geller's phase II has been studied extensively in Geller's laboratory [129, 152, 153, 251] and elsewhere [335, 403, 405, 406, 411]. X-ray spectra of this phase taken in different laboratories [151, 335, 406] agree well, but the reported physical properties vary considerably. It apparently has monoclinic symmetry and is composed of fibers of right- and left-handed helices. Some investigators report that it slowly reverts to normal orthorhombic S at RTP [335] whereas others indicate that it does not [251, 406]. There is strong evidence [129, 151, 153] that this phase II S is the same as fiberous ψ-S prepared at atmospheric pressure.

The most extensive investigation of the $P-T$ behavior of S has been made by Vezzoli, et al. [402–406]. Following examination of data from over 700 runs, they reported a diagram of "stability fields" which designates the $P-T$ regions in which twelve different phases of solid S exist [403, 405]. The fact that some of these "stability field" boundaries join the melting curve at apparent triple points may lead some to interpret them as equilibrium phase boundaries. In view of the difficulties discussed in the preceeding paragraphs, plus disagreements among different investigators concerning the position and/or existence of liquid-solid-solid triple points (see below), this would be extremely hazardous. The evidence indicates that, due to the nature of S, phase boundaries between thermodynamically stable phases will be broad and ill defined. In our present state of knowledge such phase boundaries are not discernable.

The melting curve has been reported a number of times [15, 33, 125, 307, 308, 326, 327, 369, 371, 372, 380, 402, 404, 411] with varying results. Two of these reported melting curves [15, 33] are actually attributable to some kind of solid-solid transition and so have been discarded. Others [125, 307, 326, 369, 371] will not be considered because they have been updated or republished in later reports from the same laboratories.

The melting curve and orthorhombic-monoclinic phase transition have been investigated at relatively low pressures [380, 402]. Even at these low pressures (to 3 kbar) the lack of agreement in the two reports is considerable. At about 0.8 kbar the melting curves are more than 10 °C apart. The more recent data [402] appear to be much too high in temperature to agree well with data extrapolated from higher pressures. In addition, the expanded graph (maximum pressure of 1 kbar) in which these data are reported [402] does not appear to agree with the solid-liquid boundary at 1 kbar in the more compact graph (maximum pressure exceeding 30 kbar) in the same report and in another report by the same authors [403]. It thus appears that the expanded graph may have been drawn incorrectly. In any case, Tammann's [380] data appear to be the more reliable in the pressure region to about 3 kbar.

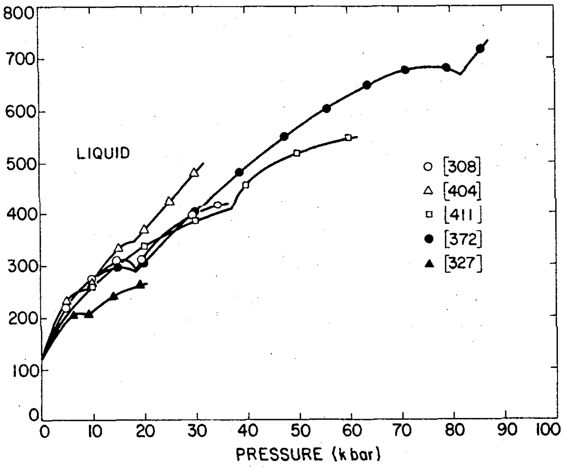

FIGURE 26. Melting curves for sulfur.

The melting curves beyond 3 kbar [308, 327, 372, 404, 411] are shown in figure 26. Particularly noteworthy is the difference in positions of triple points. Apparently the behavior of S under increased pressure and temperature conditions is unusually sensitive to the environment (shear forces, heating rate) and the type of starting material (polymorphic form of S used, different type and amounts of impurities). Consequently it is not possible at present to suggest a definite best melting curve for this element.

7.2. Selenium

Early work by Bridgman [69, 70] on amorphous Se showed breaks in the V(p) curve suggesting that some sort of permanent change had occurred. Later X-ray studies by McCann and Cartz [271] showed that amorphous Se begins to crystallize by about 60 kbar. They suggest that this crystallization was the cause of the break in V(p) observed by Bridgman.

Later work by Bridgman [75] on single crystals of Se (crystalline form not specified) showed a discontinuity in R(p) at about *52* kbar. This discontinuity has not been confirmed by later work [21, 296a, 323, 423], but lack of details concerning the specific crystalline form of the starting material makes any definite conclusion impossible.

Studies employing resistance [21, 296a, 323, 423] and superconductivity [418] methods indicate that there is a sluggish phase transition in amorphous Se at about *95–115* kbar. The very recent work of Moodenbaugh, et al. [296a] has shown that this transition does not occur in hexagonal Se, but that a similar transition does occur in monoclinic Se. The transition is to a metallic, superconducting phase which decays slowly (in 100–240 hours) at pressure to a non-metallic, non-superconducting phase believed to be hexagonal Se. Post-pressure

X-ray patterns show that amorphous and monoclinic Se become hexagonal after exposure to pressures exceeding 95–115 kbar. Vereshchagin, et al. [393] did not observe this transition in their experiments on an unspecified form of Se. Their results are consistant with others' if their Se was in the hexagonal form.

X-ray studies by McCann and Cartz [271] have indicated that amorphous and hexagonal Se both undergo a transition in the vicinity of 140 ± 10 kbar to a new phase that is metastable at RTP. They report the *d*-spacings for this new phase but were unable to determine a structure consistent with the data. They suggested that their new phase was identical to the metallic, superconducting phase discussed in the preceeding paragraph. Data published subsequently [296a, 423] showed this not to be true and further revealed the instability of the high-pressure metallic, superconducting form.

X-ray exposure times required by the high-pressure apparatus used by McCann and Cartz [271] were on the order of 100 hours. This could explain why they did not observe a structure that could be attributed to the unstable metallic, superconducting form. Moodenbaugh, et al. [296a] reported that they did not observe the metastable phase of McCann and Cartz even to pressures of 160 kbar. However, analysis of their method of pressure calibration indicates that they probably did not attain pressures substantially above 130 kbar. This, of course, would account for their lack of success in reproducing the data of McCann and Cartz.

The melting curve has been investigated on several occasions [5, 16, 125, 236, 298, 308, 370, 383] with fair agreement. The data of Nasledov and Kozyrev [298] give a melting curve that is concave toward the temperature axis and is about 8 °C below the data of Babb [16] at 3.5 kbar. It is felt that these deviations are attributable to their unusual method of obtaining melting point data. Consequently, their data have been discarded. The melting curve is shown in figure 27.

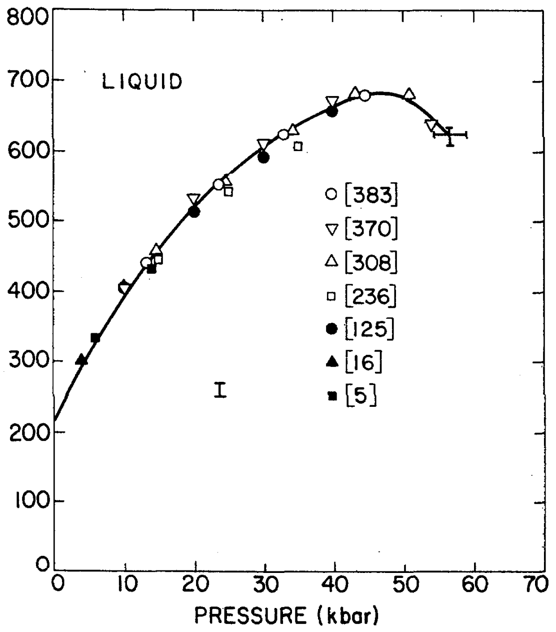

FIGURE 27. Phase diagram for selenium.

7.3. Tellurium

There are two well established solid-solid phase transitions in Te. The first of these occurs at about 42 kbar at RT and has been observed by resistance [22, 41, 75, 393], volume [61, 225, 386], Mössbauer [38], thermal [41, 356], superconductivity [39, 187, 270], and X-ray [198, 215] methods. The second is found in the vicinity of 63 kbar at RT and has also been detected by resistance [22, 41], volume [61], Mössbauer [38], thermal [356], superconductivity [39, 187] and X-ray [198] methods, although some reports indicate that resistance [41, 393] and X-ray [215] studies failed to detect this transition at RT.

Three questionable transitions have also been reported. Early studies by Bridgman [61] indicated a very small volume transition preceeding the 40 kbar phase change. Indications of this transition were not seen by later workers [225] and Bridgman himself did not mention it in later [69, 70] publications. Kabalkina, et al. [215] have reported an apparent phase change at 15–20 kbar and RT. They interpreted their X-ray data to indicate a subtle hexagonal (Se-type) to hexagonal (As-type) transition with no volume change. Stishov and Tikhomirova [356] have reported a very slight (on the order of 0.1–0.2 °C) dip in the melting curve at 14.4 kbar and 467.0 °C which they interpret as the triple point associated with the transition reported by Kabalkina, et al. This transition has not been found by resistance or thermal methods and could not be detected, even with careful searching, by Jamieson and McWhan in their X-ray studies [198]. Furthermore, the interpretation of a 0.1–0.2 °C dip in the melting curve as evidence of a triple point is extremely hazardous, even considering the excellent reproducibility of temperatures (± 0.15 °C) reported for the study. Stishov and Tikhomirova [356] have also reported a new solid-solid transition on the basis of a single data point near their Te(III–IV) [Te(II–III) in figure 28] phase boundary. None of these transitions has been adequately established and all are assumed not to exist.

Finally, suggestions of higher-pressure transitions in Te have been made on the basis of superconductivity data [39, 187]. At about *70* kbar there is a discontinuity in the variation of the superconducting transition temperature (T_c) with pressure. This has been interpreted as an indication of a Te(III–IV) transition. Discontinuous changes in the slope of the T_c versus pressure curve at high pressures (*92* and *143* kbar) are suggestive [39] of yet more Te phase transitions. Further study of these transitions is necessary before definite

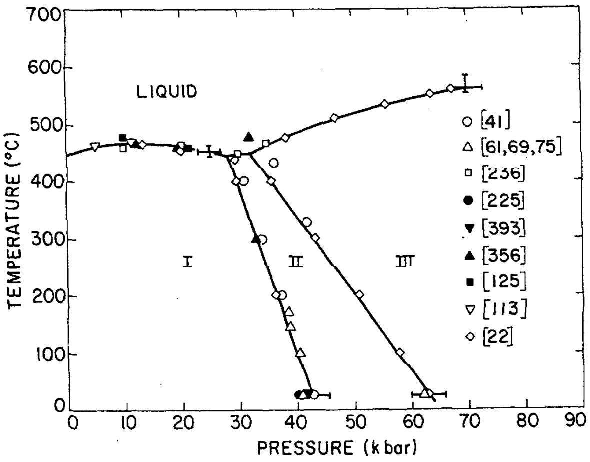

FIGURE 28. Phase diagram for tellurium.

conclusions can be drawn, particularly with regard to the possible 92 and 143 kbar transitions.

The Te(I–II) boundary above RT has been investigated three times [22, 61, 356] with good agreement. The Te(II–III) boundary has likewise been investigated three times [22, 41, 356] above RT, but the agreement is not as good. Stishov and Tikhomirova [356] illustrate this phase boundary with such large curvature that it terminates on the Te(I–II) boundary rather than on the melting curve. Since solid-solid phase boundaries tend to have little (if any) curvature and since the other two investigations [22, 41] found Te(II–III) terminating on the liquids, the data of Stishov and Tikhomirova have been discarded.

The melting curve has been investigated a number of times with varying results [22, 41, 113, 125, 227, 236, 356, 357, 381]. Some of these [41, 227, 381] have been superseded by later reports from the same laboratory and will not be considered further. The rest of the data are in good agreement with the exception of that reported by Deaton and Blum [125] which is in fair agreement. Klement, et al. [236] have made a study of the effect of sample container on the melting curve. They pointed out that none of the containers (Fe, Ta, Pt, C) proved entirely satisfactory. The region of data scatter they show roughly includes the data points of those reports considered here with the exception of the one by Deaton and Blum [125].

X-ray data [198] indicate that Te(III) has a β-Po-type structure. Data [198, 215] taken on Te(II) could not be indexed by either of the groups reporting the data. Vezzoli [407] has proposed an indexing based on the data of Jamieson and McWhan [198] which suggests that Te(II) has a distorted white-Sn-type structure. Upon comparison of the observed *d*-values with those calculated on the basis of Vezzoli's proposed structure, one finds differences of up to 5 percent. Since these differences are unreasonably high [differences calculated on the basis of the correct solution of Te(III) data do not exceed 1.2%] this proposed Te(II) structure cannot be accepted.

8. Group VII A (The Halogens)

8.1. Chlorine

This element has no polymorphic changes with pressure to about 7 kbar. The melting curve has been investigated only once [17] and is shown in figure 29.

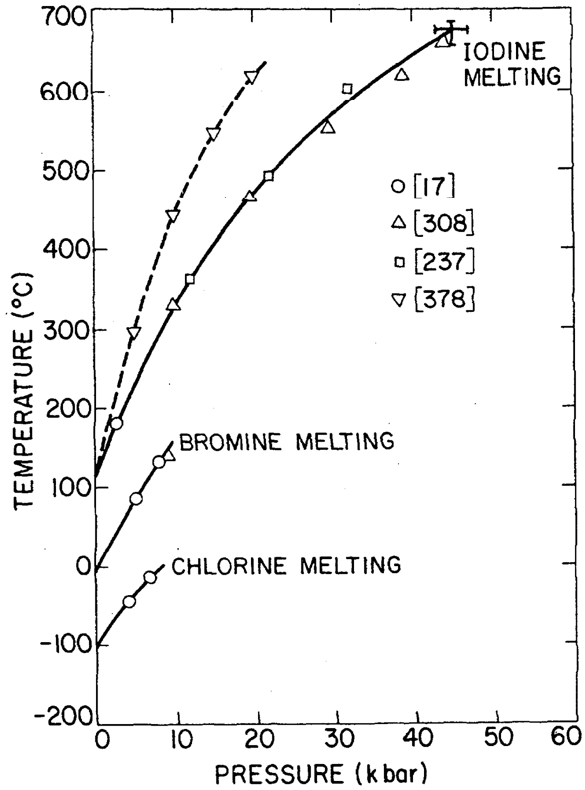

FIGURE 29. Melting curves for chlorine, bromine, and iodine.

8.2. Bromine

There are no high pressure polymorphs of Br to about 9 kbar. The melting curve has been investigated twice [17, 308], but it is very difficult to accurately compare the work since the earliest report [308] presented the data only on a very small graph. As near as can be determined from the graph, the data of Paukov, et al. [308] is somewhat below (about 5 °C lower at 8 kbar) that of Babb [17]. The melting curve shown in figure 29 is entirely attributable to Babb.

8.3. Iodine

Early V(p) studies by Bridgman [61] indicated a 2 percent volume discontinuity with large hysteresis beginning at about 20 kbar with increasing pressure and having an equilibrium value of about 13 kbar. An X-ray study reported by Kabalkina, et al. [216] gave indications of the appearance of a new phase at 10 kbar. The structure of the new phase is very similar to the original structure, the difference apparently being attributable to the rotation of the I_2 molecules. Resistance data reported by Vereshchagin and Zubova [391] could be interpreted to indicate a phase transition near 20 kbar, but the data are sparce and such an interpretation was not suggested in the report. Compressibility data taken by Grover, et al. [161] with a reported sensitivity of 0.5 percent in volume change gave no indication of a phase transition to about 40 kbar. None of the reported melting curves show evidence of a triple point to about 50 kbar. In view of the conflicting reports, the existence of this transition is questionable.

Studies using shock pressures first indicated that I may become metallic at pressures near 250 kbar [6, 171]. Resistance measurements under static pressure conditions later confirmed that the resistance becomes very low at very high static pressures [21, 176, 323, 393]. Reports from Drickamer's laboratory [263, 323] discuss the transition to the metallic state in some detail, suggesting that the transition occurs at different pressures for different crystal orientations.

The melting curve has been investigated four times [17, 237, 308, 378] with variable results. The melting data of Tamayama, et al. [378] is considerably higher than that from the other reports (about 140 °C high at 20 kbar). The other melting curves [237, 308] are in good agreement to about 20 kbar, but they diverge thereafter, showing a 35 °C difference at 30 kbar. It is not apparent why these large differences should exist, although Tamayama, et al. suggest some possible reasons. The three lower temperature curves [17, 237, 308] have been combined and are shown in figure 29. The data of Tamayama, et al. [378] are also shown.

9. Group I B

9.1. Copper

The melting curve has been reported four times [3, 119, 159, 294] with rather poor agreement. The most recent report [3] shows very little data scatter, accounts for the pressure effect on the thermocouple, and generally appears to be high quality work; but for undetermined reasons the melting curve is considerably below those reported by others. Pressure and/or temperature corrections to the earlier data would only serve to increase the difference. Because of these factors, the individual solid-liquid boundaries are each shown in figure 30 with no attempt made to arrive at a best curve. No other data are available.

9.2. Silver

Liu and Bassett [253] have studied Ag to about 300 kbar at RT by X-ray methods. They reported no phase changes. The melting curve has been investigated on four occasions [3, 119, 227, 294]. Data from Kennedy and Newton [227] are "obviously in error" according to Akella and Kennedy [3] and have therefore been discarded. The remaining reports are in poor agreement, so the curves from each are shown in figure 31 with no attempt to determine a best curve. No other data are available.

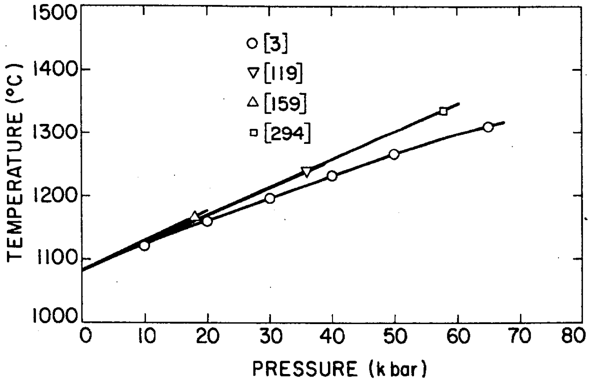

FIGURE 30. Phase diagram for copper.

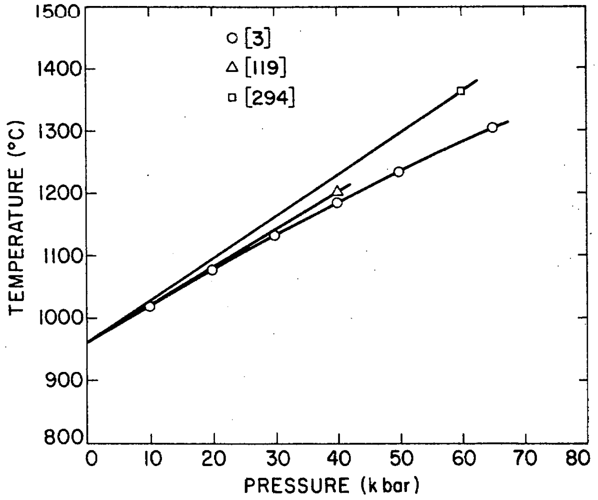

FIGURE 31. Phase diagram for silver.

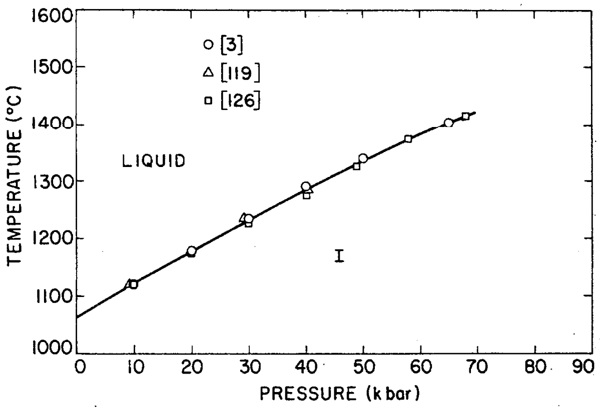

FIGURE 32. Phase diagram for gold.

9.3. Gold

The melting curve has been investigated three times [3, 119, 126, 294] with fair agreement. The data have been averaged and are shown in figure 32.

10. Group II B

10.1. Zinc

Resistance [262] and X-ray [262, 281, 311] studies at high pressure indicate that there are no phase transitions in Zn at RT to about *100* kbar and about *370* kbar, respectively. The melting curve has been studied in five laboratories [4, 107, 110, 114, 227, 247, 291]. The data to about 45 kbar are in fair to good agreement. Above 45 kbar some divergence takes place. Appropriate corrections for pressure and temperature to those data not already corrected would not tend to reduce this divergence. Thus the reason for the spread in the melting curve data for Zn remains unexplained. The best curve (shown in figure 33) is an average of the available data and must be assigned a fairly high degree of uncertainty.

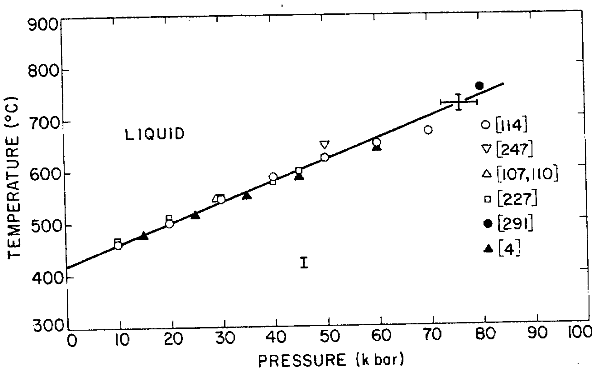

FIGURE 33. Phase diagram for zinc.

10.2. Cadmium

Early work by Bridgman [55, 61] indicated that there may be two RT polymorphic transitions below 10 kbar in Cd. Subsequent X-ray studies [190, 191, 262, 281, 311] revealed no structural change below 10 kbar, and determinations of the melting curve [107, 212, 227, 291] give no indication of a triple point. The discontinuities noted by Bridgman must therefore be attributable to some phenomena not associated with a first order phase change.

Later work in Drickamer's laboratory [262, 311] revealed a possible first order phase transition near *115* kbar. McWhan [281] found no indication of polymorphism to about *93* kbar using X-ray diffraction. No definite structural change was observed by X-ray methods in Drickamer's laboratory, but the change (possibly hcp to dhcp) is subtle and could easily be masked.

The melting curve has been investigated at four laboratories [107, 212, 227, 291] with poor agreement. Pressure and temperature corrections to the data of Kennedy and Newton [227] would tend to bring their curve closer to the results of Miller [291] and of Butuzov [107]. Also the method used by Kennedy and Newton does allow liquid Cd to be in contact with its Pt container for relatively long periods (up to 120 seconds at each of 10 pressure intervals). If this is introducing impurity into the sample it could partially account for the lower melting temperatures. The melting curve in figure 34 was determined from available data excepting that of Kennedy and Newton.

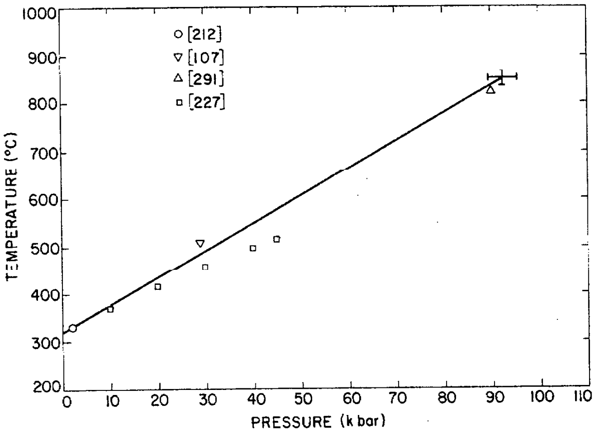

FIGURE 34. Phase diagram for cadmium.

10.3. Mercury

Bridgman [61, 75] first reported the Hg(I–II) transition and determined the phase boundary from RT down to −77° C. This transition has since been confirmed and studied in two other laboratories [235, 332, 374]. Atoji, et al. [13] have reported the crystal structure of Hg(II) as bct. The phase boundary shown in figure 35 is an average of the available data.

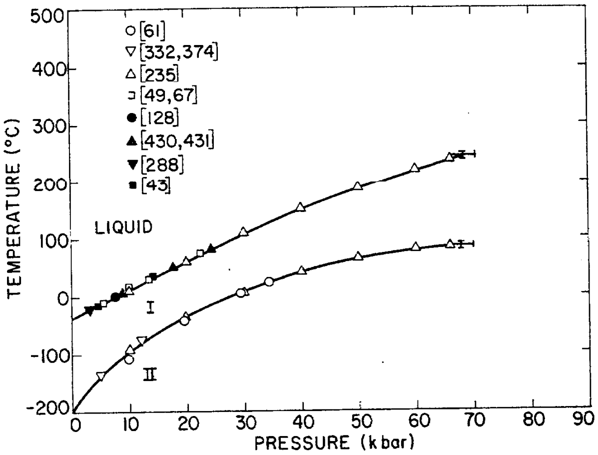

FIGURE 35. Phase diagram for mercury.

The melting curve has been determined a number of times with good agreement [43, 49, 67, 235, 288, 430, 431]. The freezing pressure at 0° C is often used as a pressure calibration point. Data for this particular point has been extensively reviewed elsewhere [128]. The melting curve in figure 35 is an average of the available data.

11. Group IV B

11.1. Titanium

At RT, Ti undergoes a phase transition at about *77* kbar [93, 201]. The high-pressure phase is metastable at RTP and has a hexagonal (distorted bcc) structure [196]. At higher temperatures Ti transforms to a bcc phase. Bundy [93] has investigated the solid-solid phase boundaries to about *125* kbar and Jayaraman, et al. [201] to about 40 kbar. The poor agreement of these two studies is in part attributable to sample contamination. The phase boundaries are presented in figure 36.

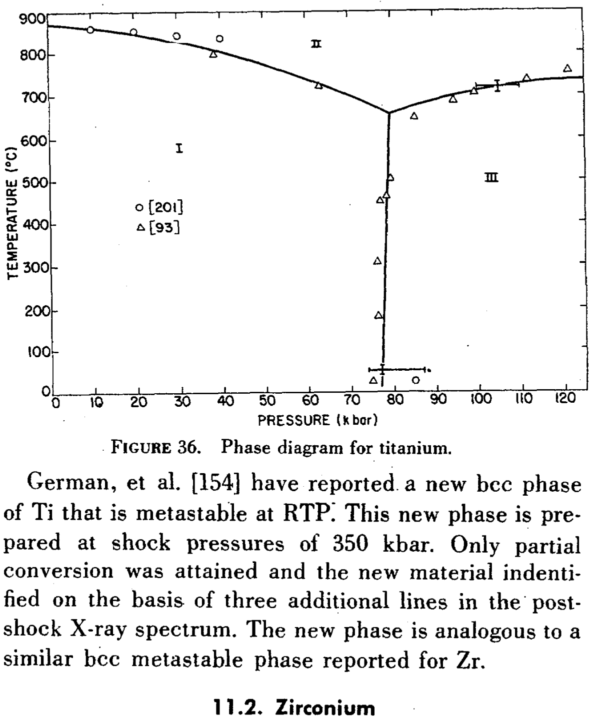

FIGURE 36. Phase diagram for titanium.

German, et al. [154] have reported a new bcc phase of Ti that is metastable at RTP. This new phase is prepared at shock pressures of 350 kbar. Only partial conversion was attained and the new material indentified on the basis of three additional lines in the post-shock X-ray spectrum. The new phase is analogous to a similar bcc metastable phase reported for Zr.

11.2. Zirconium

Resistance [75, 201] and superconductivity [134] measurements indicate a RT phase change at 50–59 kbar. This transition apparently has no detectable volume change [73]. Jamieson [196] has determined the structure of the high pressure phase and has shown that it is metastable at RTP. The phase boundaries have been investigated by Jayaraman, et al. [201], but their positions are affected by impurity from the Ta container. There is an apparent discontinuity at the triple point that cannot be explained at present. German, et al. [154] have reported a metastable (at RTP) bcc phase prepared at shock pressures of 350 kbar and up.

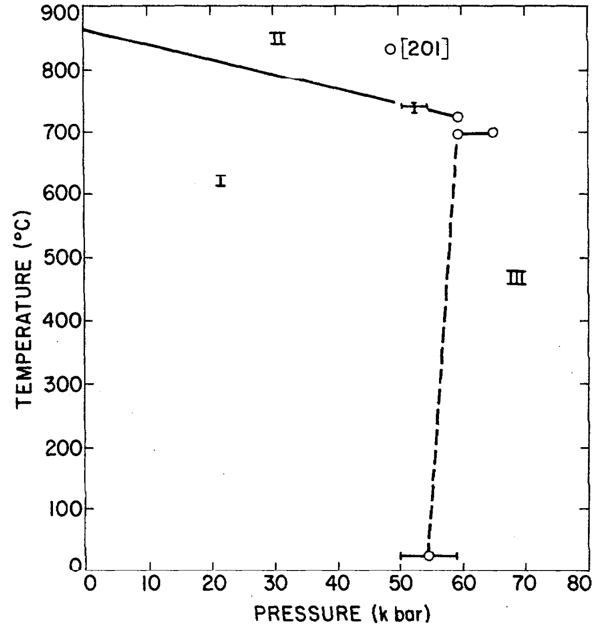

FIGURE 37. Phase diagram for zirconium.

11.3. Hafnium

X-ray [196] and resistance [76, 201] measurements show no indication of a transition at RT. Shock experiments [18] indicate a possible transition in the vicinity of 500 kbar.

12. Group V B

12.1. Tantalum

Fateeva and Vereshchagin [142] have made a rough determination of the melting curve to about *55* kbar. No other data are available.

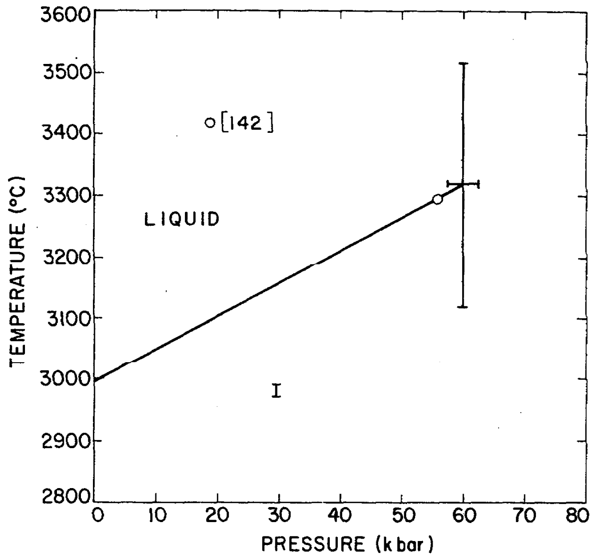

FIGURE 38. Phase diagram for tantalum.

12.2. Molybdenum

Fateeva and Vereshchagin [143] have reported a rough determination of the melting curve to about *77* kbar. No other data are available.

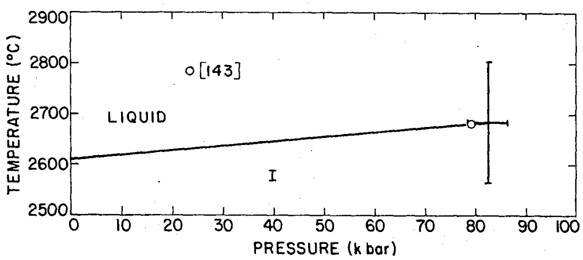

FIGURE 39. Phase diagram for molybdenum.

12.3. Tungsten

A rough determination of the melting curve has been reported for pressures to about 45 kbar [399]. No other data are available.

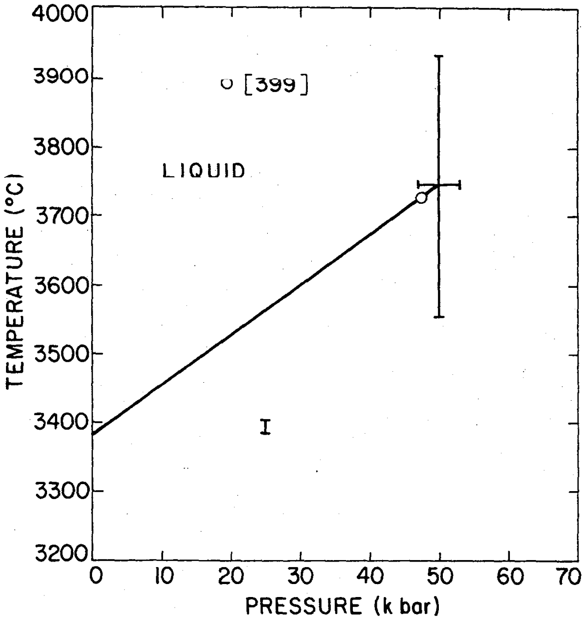

FIGURE 40. Phase diagram for tungsten.

13. Group VII B

13.1. Manganese

Rapoport and Kennedy [321] have investigated the variation of the three known polymorphic transitions with pressure. There are no triple points to 40 kbar, but the phase boundaries appear to be converging with increasing pressure. The melting curve was also reported. No other data are available.

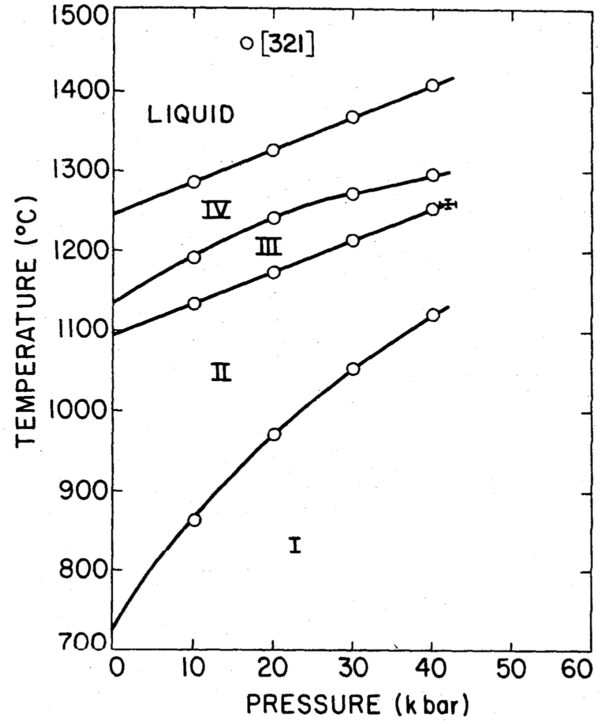

FIGURE 41. Phase diagram for manganese.

14. Group VIII

14.1. Iron

This element has been extensively studied at high pressures and temperatures because of its importance in the fields of geology and metallurgy and because the Fe(I–IV) transition is widely used as a RT pressure calibration point. Unfortunately, polymorphic transitions in Fe are generally sluggish and occur over wide ranges of pressure at constant temperature.

The RT Fe(I–IV) transition has been investigated many times [20, 118, 121, 131, 158, 264, 347, 375, 376, 398] with reported initiation pressures ranging from *110–115* kbar [20, 118, 131] to 140±15 kbar [121]. Bridgman [78] did not observe Fe(I–IV) to a reported pressure of 175,000 kg/cm^2, but this is understandable since the corrected pressure is only about *107* kbar. Stromberg and Stephens [360] did not observe the transition to their maximum pressure—about *122* kbar. It is confusing to note that Drickamer's new pressure scale [131], based on X-ray work, gives 110–115 kbar as the RT value for the initiation of Fe(I–IV), whereas other recent X-ray work [158, 376] places the initiation pressure in the 134–137 kbar range. Giles, et al. [158] feel that the initiation pressure is considerably higher than the equilibrium pressure and have determined an equilibrium pressure of 112±8 kbar. This lower value is supported by the Mossbauer work of Millet and Decker [292] who reported that the I–II–IV triple point must be lower in pressure than the usually accepted value of 110 kbar.

In view of the differences concerning the initiation pressure for this transition, it is suggested that it not be used as a pressure calibration point. One may raise questions whether the transition is inherently sluggish, whether the purity and physical condition of the sample has considerable effect, and whether the pressure field conditions in the cell might be unfavorable (such as large pressure gradients across the sample) [103]. In the case of Fe(I–IV) each of the above conditions probably contributes to the large variation in results from different sources. If Fe (I–IV) is used as a pressure calibration point, care should be taken to specify in detail the source (including purity) and physical conditions of the sample and the experimental conditions as well as the value used for the transition pressure. If this is done then corrections may be made later when the transition is better understood. At present, the best value for the equilibrium transition point appears to be the 112±8 kbar value of Giles, et al. [158]. As stated in the introduction, the initiation value used for pressure standardization purposes of this review is 110–115 kbar. This value was chosen to maintain consistency with the other very-high-pressure (above 100 kbar) fixed points taken from Drickamer [131].

The Fe(I–IV) boundary (at other than RT) has been investigated twice [98, 213], but data from the second of these [98] was adjusted to reflect the values of the first [213]. The first study employed shock methods of generating high pressure. For a reaction of a sluggish nature this is not a reliable technique for establishing an equilibrium phase boundary. Consequently, data from both of these studies have been discarded. The data of Millet and Decker [292] indicate that the triple point (I–II–IV) pressure is below 112 kbar, so the slope of the Fe(I–IV) boundary is certainly negative.

Many investigators have reported data for the Fe(I–II) boundary [40, 91, 98, 115, 116, 179, 213, 220, 222, 227, 304, 363, 364, 366]. Data based on shock pressures [98, 213] have been discarded for reasons mentioned above. Strong's [363, 364] early data is in very poor agreement with that of other investigators (about 60 °C higher at 50 kbar) and extrapolates considerably above any reasonable estimate of the I–II–IV triple point. Later data by Strong [91, 366] are different and in much better agreement with other published results. Claussen's early work [115] has also been replaced by later, more accurate data [116]. Data from references [40, 91, 116, 179, 220, 222, 227, 304] have been averaged and are shown in figure 42.

Bundy [98] is the only person who has reported data on Fe(II–IV). Because he corrected his data on the basis of shock work, his pressures are undoubtedly too high. His work does give an indication of the relative position of the Fe(II–IV) boundary. This information is reflected by the dashed line in figure 42.

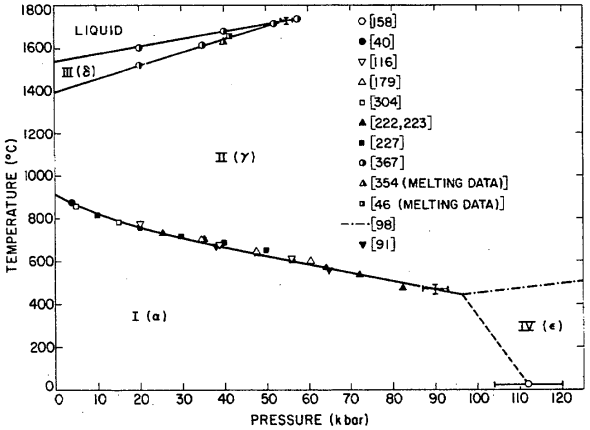

FIGURE 42. Phase diagram for iron.

In a very recent work Strong, et al. [367] have published the only data available on the Fe(II–III) phase boundary. They employed all of the latest experimental techniques, including pressure corrections to the thermocouple and simultaneous high-pressure, high-temperature calibration of their belt apparatus against the Au melting curve and the Fe(I–II) phase boundary. The Fe(L–II–III) triple point is placed at 52 kbar and 1718 °C. It is interesting to note that this is in accordance with earlier predictions of Sterrett, et al. [354] that this triple point lies above (perhaps considerably above) 25 kbar. The Fe(II–III) boundary shown in figure 42 is entirely attributable to Strong, et al. [367].

The melting curve is of considerable interest because of its geological significance. Unfortunately, the highest pressures for which the melting of Fe can be measured in the laboratory fall far short of those in effect near the earth's center. Consequently, enormous extrapolations have been made in an attempt to estimate the temperature at the earth's core boundary where the pressure is about 1400 kbar. Such extrapolations are interesting but probably bear little relation to the actual temperature at the core boundary [354]. Data for the melting curve have been reported from three laboratories [46, 354, 363–365, 367] with fair agreement. The data from each report can be fit to a straight line within experimental error. Data from the latest report of Strong, et al. [367] had been corrected for pressure effect on the thermocouple and is based on up-to-date calibration proceedures for the belt apparatus. Estimates of corrections to earlier data tend to move them toward the Strong data, so the melting curve shown in figure 42 has been drawn in accordance with Strong's latest results [367].

The crystal structure of Fe(IV) was first correctly reported by Jamieson and Lawson [192, 193] to be hcp. This structure has since been confirmed by others [118, 158, 264, 375, 376]. The latest data by Bassett's group [376] have been accepted as the best available lattice parameter determinations because of improved pressure determination. The lattice parameters for a pressure of *151* kbar are shown in table 3. Data at other pressures are available from the source literature.

14.2. Rhodium

Strong and Bundy [365] have reported a melting curve for Rh, but upon extrapolation to RP it gives a melting point about 170 °C low. The curve was fit to the Simon equation and then corrected uniformly upward 170 °C to agree with the accepted RP melting point. The curve is based on only four data points and must be viewed as a rough approximation. No other data are available.

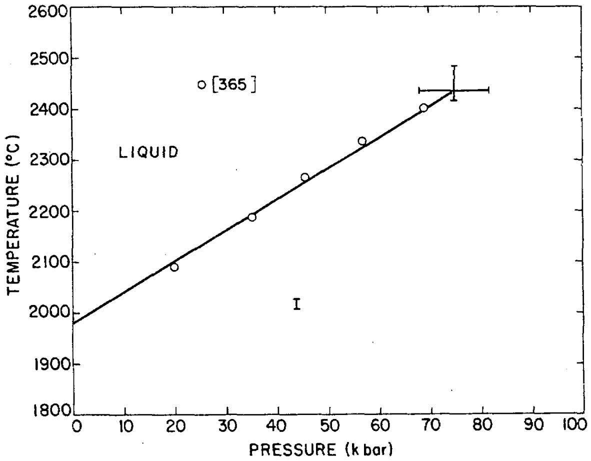

FIGURE 43. Phase diagram for rhodium.

14.3. Iridium

Zil'bershteyn and Estrin [429], on the basis of thermodynamic calculations, predicted a RT first order phase transition in Ir at about 90 kbar. X-ray and R(p) studies [334] to about 175 kbar and *120* kbar, respectively, show no indication of this transition. Shock data of McQueen, et al. [276] indicate a possible transition above about 1.1 Mbar, but the data are not sufficient for a definite conclusion.

14.4. Nickel

The melting curve has been reported by Strong and Bundy [365]. No other data are available.

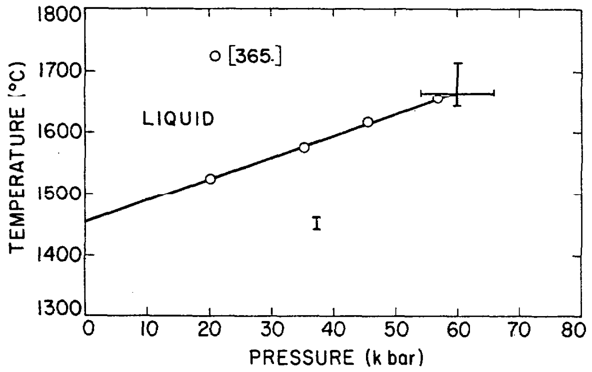

FIGURE 44. Phase diagram for nickel.

14.5. Platinum

The melting curve has been reported on three occasions [294, 365, 399]. The reported data sets show scatter ranging from 60–80 °C [294, 365] to over 200 °C [399]. Taking this scatter into consideration, the agreement among reports is good, but, of course, there is a high uncertainty in the final result. The data have been averaged and are shown in figure 45. No other data are available.

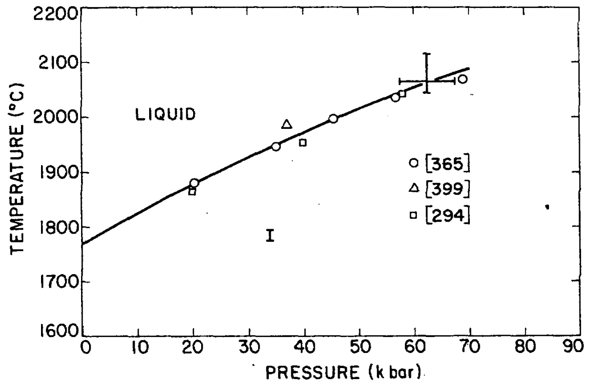

FIGURE 45. Phase diagram for platinum.

15. The Lanthanides and Yttrium

15.1. Yttrium

Investigation of superconductivity to about 150 kbar indicates that Y becomes a superconducter ($T_C = 1.3$ K) at about 110 kbar [296, 422]. The report concludes that superconductivity results from decreasing the hexagonal unit cell size and not from a phase change. There is no evidence for any polymorphic changes at RT to about 150 kbar. No melting curve data have been reported.

15.2. Lanthanum

The RT La(I–II) transition was first observed by Bridgman [72, 73] during V(p) studies, although similar studies by Vaidya and Kennedy [385] did not reveal the transition. It has since been confirmed by R(p) [75, 231, 277] and superconductivity [266, 337, 427] measurements, and X-ray studies [279, 313] have shown that La(II) has a fcc structure. A unique feature of this transition is that it apparently consists of two separable events that occur at roughly the same pressure. One event involves the hexagonal to cubic structure change, and the other consists of an electron transfer analogous to the Ce(I–III) transition. This results in the interesting fact that at RT one may start with either hexagonal or cubic La and still observe a transition in the vicinity of 23–27 kbar [75, 231]. During R(p) studies above RT, McWhan, et al. [277] observed that the transition could only be observed on the upstroke. This indicates that at higher temperatures the cubic to cubic transition is not observed and that a critical point for this aspect of the transition may exist as in Ce(I–III).

Resistance studies to very high pressures by Vereshchagin, et al. [389] indicate a possible phase transition at about *7.0* kbar in 99.48 percent pure La. Samples of 98.51 percent purity gave no indication of this possible transition. Similar studies by Maple, et al. [266] suggested a transition at about the same pressure only in La with 1.3 atomic percent Ce added. McWhan and Bond [279] determined the crystal structure of 99.9 percent pure La at 70 ± 10 kbar and found it to be fcc, thus indicating no further phase change to that pressure. The evidence is not sufficient to establish the presence or absence of a 70 kbar transition in La.

The melting curve and La(II–III) boundary have been investigated by Jayaraman [209] and are shown in figure 46.

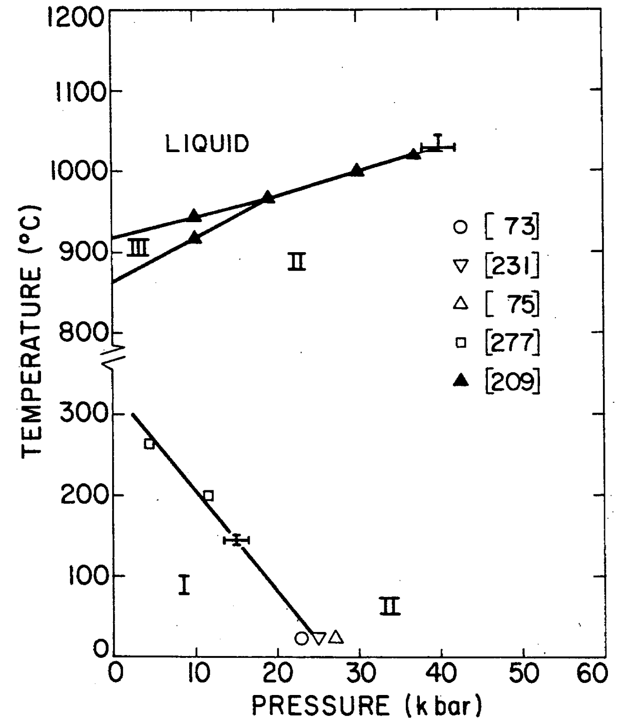

FIGURE 46. Phase diagram for lanthanum.

15.3. Cerium

The Ce(I–III) transition was first discovered by Bridgman [58, 72, 74, 75] and has been extensively investigated by resistance [58, 74, 188, 208, 256, 257, 319, 389], volume [32, 58, 72, 137, 162, 178, 250, 256], DTA [160, 208, 315], X-ray [123, 137, 149, 313] and ultrasonic [408] methods. Gschneidner, et al. [162–164] and Livshitz, et al. [256] have reported the effects of various impurity concentrations on the position of the Ce(I–III) phase boundary. Frolov, et al. [149] have used X-ray methods to detect Ce(III) at pressures as low as 1.1 kbar while Evdokimova and Genshaft [137] have observed Ce(I) at pressures as high as 13.7 kbar. In general, the transitions in Ce are characterized by large hysteresis and by relatively high sensitivity to impurity levels. Because of these factors, the positions of the phase lines in figure 47 may not be representative of true equilibrium.

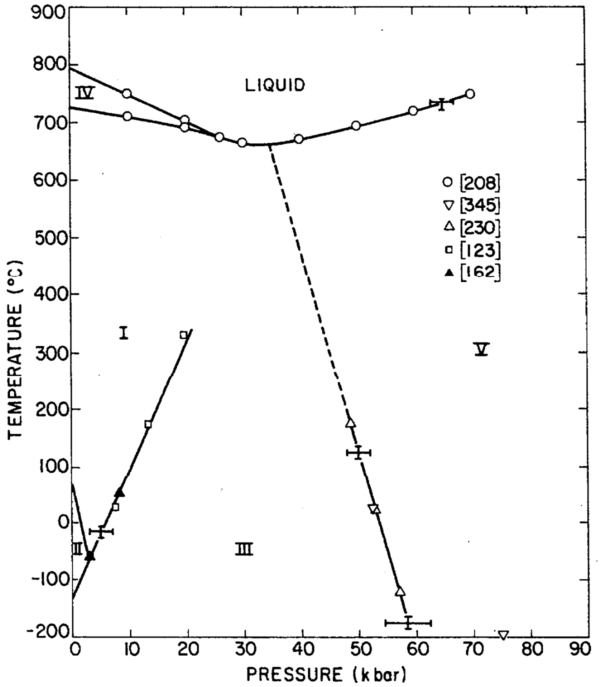

FIGURE 47. Phase diagram for cerium.

To determine the best values for the phase boundaries, all reports involving Ce with unknown purity or purity less than 99.9 percent were discarded [32, 58, 72, 74, 75, 137, 149, 178, 188, 250, 256, 257, 313, 315, 319, 389, 408] except that of Jayaraman [208] whose report contained the only available melting curve (99.5% Ce was used). Gschneidner, et al. [162] were the only ones to report the I–II–III triple point and the Ce(I–II) and Ce(II–III) phase lines, and Jayaraman [208] was the only one to report the L–I–IV triple point, so their values have been accepted without revision. The Ce(III–IV) boundary has been determined by King, et al. [230]. Stager and Drickamer [345] reported Ce(III–V) transition pressures, which (corrected) are in good agreement with King, et al. at 25 °C but in only fair agreement at − 196 °C. Because King, et al. report more data over a larger temperature range, their work is preferred over that of Stager and Drickamer. It is interesting to note that Livshitz, et al. [257], using Ce of less than 98.5 percent purity, determined the Ce(III–V) boundary as having a slight *positive* slope. One further transition, Ce(V–VI), has been reported by Stager and Drickamer [345] at pressures near *130* kbar. This transition was not observed in earlier work to about *150* kbar reported by Vereshchagin, et al. [389], but impurities in their Ce (purity not reported) may have suppressed it.

The crystal structure of Ce(III) was first determined at high pressure by Lawson and Tang [245]. They found that it had the same fcc structure as Ce(I), but that the lattice parameter was considerably smaller. There seems to be universal agreement that the structure of Ce(III) is fcc [1, 146, 149, 245, 313], but the value determined for the lattice parameter varies somewhat. Most of the reports give no information concerning the purity of the Ce used [1, 313] or the method of pressure calibration [1, 149, 245]. Consequently, the paper by Franceschi and Olcese [146] is the only one for which both Ce purity (99.95%) and pressure calibration were reported. Their values for the lattice parameter of Ce(III) is therefore accepted without revision.

The structure of Ce(V) has been investigated in two laboratories with totally different results. Franceschi and Olcese [146] report that Ce(V) is fcc while McWhan [285] claims that it is a slightly-distorted hcp. A comparison of the *d*-values and associated intensities for the two structures [147, 285] reveals that none match. There is currently no explanation for this discrepancy, so further work must be done to resolve the difference.

The Ce(I–III) transition is of considerable interest since it apparently is the only [with the possible exception of La(I–II)] solid-solid transition known to end in a critical point (in the vicinity of 21.5 kbar and 340 °C [123, 162] for pure Ce). Most persons who have investigated this phenomenon agree that a critical point does exist [123, 162, 188, 208, 242, 315, 319]. Exceptions include Beecroft and Swenson [32], who were merely noncommital on the subject, and Livshitz, et al. [257], who reported having observed the Ce(I–III) transition even at their highest attainable temperatures (350 °C). Since other aspects of the Livshitz report are probably in error [see discussion above on Ce(III–V)], it seems reasonable to conclude that the weight of evidence supports the existence of a critical point on the Ce(I–III) boundary.

15.4. Praseodymium

A maximum in R(p) has been reported [75, 229, 345, 360] at about 37–40 kbar at RT and is interpreted by some to indicate a first order phase transition. There is no detectable volume discontinuity [73, 349] or DTA event [209, 350] associated with this transition, but X-ray studies at high pressure [313] and at RP and −196 °C following pressure treatment [273] indicate that normally hexagonal Pr becomes fcc above 40 kbar at RT.

Stager and Drickamer [345] have investigated Pr(I–III) at lower than RT. Their apparatus does not allow very accurate measurements below 100 kbar and transitions tend to be very sluggish at lower temperatures, so their data for this boundary are quite uncertain. Jayaraman [209] has suggested a position for the I–II–III triple point, but his conclusion is based on very little data and must be regarded as highly uncertain.

Two studies on R(p) have been made to pressures above 100 kbar [345, 392]. The data are similar to about 100 kbar but deviate somewhat after that. Vereshchagin, et al. [392] did not interpret any of their data as indicative of phase transformations (maximum pressure about 150 kbar), whereas Stager and Drickamer [345] report three phase changes (maximum pressure about 450 kbar), including two below 150 kbar.

The Pr(I–II) boundary and the melting curve have been studied on two occasions [209, 350] with fair agreement. The combined data are shown in figure 48.

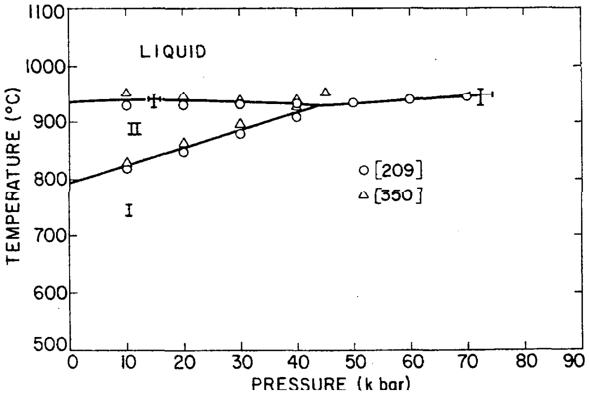

FIGURE 48. Phase diagram for praseodymium.

15.5. Neodymium

The resistance behavior of Nd with pressure has been examined on three occasions [75, 345, 389] with fair agreement to about 60–70 kbar and poor agreement thereafter. There is some indication of a phase transition near 50 kbar but interpretations vary. The X-ray work at high pressure reported by Piermarini and Weir [313] indicate that normally hexagonal Nd transforms to fcc by 50 kbar at RT. This conclusion is supported by the work of McDonald, et al. [273, 274], who retained the high pressure fcc phase at RP by cooling to −196 °C before releasing the pressure.

The melting curve and Nd(I–II) boundary have been investigated only once [209] and are shown in figure 49.

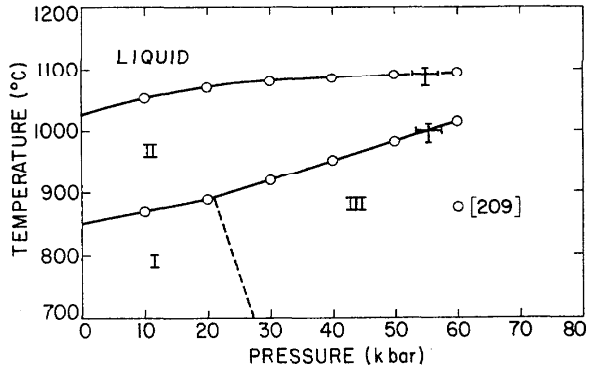

FIGURE 49. Phase diagram for neodymium.

15.6. Samarium

Studies of R(p) [77, 345] and V(p) [77] gave no certain indication of a phase change below 100 kbar at RT. Jayaraman and Sherwood [205] have reported that rhombohedral Sm converts to a dhcp (La-type) structure at about 40 kbar. The dhcp phase is metastable at RTP but reverts to rhombohedral when heated to 600 °C. The melting curve and Sm(I–II) boundary shown in figure 50 are attributable to Jayaraman [209].

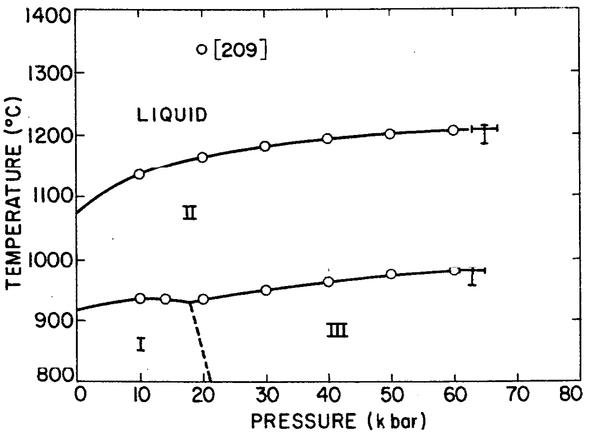

FIGURE 50. Phase diagram for samarium.

15.7. Europium

The R(p) studies of Stager and Drickamer [345] indicate a phase transition at about 122–130 kbar at RT. Stromberg and Stephens [360] investigated R(p) to about *130* kbar without observing the rapid rise in resistance characteristic of the transition. McWhan, et al. [282] examined Eu to *130* ± 15 kbar with X-rays and reported no structure change.

The melting curve has been reported on two occasions [207, 350] with fair agreement to about 30 kbar but poor agreement thereafter. Stephens [350] found it necessary to adjust his data to force the RP melting point (extrapolated from high pressure melting points) to agree with the known RP melting point for Eu. Since the melting curve of Eu shows large curvature, such an extrapolation procedure is a dangerous practice subject to wide differences of interpretation. Alternate interpretations of the "correct" extrapolation back to RP could easily result in better agreement with Jayaraman's work. Consequently, Jayaraman's [207] data are accepted as representative of the best melting curve.

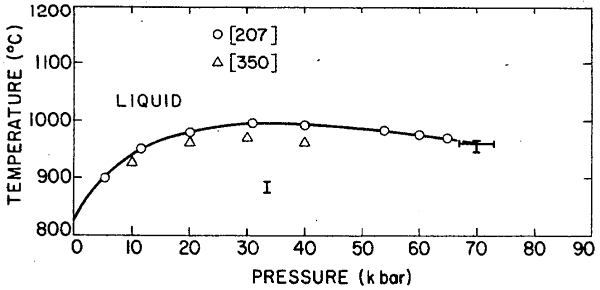

FIGURE 51. Phase diagram for europium.

15.8. Gadolinium

A phase transition beginning at 20–25 kbar at RT has been detected by resistance [76], volume [76], Curie point [280, 324], and X-ray [280, 410] measurements. The high pressure phase is metastable at RTP and has been studied by X-ray analysis under ambient conditions [35, 206]. This transition is not detectable by DTA [350] and for unknown reasons was not observed by Stromberg and Stephens [360] during resistance studies or by Livshitz and Genshaft [258] during examination of pressure effects on the Curie point. If a pressure "seasoning" process was used by these latter investigators, the irreversible nature of the Gd(I–III) transition could account for their failure to observe the transition when measurements were taken. The X-ray data leave no doubt that a phase change does occur and that the high pressure phase may be retained at RTP.

The melting curve and Gd(I–II) boundary have each been studied twice [209, 350] with good agreement [if the difference in the RP value for Gd(I–II) is considered]. Jayaraman [209] interprets his data as indicating the position of the I–II–III triple point. He shows no data between RP and the proposed triple point, and his data follow a straight line thereafter. A straight-line extrapolation of his data yields a RP Gd(I–II) point within the combined estimated errors of his work and the Gd(I–II) value quoted from the literature. Thus, there is no basis for suggesting the position of the triple point. The information in figure 52 is an average of the available data.

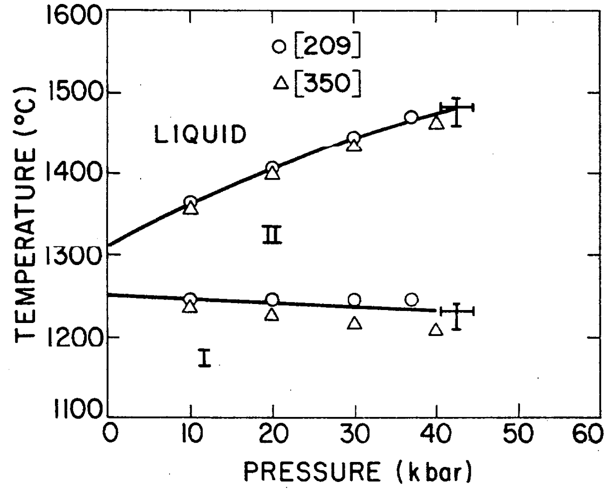

FIGURE 52. Phase diagram for gadolinium.

15.9. Terbium

The Tb(I–III) transition has been reported three times [280, 353, 360] although one of the reports [360] did not recognize it as such. Early work by Stephens [349] in which the transition was not seen has been superceded by later work [353] which did reveal a change. Reported transition pressures (determined only roughly) vary from 25 to 35 kbar. X-ray studies [280, 353] show that Tb(III) has a Sm-type structure.

The melting curve and Tb(I–II) boundary have been investigated only by Jayaraman [209]. His data are illustrated in figure 53.

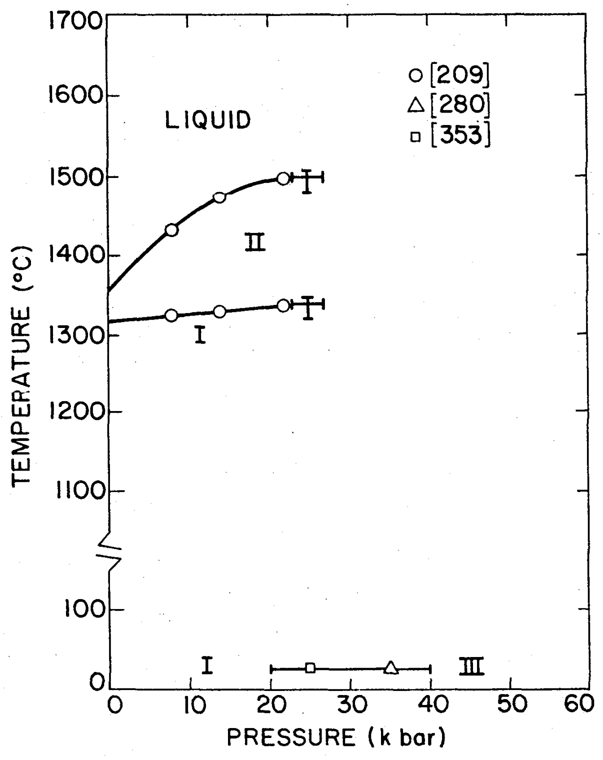

FIGURE 53. Phase diagram for terbium.

15.10. Dysprosium

A phase change has been detected at RT by Curie point [280] and resistance [77, 340, 345, 360, 392] measurements in the pressure region 45–70 kbar. X-ray measurements have been made at pressure in the Dy(III) stability region. Jamieson [197] was not able to draw any definite conclusions regarding the structure of Dy(III), but McWhan and Stevens [280] suggest that it has a Sm-type structure.

Jayaraman [209] used DTA to determine dT/dP for the melting curve (≈ 12°/kbar) and the Dy(I–II) boundary (≈ 5°/kbar). He took only two points (8 and 25 kbar) and his work was more exploratory than definitive.

15.11. Holmium

Initial work by Bridgman [77] on R(p) indicated a possible transition in the vicinity of 35 kbar at RT, but later reports of X-ray [311], Curie point [280] and resistance [345] studies show that the hcp to Sm-type transition occurs at higher pressures, nearer 70 kbar. McWhan and Stevens [280] have reported the Sm-type lattice parameters. Jayaraman's [209] work gives an approximation of dT/dP for the melting curve (≈ 15°/kbar) and Ho(I–II) (≈ 12°/kbar) boundary.

15.12. Erbium

Bridgman [77] and Perez-Albuerne, et al. [311] report evidence for a phase change in Er, and Stager and Drickamer [345] suggest the possibility of such a change. No evidence for a phase change was reported by Stromberg and Stephens [360] or by Vereshchagin, et al. [392]. Apparently, Er(I–III) is very sluggish and exhibits large pressure hysteresis [77]. Jayaraman's [209] preliminary investigations did not reveal any indication of an hcp–bcc transition but did suggest an estimate for the initial slope of the melting curve (≈ 15°/kbar).

15.13. Thulium

Recent X-ray studies [254] have established the existence of a Tm(I–II) transition at RT between 60 and 116 kbar. Earlier reports also based on X-ray data [311] suggested the possibility of a phase change at about 110 kbar, but no definite conclusions were possible. Studies of R(p) did not reveal any certain indication of the change [345]. The Tm(I–II) transition involves the same subtle hcp to Sm-type structure change seen in other lanthanide elements. There has been no report of a bcc phase of Tm [209]. Jayaraman [209] has estimated the initial slope of the melting curve (≈ 12°/kbar).

15.14. Ytterbium

The Yb(I–III) transition is often used as a RT pressure calibration point even though the transition is fairly sluggish and exhibits large hysteresis. Because of the large hysteresis, the only information valuable for pressure calibration is the transition pressure on the upstroke (increasing pressure cycle). The transition has been investigated numerous times [77, 168, 207, 211, 283, 339, 342, 349, 350, 392] with reported RT transition pressures varying from 38 kbar [342] to 40 kbar [207, 339]. Only two reports [211, 349] have given careful error analysis, and their data indicate the best value to be 39.4 ± 0.8 kbar at RT for upstroke only.

The phase boundary for Yb(I–III) has been investigated four times [168, 207, 339, 350] with variable results. The data of Hall, et al. [168] do not extrapolate to the RP transition point and have been discarded. Stephens' [350] data were apparently affected by oxygen and/or nitrogen impurity and have also been discarded. The remaining data are in good agreement and are shown in figure 54. Hall, et al. [168, 169] have shown that the structure of Yb(III) is bcc.

Three other phase transitions have been reported for Yb. One, reported by Stephens [350], is apparently stabilized by oxygen and/or nitrogen impurities and will

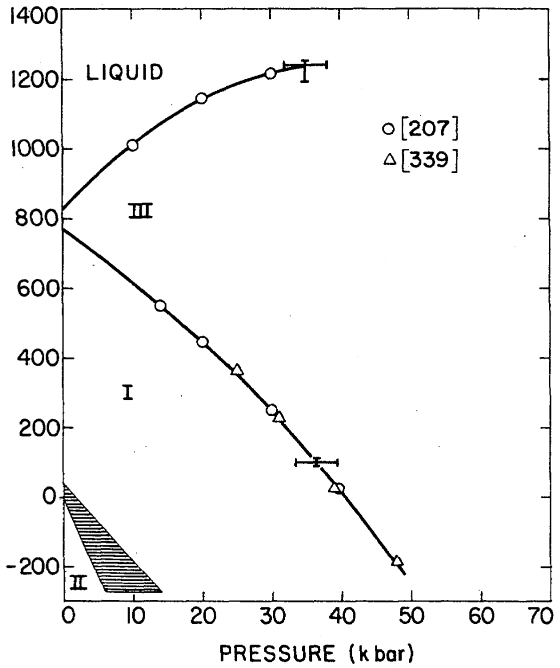

FIGURE 54. Phase diagram for ytterbium.

not be considered further. The second is not well understood and has been reported only twice on the basis of resistance measurements [168, 207]. The temperature for this "transition" is uneffected by pressure above about 30 kbar. Below 30 kbar it is not observed. The third transition as first reported by Kayser [223] involves an fcc to hcp transformation just below RT in very pure Yb. It has since been confirmed and further studied by Kayser [224] and others [84, 322]. The data do not agree well, but this is undoubtedly attributable to the sluggishness of phase transitions at low temperatures and to the method of interpreting the data. The Yb(I–II) phase boundary is accordingly shown as a broad band.

The melting curve has been investigated twice [207, 350] with poor agreement. Since it appears that Stephens' [350] melting data may have been lowered by the presence of impurities, the data of Jayaraman [207] is accepted without revision.

15.15. Lutetium

Preliminary results [255] indicate that Lu may have an hcp to dhcp transition between 100 and 200 kbar. The initial slope of the melting curve has been estimated by Jayaraman [209] to be about 8.5°/kbar.

16. The Actinides

16.1. Thorium

Superconductivity measurements [144] to about *130* kbar indicate that there may be a polymorphic change near 70 kbar. No other data are available.

16.2. Uranium

Assami, et al. [12] investigated R(p) to about *192* kbar at RT and found no evidence for a first order phase change. The phase changes already known to occur at high temperatures and RP have been investigated at high pressure on three occasions [12, 232, 259]. The material (hexagonal BN) used by Lloyd, et al. [259] to contain their U caused contamination problems when used in the other studies [12, 232]. The results reported for BN containers vary, and since the data of Lloyd, et al. fall below that reported by others (indicating possible contamination) it has been discarded. The other two studies show good agreement. Leman [249] has made an extrapolation of the U(I–III) boundary to 500 kbar. Such a large extrapolation must be regarded with skepticism.

The melting curve has been reported only once [12] and is shown in figure 55.

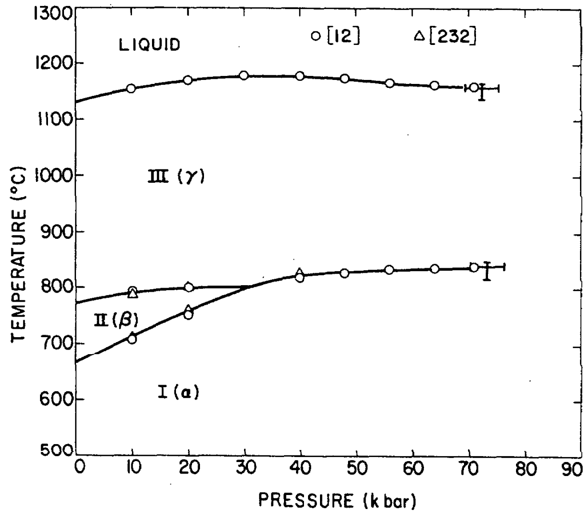

FIGURE 55. Phase diagram for uranium.

16.3. Neptunium

The two solid-solid phase boundaries and the melting curve have been investigated by Stephens [351] to about 35 kbar. The Np(I–II) boundary data reported by McWhan, et al. [277] to 12 kbar show poor agreement with Stephens' data. The strong upward curvature found by McWhan, et al. was not confirmed by Stephens and since Stephens' data extends to much higher pressure it is to be preferred in deciding this issue. The phase diagram shown in figure 56 is attributable entirely to Stephens [351].

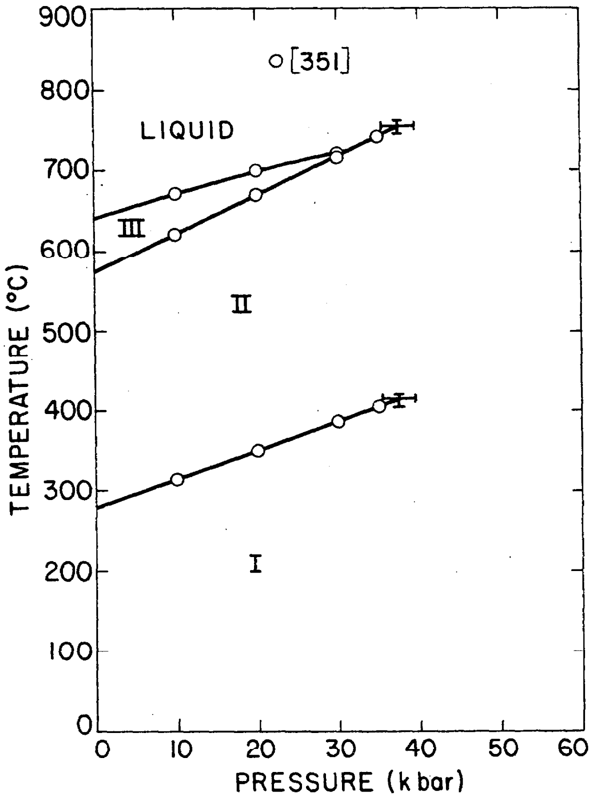

FIGURE 56. Phase diagram for neptunium.

16.4. Plutonium

The Pu(I–II) boundary has been investigated five times [79, 252, 277, 329, 348] with fair agreement. Three of these investigators [252, 329, 348] have also reported the Pu(II–III) and Pu(III–V) boundaries and the melting curve—again with fair agreement. The data of Liptai and Friddle [252] have also been reported and discussed by Brodsky at the Third International Conference on Plutonium [81]. The Pu(III–IV) and Pu(IV–V) boundaries have been reported on two occasions [329, 348] with poor agreement, but considering the small amount of data upon which these boundaries are based, this is not surprising. Roux, et al. [329] originally reported their data at a meeting of the European High Pressure Research Group for which there are no published proceedings. In the subsequent publication [329], no information was given concerning pressure calibration beyond 40 kbar. Consequently, it is not known whether the data points beyond 40 kbar attributable to Roux, et al. conform to the calibration standards given in the introduction. The phase diagram in figure 57 is an average of the available data.

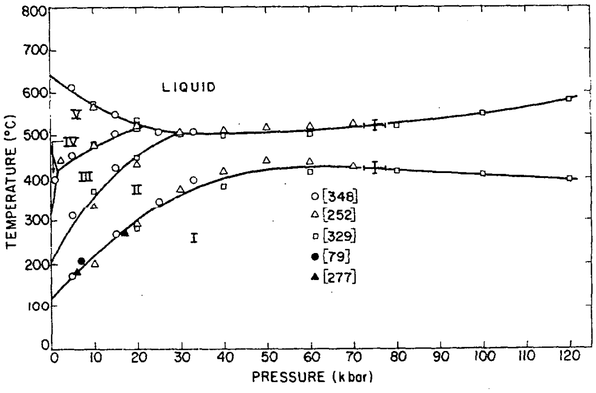

FIGURE 57. Phase diagram for plutonium.

16.5. Americium

The Am(I–II) boundary and the melting curve have been investigated only once [352]. The data are shown in figure 58. McWhan [277] did some R(p) work on this element but found no reproducible features in the data at RT to about 36 kbar.

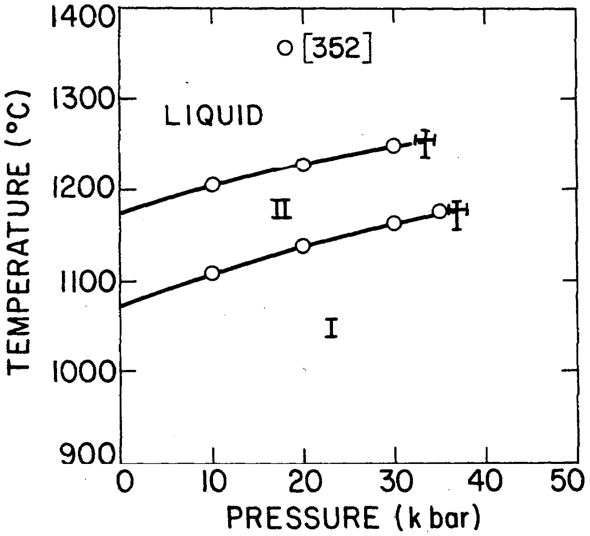

FIGURE 58. Phase diagram for americium.

17. Acknowledgments

I am happy to acknowledge with thanks the helpful advice of J. Dean Barnett, M. Duane Horton, H. Tracy Hall, and Leo Merrill.

18. References

[1] Adams, L. H., Davis, B. L., Proc. Nat. Acad. Sci., **48**, 982–990 (1962).

[2] Adler, P. N., Margolin, H., Trans. AIME, **230**, 1048–1052 (1964).

[3] Akella, J., Kennedy, G. C., J. Geophys. Res., **76**, 4969–4977 (1971).

[4] Akella, J., Ganguly, J., Grover, R., Kennedy, G., J. Phys. Chem. Solids, **34**, 631–636 (1973).

[5] Alekseev, K. A., Sov. Phys. Solid State, **7**, 1440–1441 (1965); Engl. Transl. of Fiz. Tverd. Tela, **7**, 1787–1789 (1965).

[6] Adler, B. J., Christian, R. H., Phys. Rev. Lett., **4**, 450–452 (1960).

[7] Anderson, D. R., Unpublished Dissertation, Brigham Young University, Provo, Utah, 156 pp., 1969.
[8] Anderson, D. R., Ott, J. B., Goates, J. R., Hall, H. T., Report COO–1707–9, Nat. Tech. Information Serv., Springfield, Va. 22151, 15 pp. (1970).
[9] Anderson, D. R., Ott, J. B., Goates, J. R., Hall, H. T., J. Chem. Phys., **54**, 234–238 (1971).
[10] Anderson, M. S., Gutman, E. J., Packard, J. R., Swenson, C. A., J. Phys. Chem. Solids, **30**, 1587–1601 (1969).
[11] Andersen, T. N., Bezirjian, O. H., Eyring, H., J. Electrochem. Soc., **114**, 805–809 (1967).
[12] Asami, N., Yamada, M., Takahashi, S., Report UCRL–Trans–10581, Nat. Tech. Information Serv., Springfield, Va. 22151, 18 pp, 1967; Engl. Transl. of Bull. Jap. Inst. Metals, **31**, 389–394 (1967).
[13] Atoji, M., Schirber, J. E., Swenson, C. A., J. Chem. Phys., **31**, 1628–1629 (1959).
[14] Aust, R. B., Drickamer, H. G., Science, **140**, 817–819 (1963).
[15] Baak, T., Science, **148**, 1220–1221 (1965).
[16] Babb, S. E., J. Chem. Phys., **37**, 922–923 (1962).
[17] Babb, S. E., J. Chem. Phys., **50**, 5271–5274 (1969).
[18] Bakanova, A. A., Dudoladov, I. P., Sutulov, Yu. N., Sov. Phys. Solid State, **11**, 1515–1518 (1970); Engl. Transl. of Fiz. Tverd. Tela, **11**, 1881–1884 (1969).
[19] Balchan, A. S., Drickamer, H. G., Rev. Sci. Instrum., **31**, 511–513 (1960).
[20] Balchan, A. S., Drickamer, H. G., Rev. Sci. Instrum., **32**, 308–313, (1961).
[21] Balchan, A. S., Drickamer, H. G., J. Chem. Phys., **34**, 1948–1949 (1961).
[22] Ball, D. L., in "Liquids: Structure, Properties, Solid Interactions," T. J. Hughel, Ed., Elsevier, Amsterdam, 1965, pp. 353–369.
[23] Barnett, J. D., Bennion, R. B., Hall, H. T., Science, **141**, 534–535 (1963).
[24] Barnett, J. D., Bennion, R. B., Hall, H. T., Science, **141**, 1041–1042 (1963).
[25] Barnett, J. D., Hall, H. T., Rev. Sci. Instrum., **35**, 175–182 (1964).
[26] Barnett, J. D., Bean, V. E., Hall, H. T., J. Appl. Phys., **37**, 875–877 (1966).
[27] Bastide, J. P., Susse, C., Epain, R., C. R. Acad. Sci. Ser. C, **267**, 857–860 (1968).
[28] Bastide, J. P., Susse, C., High Temp. High Pressures, **2**, 237–240 (1970).
[29] Bastide, J. P., Private Communication.
[30] Bates, C. H., Dachille, F., Roy, R., Science, **147**, 860–862 (1965).
[31] Bates, C. H., Report AD–625–428, Nat. Tech. Information Serv., Springfield, Va. 22151, 79 pp., 1966.
[32] Beecroft, R. I., Swenson, C. A., J. Phys. Chem. Solids, **15**, 234–239 (1960).
[33] Bell, P. M., England, J. L., Kullerud, G., Carnegie Inst. Wash. Yearbook, **65**, 354–356 (1966).
[34] Bell, P. M., Boyd, F. R., England, J. L., Nat. Bur. Stand. (U.S.) Spec. Publ. 326, pp. 63–65 (1971).
[35] Belov, K. P., Ergin, Yu. V., Katsnel'son, A. A., Ped'ko, A. V., JETP Lett., **1**, 43–47 (1965); Engl. Transl. of Zh. Eksp. Teor. Fiz. Pis'ma Red., **1**, 8 (1965).
[36] Berman, I. V., Brandt, N. B., JETP Lett., **7**, 323–326 (1968); Engl. Transl. of Zh. Eksp. Teor. Fiz. Pis'ma Red., **7**, 412–416 (1968).
[37] Berman, I. V., Brandt, N. B., JETP Lett., **10**, 55–57 (1969); Engl. Transl. of Zh. Eksp. Teor. Fiz. Pis'ma Red., **10**, 88–91 (1969).
[38] Berman, I. V., Brandt, N. B., Kuz'min, R. N., Opalenko, A. A., Slobodchikov, S. S., JETP Lett., **10**, 237–239 (1969); Engl. Transl. of Zh. Eksp. Teor. Fiz. Pis'ma Red., **10**, 373–377 (1969).
[39] Berman, I. V., Bynzarov, Zh. I., Kurkin, Yu. P., Sov. Phys. Solid State, **14**, 2192–2194 (1973); Engl. Transl. of Fiz. Tverd. Tela, **14**, 2527–2530 (1972).
[40] Birch, F., Amer. J. Sci., **283**, 192–211 (1940).
[41] Blum, F. A., Deaton, B. C., Phys. Rev. A, **137**, 1410–1417 (1965).
[42] Bogdanov, V. S., JETP Lett., **3**, 26–28 (1966); Engl. Transl. of Zh. Eksp. Teor. Fiz. Pis'ma Red., **3**, 44–47 (1966).
[43] Bogdanov, V. S., Meas. Tech (USSR), **1967**, 928–930 (1967); Engl. Transl. of Izmer. Tekh., **1967**, 29–30 (1967).
[44] Bosio, L., Defrain, A., Epelboin, I., Vidal, J., J. Chim. Phys. Physicochim. Biol., **65**, 719–721 (1968).
[45] Bosio, L., C. R. Acad. Sci. Ser. B, **270**, 1453–1456 (1970).
[46] Boyd, F. R., England, J. L., Carnegie Inst. Wash. Yearbook, **62**, 134–137 (1963).
[47] Brandt, N. B., Ginzburg, N. I., Sov. Phys. Solid State, **3**, 2510–2519 (1962); Engl. Transl. of Fiz. Tverd. Tela, **3**, 3461–3472 (1961).
[48] Brandt, N. B., Ginzburg, N. I., Instrum. Exp. Tech., **1962**, 1024–1027 (1962); Engl. Transl. of Prib. Tekh. Eksp., **1962**, 161–164 (1962).
[49] Bridgman, P. W., Proc. Amer. Acad. Arts Sci., **47**, 347–438 (1911).
[50] Bridgman, P. W., Phys. Rev., **3**, 126–141, 153–203 (1914).
[51] Bridgman, P. W., J. Amer. Chem. Soc., **36**, 1344–1363 (1914).
[52] Bridgman, P. W., Phys. Rev., **6**, 1–33, 94–112 (1915).
[53] Bridgman, P. W., J. Amer. Chem. Soc., **38**, 609–612 (1916).
[54] Bridgman, P. W., Proc. Amer. Acad. Arts Sci., **56**, 61–154 (1921).
[55] Bridgman, P. W., Proc. Amer. Acad. Arts Sci., **60**, 305–383 (1925).
[56] Bridgman, P. W., Proc. Amer. Acad. Arts Sci., **60**, 385–421 (1925).
[57] Bridgman, P. W., Phys. Rev., **27**, 68–86 (1926).
[58] Bridgman, P. W., Proc. Amer. Acad. Arts Sci., **62**, 207–226 (1927).
[59] Bridgman, P. W., Phys. Rev., **45**, 844–845 (1934).
[60] Bridgman, P. W., Phys. Rev., **48**, 825–847 (1935).
[61] Bridgman, P. W., Phys. Rev., **48**, 893–906 (1935).
[62] Bridgman, P. W., Proc. Amer. Acad. Arts Sci., **71**, 387–460 (1937).
[63] Bridgman, P. W., Proc. Amer. Acad. Arts Sci., **72**, 207–225 (1938).
[64] Bridgman, P. W., Proc. Amer. Acad. Arts Sci., **72**, 157–205 (1938).
[65] Bridgman, P. W., Phys. Rev., **57**, 237–239 (1940).
[66] Bridgman, P. W., Proc. Amer. Acad. Arts Sci., **74**, 21–51 (1940).
[67] Bridgman, P. W., Proc. Amer. Acad. Arts Sci., **74**, 1–10 (1940).
[68] Bridgman, P. W., J. Appl. Phys., **12**, 461–469 (1941).
[69] Bridgman, P. W., Phys. Rev., **60**, 351–354 (1941).
[70] Bridgman, P. W., Proc. Amer. Acad. Arts Sci., **74**, 425–440 (1942).
[71] Bridgman, P. W., Proc. Amer. Acad. Arts Sci., **76**, 1–7 (1945).
[72] Bridgman, P. W., Proc. Amer. Acad. Arts Sci., **76**, 71–87 (1948).
[73] Bridgman, P. W., Proc. Amer. Acad. Arts Sci., **76**, 55–70 (1948).
[74] Bridgman, P. W., Proc. Amer. Acad. Arts Sci., **79**, 149–179 (1951).
[75] Bridgman, P. W., Proc. Amer. Acad. Arts Sci., **81**, 167–251 (1952).
[76] Bridgman, P. W., Proc. Amer. Acad. Arts Sci., **82**, 83–100 (1953).
[77] Bridgman, P. W., Proc. Amer. Acad. Arts Sci., **83**, 3–21 (1954).
[78] Bridgman, P. W., J. Appl. Phys., **27**, 659 (1956).
[79] Bridgman, P. W., J. Appl. Phys., **30**, 214–217 (1959).
[80] Bridgman, P. W., "Collected Experimental Papers," Vols. I–VII, Harvard University Press, Cambridge, Mass., 1964.
[81] Brodsky, M. B., in "Plutonium 1965, Proc. Int. Conf. 3rd", A. E. Kay and M. B. Waldron, Eds., Royal Commonwealth Hall, London, 1967, pp. 137–139.

[82] Brugger, R. M., Bennion, R. B., Worlton, T. G., Phys. Lett. A, **24**, 714–717 (1967).

[83] Brugger, R. M., Bennion, R. B., Worlton, T. G., Myers, W. R., Trans. Amer. Crystallographic Assn., **5**, 141–153 (1969).

[84] Bucher, E., Schmidt, P. H., Jayaraman, A., Andres, K., Maita, J. P., Nassau, K., Dernier, P. D., Phys. Rev. B, **2**, 3911–3917 (1970).

[85] Buckel, W., Gey, W., Z. Phys., **176**, 336–350 (1963).

[86] Bundy, F. P., Phys. Rev., **110**, 314–318 (1958).

[87] Bundy, F. P., Phys. Rev., **115**, 274–277 (1959).

[88] Bundy, F. P., Bovenkerk, H. P., Strong, H. M., Wentorf, R. H., J. Chem. Phys., **35**, 383–391 (1961).

[89] Bundy, F. P., Science, **137**, 1055–1057 (1962).

[90] Bundy, F. P., Science, **137**, 1057–1058 (1962).

[91] Bundy, F. P., Strong, H. M., Solid State Phys., **13**, 81–146 (1962).

[92] Bundy, F. P., Kasper, J. S., Science, **139**, 340–341 (1963).

[93] Bundy, F. P., General Electric Report 63-RL-3481C, 5 pp, 1963.

[94] Bundy, F. P., J. Chem. Phys., **38**, 618–630 (1963).

[95] Bundy, F. P., J. Chem. Phys., **38**, 631–643 (1963).

[96] Bundy, F. P., J. Chem. Phys., **41**, 3809–3814 (1964).

[97] Bundy, F. P., Ann. N. Y. Acad. Sci., **105**, 951–982 (1964).

[98] Bundy, F. P., J. Appl. Phys., **36**, 616–620 (1965).

[99] Bundy, F. P., Kasper, J. S., J. Chem. Phys., **46**, 3437–3446 (1967).

[100] Bundy, F. P., Proc. Kon. Ned. Akad. Wetensch. Ser. B, **72**, 302–316 (1969).

[101] Bundy, F. P., Reactiv. Solids, Proc. Int. Symp. 6th, J. W. Mitchell, Ed., Wiley-Interscience, New York, 1969, pp. 817–826.

[102] Bundy, F. P., Kasper, J. S., High Temp. High Pressures, **2**, 429–436 (1970).

[103] Bundy, F. P., Private Communication.

[104] Butuzov, V. P., Gonikberg, M. G., Smirnov, S. P., Engl. Transl. of Dokl. Akad. Nauk SSSR, **89**, 651–653 (1953).

[105] Butuzov, V. P., Gonikberg, M. G., Engl. Transl. of Dokl. Akad. Nauk SSSR, **91**, 1083–1084 (1953).

[106] Butuzov, V. P., Ponyatovskii, E. G., Sov. Phys. Crystallogr., **1**, 577 (1956); Engl. Transl. of Kristallografiya, **1**, 736–737 (1956).

[107] Butuzov, V. P., Ponyatovskii, E. G., Shakhovskii, G. P., Engl. Transl. of Dokl. Akad. Nauk SSSR, **109**, 519–520 (1956).

[108] Butuzov, V. P., Boksha, S. S., Gonikberg, M. G., Dokl. Akad. Nauk SSSR, **108**, 837–840 (1956); Chem. Abstr., **51**, 3259a (1958).

[109] Butuzov, V. P., Ponyatovskii, E. G., Sov. Phys. Crystallogr., **1**, 453–455 (1956); Engl. Transl. of Kristallografiya, **1**, 572–576 (1956).

[110] Butuzov, V. P., Sov. Phys. Crystallogr., **2**, 533–543 (1957); Engl. Transl. of Kristallografiya, **2**, 536 (1957).

[111] Cannon, J. F., Merrill, L., "A Compilation of Volumes I–IV of Bibliography on High Pressure Research with Author and Subject Indexes," Vol. II, High Pressure Data Center, Brigham Young University, Provo, Utah 84602, 1972.

[112] Cedergren, M., Backstrom, G., Rev. Sci. Instrum., **43**, 686–688 (1972).

[113] Chaney, P. E., Babb, S. E., J. Chem. Phys., **43**, 1071 (1965).

[114] Christensen, H. E., Unpublished Thesis, Brigham Young University, Provo, Utah, 24 pp., 1961.

[115] Claussen, W. F., Rev. Sci. Instrum., **31**, 878–881 (1960).

[116] Claussen, W. F., ASME Paper 62-WA-277. Also in "High Pressure Measurement," A. A. Giardini and E. C. Lloyd, Eds., Butterworths, Washington, D.C., 1963, pp. 125–151.

[117] Clendenen, G. L., Drickamer, H. G., Phys. Rev. A, **135**, 1643–1645 (1964).

[118] Clendenen, R. L., Drickamer, H. G., J. Phys. Chem. Solids, **25**, 865–868 (1964).

[119] Cohen, L. H., Klement, W., Kennedy, G. C., Phys. Rev., **145**, 519–525 (1966).

[120] Compy, E. M., J. Appl. Phys., **41**, 2014–2018 (1970).

[121] Contre, M., Nat. Bur. Stand. (U.S.) Spec. Publ. 326, pp. 291–296 (1971).

[122] Contre, M., Private Communication.

[123] Davis, B. L., Adams, L. H., J. Phys. Chem. Solids, **25**, 379–388 (1964).

[124] Deaton, B. C., Bowen, D. E., Appl. Phys. Lett., **4**, 97–99 (1964).

[125] Deaton, B. C., Blum, F. A., Phys. Rev. A, **137**, 1131–1138 (1965).

[126] Decker, D. L., Vanfleet, H. B., Phys. Rev. A, **138**, 129–133 (1965).

[127] Decker, D. L., J. Appl. Phys., **42**, 3239–3244 (1971).

[128] Decker, D. L., Bassett, W. A., Merrill, L., Hall, H. T., Barnett, J. D., J. Phys. Chem. Ref. Data, **1**, 773–836 (1972).

[129] Donohue, J., Goodman, S. H., Crisp, M., Acta Crystallogr. B, **25**, 2168 (1969).

[130] Drickamer, H. G., Solid State Phys., **17**, 1–133 (1965).

[131] Drickamer, H. G., Rev. Sci. Instrum., **41**, 1667–1668 (1970).

[132] Dudley, J. D., Hall, H. T., Phys. Rev., **118**, 1211–1216 (1960).

[133] Duggin, M. J., J. Phys. Chem. Solids, **33**, 1267–1271 (1972).

[134] Eichler, A., Gey, W., Z. Phys., **251**, 321–332 (1972).

[135] El Goresy, A., Donnay, G., Science, **161**, 363–364 (1968).

[136] Ergun, S., Alexander, L. E., Nature, **195**, 765–767 (1962).

[137] Evdokimova, V. V., Genshaft, Yu. S., Sov. Phys. Solid State, **6**, 1941–1944 (1965); Engl. Transl. of Fiz. Tverd. Tela, **6**, 2449–2452 (1964).

[138] Fadeev, V. E., Russ. J. Phys. Chem., **45**, 1051–1052 (1971); Engl. Transl. of Zh. Fiz. Khim., **45**, 1843 (1971).

[139] Fateeva, N. S., Vereshchagin, L. F., Kolotygin, V. S., Sov. Phys. Dokl., **8**, 893–895 (1964); Engl. Transl. of Dokl. Akad. Nauk SSSR, **152**, 88–91 (1963).

[140] Fateeva, N. S., Vereshchagin, L. F., Kolotygin, V. S., Sov. Phys. Dokl., **8**, 904–906 (1964); Engl. Transl. of Dokl. Akad. Nauk SSSR, **152**, 317–319 (1963).

[141] Fateeva, N. S., Vereshchagin, L. F., JETP Lett., **13**, 110–111 (1971); Engl. Transl. of Zh. Eksp. Teor. Fiz. Pis'ma Red., **13**, 157–159 (1971).

[142] Fateeva, N. S., Vereshchagin, L. F., Sov. Phys. Dokl., **16**, 322–323 (1971); Engl. Transl. of Dokl. Akad. Nauk SSSR, **197**, 1060–1061 (1971).

[143] Fateeva, N. S., Vereshchagin, L. F., JETP Lett., **14**, 153–155 (1971); Engl. Transl. of Zh. Eksp. Teor. Fiz. Pis'ma Red., **14**, 233–235 (1971).

[144] Fertig, W. A., Moodenbaugh, A. R., Maple, M. B., Phys. Lett. A, **38**, 517–518 (1972).

[145] Francois, M., Contre, M., Conf. Int. Met. Beryllium, Commun., **3rd.**, pp. 201–211, 1965.

[146] Franceschi, E., Olcese, G. L., Phys. Rev. Lett., **22**, 1299–1300 (1969).

[147] Franceschi, E., Private Communication.

[148] Freud, P. J., La Mori, P. N., Nat. Bur. Stand. (U.S.) Spec. Publ. 326, pp. 67–75 (1971).

[149] Frolov, A. P., Rodionov, K. P., Vereshchagin, L. F., Phys. Metals Metallogr., **28**, 34–40 (1969); Engl. Transl. of Fiz. Metal. Metalloved., **28**, 993–998 (1969).

[150] Gabrysh, A. F., Eyring, H., Van Hook, A., J. Phys. Chem. Solids, **25**, 129–133 (1964).

[151] Geller, S., Science, **152**, 644–646 (1966).

[152] Geller, S., Science, **161**, 290–291 (1968).

[153] Geller, S., Lind, M. D., Acta Crystallogr. B, **25**, 2166–2167 (1969).

[154] German, V. N., Bakanova, A. A., Tarasova, L. A., Sumulov, Y. N., Sov. Phys. Solid State, **12**, 490–491 (1970); Engl. Transl. of Fiz. Tverd. Tela, **12**, 637–639 (1970).

[155] Getting, I. C., Kennedy, G. C., J. Appl. Phys., **41**, 4552–4562 (1970).

[156] Getting, I. C., Kennedy, G. C., Nat. Bur. Stand. (U.S.) Spec. Publ. 326, pp. 77–80 (1971).

[157] Giardini, A. A., Samara, G. A., J. Phys. Chem. Solids, **26**, 1523–1528 (1965).

[158] Giles, P. M., Longenbach, M. H., Marder, A. R., J. Appl. Phys., **42**, 4290–4295 (1971).

[159] Gonikberg, M. G., Shakhovskoi, G. P., Butuzov, V. P., Engl. Transl. of Zh. Fiz. Khim., **31**, 1839–1842 (1957).

[160] Gonikberg, M. G., Shakhovskoi, G. P., Butuzov, V. P., No. AEC-TR-3222, Nat. Transl. Cent., John Crerar Lib., 35 W. 33rd St., Chicago, Ill. 60616; Engl. Transl. of Zh. Fiz. Khim., **31**, 350–353 (1957).

[161] Grover, R., Kusubov, A. S., Stromberg, H. D., J. Chem. Phys., **47**, 4398–4399 (1967).

[162] Gschneidner, K. A., Elliott, R. O., McDonald, R. R., J. Phys. Chem. Solids, **23**, 555–566 (1962).

[163] Gschneidner, K. A., Elliott, R. O., McDonald, R. R., J. Phys. Chem. Solids, **23**, 1191–1199 (1962).

[164] Gschneidner, K. A., Elliott, R. O., McDonald, R. R., J. Phys. Chem. Solids, **23**, 1201–1208 (1962).

[165] Gust, W. H., Royce, E. B., J. Appl. Phys., **42**, 1897–1905 (1971).

[166] Hall, H. T., J. Phys. Chem., **59**, 1144–1146 (1955).

[167] Hall, H. T., Rev. Sci. Instrum., **31**, 125–131 (1960).

[168] Hall, H. T., Merrill, L., Inorg. Chem., **2**, 618–624 (1963).

[169] Hall, H. T., Barnett, J. D., Merrill, L., Science, **139**, 111–112 (1963).

[170] Hall, H. T., Merrill, L., Barnett, J. D., Science, **146**, 1297–1299 (1964).

[171] Hamann, S. D., Aust. J. Chem., **11**, 391–398 (1958).

[172] Hanneman, R. E., Strong, H. M., General Electric Report 65-RL-4033X, 6 pp., 1965.

[173] Hanneman, R. E., Strong, H. M., J. Appl. Phys., **36**, 523–528 (1965).

[174] Hanneman, R. E., Strong, H. M., J. Appl. Phys., **37**, 612–614 (1966).

[175] Hanneman, R. E., Strong, H. M., Bundy, F. P., Nat. Bur. Stand. (U.S.) Spec. Publ. 326, pp. 53–62 (1971).

[176] Harris, R. E., Vaisnys, R. J., Stromberg, H., Jura, G., in "Progress in Very High Pressure Research," F. P. Bundy, W. R. Hibbard and H. M. Strong, Eds., John Wiley & Sons, N.Y., 1961, pp. 165–172.

[177] Haygarth, J. C., Luedmann, H. D., Getting, I. C., Kennedy, G. C., J. Phys. Chem. Solids, **30**, 1417–1424 (1969).

[178] Herman, R., Swenson, C. A., J. Chem. Phys., **29**, 398–400 (1958).

[179] Hilliard, J. E., Trans. AIME, **227**, 429–438 (1963).

[180] Hoffman, R. E., Hudson, J. B., Kouvel, J. S., Meiklejohn, W. H., Rodbell, D. S., Wilson, R. H., Report 60–GC–120 under Contract AF-33(616)-5951, Project 7021, Task 70645, Wright Air Development Division, USAF, 1960.

[181] Holzapfel, W. B., Severin, D., High Temp. High Pressures, **1**, 713–717 (1969).

[182] Houck, J. C., J. Res. Nat. Bur. Stand. Sect. A, **74**, 51–54 (1970).

[183] Il'ina, M. A., Itskevich, E. S., Sov. Phys. Solid State, **8**, 1873–1876 (1967); Engl. Transl. of Fiz. Tverd. Tela, **8**, 2349–2354 (1966).

[184] Il'ina, M. A., Itskevich, E. S., JETP Lett., **11**, 15–17 (1970); Engl. Transl. of Zh. Eksp. Teor. Fiz. Pis'ma Red., **11**, 26–28 (1970).

[185] Il'ina, M. A., Itskevich, E. S., JETP Lett., **11**, 218–221 (1970); Engl. Transl. of Zh. Eksp. Teor. Fiz. Pis'ma Red., **11**, 328–332 (1970).

[186] Il'ina, M. A., Itskevich, E. S., Sov. Phys. Solid State, **12**, 965–967 (1970); Engl. Transl. of Fiz. Tverd. Tela, **12**, 1240–1243 (1970).

[187] Il'ina, M. A., Itskevich, E. S., JETP Lett., **13**, 15–17 (1971); Engl. Transl. of Zh. Eksp. Teor. Fiz. Pis'ma Red., **13**, 23–26 (1971).

[188] Itskevich, E. S., Sov. Phys. JETP, **15**, 811–817 (1962); Engl. Transl. of Zh. Eksp. Teor. Fiz., **42**, 1173–1182 (1962).

[189] Jacobs, R. B., J. Chem. Phys., **5**, 945–953 (1937).

[190] Jacobs, R. B., Phys. Rev., **54**, 325–331 (1938).

[191] Jamieson, J. C., J. Geol., **65**, 334–343 (1957).

[192] Jamieson, J. C., Lawson, A. W., J. Appl. Phys., **33**, 776–780 (1962).

[193] Jamieson, J. C., Paper presented at the ASME Winter Annual Meeting, New York, 1962.

[194] Jamieson, J. C., Science, **139**, 762–764 (1963).

[195] Jamieson, J. C., Science, **139**, 1291–1292 (1963).

[196] Jamieson, J. C., Science, **140**, 72–73 (1963).

[197] Jamieson, J. C., Science, **145**, 572–574 (1964).

[198] Jamieson, J. C., McWhan, D. B., J. Chem. Phys., **43**, 1149–1152 (1965).

[199] Jamieson, J. C., Private Communication.

[200] Jayaraman, A., Klement, W., Kennedy, G. C., Phys. Rev., **132**, 1620–1624 (1963).

[201] Jayaraman, A., Klement, W., Kennedy, G. C., Phys. Rev., **131**, 644–649 (1963).

[202] Jayaraman, A., Klement, W., Kennedy, G. C., Phys. Rev., **130**, 540–547 (1963).

[203] Jayaraman, A., Klement, W., Kennedy, G. C., Phys. Rev. Lett., **10**, 387–389 (1963).

[204] Jayaraman, A., Klement, W., Newton, R. C., Kennedy, G. C., J. Phys. Chem. Solids, **24**, 7–18 (1963).

[205] Jayaraman, A., Sherwood, R. C., Phys. Rev. A, **134**, 691–692 (1964).

[206] Jayaraman, A., Sherwood, R. C., Phys. Rev. Lett., **12**, 22–23 (1964).

[207] Jayaraman, A., Phys. Rev. A, **135**, 1056–1059 (1964).

[208] Jayaraman, A., Phys. Rev. A, **137**, 179–182 (1965).

[209] Jayaraman, A., Phys. Rev. A, **139**, 690–696 (1965).

[210] Jayaraman, A., Newton, R. C., McDonough, J. M., Phys. Rev., **159**, 527–533 (1967).

[211] Jeffery, R. N., Barnett, J. D., Vanfleet, H. B., Hall, H. T., J. Appl. Phys., **37**, 3172–3180 (1966).

[212] Johnston, J., Adams, L. H., Amer. J. Sci., **31**, 501–517 (1911).

[213] Johnson, P. C., Stein, B. A., Davis, R. S., J. Appl. Phys., **33**, 557–561 (1962).

[214] Kabalkina, S. S., Vereshchagin, L. F., Mylov. V. P., Sov. Phys. Dokl., **8**, 917–918 (1964); Engl. Transl. of Dokl. Akad. Nauk SSSR, **152**, 585–586 (1963).

[215] Kabalkina, S. S., Vereshchagin, L. F., Shulenin, B. M., Sov. Phys. JETP, **18**, 1422–1423 (1964); Engl. Transl. of Zh. Eksp. Teor. Fiz., **45**, 2073–2076 (1963).

[216] Kabalkina, S. S., Kolobyanina, T. N., Vereshchagin, L. F., Sov. Phys. Dokl., **12**, 50–54 (1967); Engl. Transl. of Dokl. Akad. Nauk SSSR, **172**, 313–316 (1967).

[217] Kabalkina, S. S., Kolobyanina, T. N., Vereshchagin, L. F., Sov. Phys. JETP, **31**, 259–263 (1970); Engl. Transl. of Zh. Eksp. Teor. Fiz., **58**, 486–493 (1970).

[218] Kasper, J. S., Richards, S. M., Acta Crystallogr., **17**, 752–755 (1964).

[219] Katz, S., Doran, D. G., Curran, D. R., J. Appl. Phys., **30**, 568–576 (1959).

[220] Kaufman, L., Clougherty, E. V., Weiss, R. J., Tech. Rept. #5, Contract Nonr 2600(00) to Metallurgy Branch, Office of Naval Research, Wash., D.C., 1962.

[221] Kaufman, L., Reported data by H. Enz, in "Solids Under Pressure," W. Paul and D. M. Warschauer, Eds., McGraw-Hill Book Co., New York, 1963, pp. 303 – 356.

[222] Kaufman, L., Clougherty, E. V., Weiss, R. J., Acta Met., **11**, 323–335 (1963).

[223] Kayser, F. X., Phys. Rev. Lett., **25**, 662–664 (1970).

[224] Kayser, F. X., Phys. Status Solidi A, **8**, 233–241 (1971).

[225] Kennedy, G. C., La Mori, P. N., J. Geophys. Res., **67**, 851–856 (1962).

[226] Kennedy, G. C., Jayaraman, A., Newton, R. C., Phys. Rev., **126**, 1363–1366 (1962).

[227] Kennedy, G. C., Newton, R. C., in "Solids Under Pressure," W. Paul and D. M. Warschauer, Eds., McGraw-Hill Book Co., New York, 1963, pp. 163–178.

[228] Kennedy, G. C., Private Communication.

[229] King, E., Harris, I. R., J. Less-Common Metals, **21**, 275–282 (1970).

[230] King, E., Lee, J. A., Harris, I. R., Smith, T. F., Phys. Rev. B., **1**, 1380–1381 (1970).

[231] King, E., Harris, I. R., J. Less-Common Metals, **27**, 51–63 (1972).

[232] Klement, W., Jayaraman, A., Kennedy, G. C., Phys. Rev., **129**, 1971–1975 (1963).

[233] Klement, W., J. Chem. Phys., **38**, 298–299 (1963).

[234] Klement, W., Jayaraman, A., Kennedy, G. C., Phys. Rev., **131**, 632–637 (1963).

[235] Klement, W., Jayaraman, A., Kennedy, G. C., Phys. Rev., **131**, 1–6 (1963).

[236] Klement, W., Cohen, L. H., Kennedy, G. C., J. Phys. Chem. Solids, **27**, 171–177 (1966).

[237] Klement, W., Cohen, L. H., Kennedy, G. C., J. Chem. Phys., **44**, 3697–3701 (1966).

[238] Klimovic, J., Cesk. Cas. Fys., **19**, 60–63 (1969).

[239] Kolobyanina, T. N., Kabalkina, S. S., Vereshchagin, L. F., Fedina, L. V., Sov. Phys. JETP, **28**, 88–90 (1969); Engl. Transl. of Zh. Eksp. Teor. Fiz., **55**, 164–169 (1968).

[240] Kolobyanina, T. N., Kabalkina, S. S., Vereshchagin, L. F., Michkov, A. Ya., Kachan, M. F., Sov. Phys. JETP, **32**, 624–629 (1971); Engl. Transl. of Zh. Eksp. Teor. Fiz., **59**, 1146–1155 (1970).

[241] Kossowsky, R., Trans. Met. Soc. AIME, **236**, 1746–1748 (1966).

[242] Kutsar, A. R., Fiz. Metal. Metalloved., **33**, 1104–1108 (1972); Phys. Abs., **75** (948), 3354 (1972).

[243] Lallemand, M., Brielles, J., Vidal, D., Malbrunot, P., J. Phys. D, **6**, 1052–1057 (1973).

[244] La Mori, P. N., in "High-Pressure Measurement," A. A. Giardini and E. C. Lloyd, Eds., Butterworths, Washington, D.C., 1963, pp. 321–338.

[245] Lawson, A. W., Tang, T. Y., Phys. Rev., **76**, 301–302 (1949).

[246] Lazarus, D., Jeffrey, R. N., Weiss, J. D., Appl. Phys. Lett., **19**, 371–373 (1971).

[247] Lees, J., Williamson, B. H. J., Nature, **208**, 278–279 (1965).

[248] Lees, J., High Temp. High Pressures, **1**, 601–602 (1969).

[249] Leman, G., Report FOA-4-4434-23, Nat. Tech. Information Serv., Springfield, Va. 22151, 48 pp. 1970.

[250] Likhter, A. I., Riabinin, Iu. N., Vereshchagin, L. F., Sov. Phys. JETP, **6**, 469–471 (1958); Engl. Transl. of Zh. Eksp. Teor. Fiz., **33**, 610–613 (1957).

[251] Lind, M. D., Geller, S., J. Chem. Phys., **51**, 348–353 (1969).

[252] Liptai, R. G., Friddle, R. J., J. Less-Common Metals, **10**, 292–294 (1966).

[253] Liu, L., Bassett, W. A., J. Appl. Phys., **44**, 1475–1479 (1973).

[254] Liu, L., Bassett, W. A., Liu, M. S., Science, **180**, 298–299 (1973).

[255] Liu, L., J. Appl. Phys., **44**, 2470–2474 (1973).

[256] Livshitz, L. D., Genshaft, Yu. S., Ruabinin, Yu. D., Phys. Metals Metallogr. (USSR), **9**, 82–88 (1960); Engl. Transl. of Fiz. Metal. Metalloved., **9**, 726–732 (1960).

[257] Livshitz, L. D., Genshaft, Yu. S., Markov, V. K., Sov. Phys. JETP, **16**, 894–898 (1963); Engl. Transl. of Zh. Eksp. Teor. Fiz., **43**, 1262–1267 (1962).

[258] Livshitz, L. D., Genshaft, Yu. S., Sov. Phys. JETP, **21**, 701–703 (1965); Engl. Transl. of Zh. Eksp. Teor. Fiz., **48**, 1050–1053 (1965).

[259] Lloyd, L. T., Liptai, R. G., Friddle, R. J., J. Nucl. Mater., **19**, 173–180 (1966).

[260] Long, L. J., Guarise, G. B., Marani, A., Corsi Semin. Chim., **5**, 97–104 (1967).

[261] Luedemann, H. D., Kennedy, G. C., J. Geophys. Res., **73**, 2795–2805 (1968).

[262] Lynch, R. W., Drickamer, H. G., J. Phys. Chem. Solids, **26**, 63–68 (1965).

[263] Lynch, R. W., Drickamer, H. G., J. Chem. Phys., **45**, 1020–1026 (1966).

[264] Mao, H., Bassett, W. A., Takahashi, T., J. Appl. Phys., **38**, 272–276 (1967).

[265] Mao, H. K., Takahashi, T., Bassett, W. A., Carnegie Inst. Wash. Yearbook, **68**, 251–253 (1969).

[266] Maple, M. B., Wittig, J., Kim, K. S., Phys. Rev. Lett., **23**, 1375–1377 (1969).

[267] Marani, A., Guarise, G. B., Chim. L'Indust., **50**, 663–665 (1968).

[268] Marder, A. R., Science, **142**, 664 (1963).

[269] Martin, J. E., Smith, P. L., Brit. J. Appl. Phys., **16**, 495–500 (1965).

[270] Matthias, B. T., Olsen, J. L., Phys. Lett., **13**, 202–203 (1964).

[271] McCann, D. R., Cartz, L., J. Chem. Phys., **56**, 2552–2554 (1972).

[272] McDaniel, M. L., Babb, S. E., Scott, G. J., J. Chem. Phys., **37**, 822–828 (1962).

[273] McDonald, T. R. R., Barberich, G. S., Gregory, E., in "1964 Symposium on High Pressure Technology," E. C. Lloyd and A. A. Giardini, Eds., ASME, New York, 1964, 12 pp.

[274] McDonald, T. R. R., Barberich, G. S., Gregory, E., ASME Paper 64–WA/PT–4, 12 pp., 1964.

[275] McQueen, R. G., Marsh, S. P., Wackerle, J., Bull. Amer. Phys. Soc., **7**, 447 (1962).

[276] McQueen, R. G., Marsh, S. P., Taylor, J. W., Fritz, J. N., Carter, W. J., in "High-Velocity Impact Phenomena," R. Kinslow, Ed., Academic Press, New York, 1970, pp. 293–417.

[277] McWhan, D. B., Montgomery, P. W., Stromberg, H. D., Jura, G., J. Phys. Chem., **67**, 2308–2311 (1963).

[278] McWhan, D. B., Jayaraman, A., Appl. Phys. Lett., **3**, 129–131 (1963).

[279] McWhan, D. B., Bond, W. L., Rev. Sci. Instrum., **35**, 626–627 (1964).

[280] McWhan, D. B., Stevens, A. L., Phys. Rev. A, **139**, 682–689 (1965).

[281] McWhan, D. B., J. Appl. Phys., **36**, 664–665 (1965).

[282] McWhan, D. B., Souers, P. C., Jura, G., Phys. Rev., **143**, 385–389 (1966).

[283] McWhan, D. B., Rice, T. M., Schmidt, P. H., Phys. Rev., **177**, 1063–1071 (1969).

[284] McWhan, D. B., Stevens, A. L., Solid State Commun., **7**, 301–304 (1969).

[285] McWhan, D. B., Phys. Rev. B, **1**, 2826 (1970).

[286] Merrill, L., "High Pressure Bibliography: 1900–1968," Vol. II, Nat. Tech. Information Serv., Springfield, Va. 22151 (PB-191-175), (1970).

[287] Merrill, L., "Bibliography On High Pressure Research" published bimonthly by the High Pressure Data Center, Brigham Young University, Provo, Utah 84602.

[288] Michels, A., Wassenaar, T., Blaisse, B., Physica, **9**, 574–576 (1942).

[289] Mii, H., Fujishiro, I., Nomura, T., in "Les Proprietes Physiques des Solides Sous Pression," R. Georges and R. Maury, Eds., Centre National de la Recherche Scientifique, Paris, 1970, pp. 441–445.

[290] Mii, H., Fujishiro, I., Senoo, M., Ogawa, K., High Temp. High Pressures, **5**, 155–160 (1973).

[291] Millet, L. E., Unpublished Dissertation, Brigham Young University, Provo, Utah, 92 pp., 1968.

[292] Millet, L. E., Decker, D. L., Phys. Lett. A, **29**, 7–8 (1969).

[293] Minomura, S., Drickamer, H. G., J. Phys. Chem. Solids, **23**, 451–456 (1962).

[294] Mitra, N. R., Decker, D. L., Vanfleet, H. B., Phys. Rev., **161**, 613–617 (1967).

[295] Moodenbaugh, A. R., Wittig, J., J. Low Temp. Phys., **10**, 203–206 (1973).

[296] Moodenbaugh, A. R., Fisk, Z., Phys. Lett. A, **43**, 479–480 (1973).

[296a] Moodenbaugh, A. R., Wu, C. T., Viswanathan, R., Solid State Commun., **13**, 1413–1416 (1973).

[297] Mori, N., Yomo, S., Mitsui, T., Phys. Lett. A., **34**, 190–191 (1971).

[298] Nasledov, D. N., Kozyrev, P. T., Engl. Transl. of Zh. Tekh. Fiz., **24**, 2124–2135 (1954).

[299] Newton, R. C., Jayaraman, A., Kennedy, G. C., J. Geophys. Res., **67**, 2559–2566 (1962).

[300] Nichols, S., J. Phys. D, **4**, 783–786 (1971).

[301] Nichols, S., J. Phys. D, **5**, 799–802 (1972).

[302] Nichols, S., J. Phys. D, **5**, 1898–1901 (1972).

[303] Nikolaev, I. N., Mar'in, V. P., Panyushkin, V. N., Pavlyukov, L. S., Sov. Phys. Solid State, **14**, 2022–2024 (1973); Engl. Transl. of Fiz. Tverd. Tela, **14**, 2337–2339 (1972).

[304] Omel'chenko, A. V., Soshnikov, V. I., Estrin, E. I., Phys. Metals Metallogr., **28**, 80–86 (1969); Engl. Transl. of Fiz. Metal. Metalloved., **28**, 77–83 (1969).

[305] Panova, G. Kh., Sekoyan, S. S., Vereshchagin, L. F., Phys. Metals Metallogr., **11**, 61–65 (1961); Engl. Transl. of Fiz. Metal. Metalloved., **11**, 215–219 (1961).

[306] Patz, K., Z. Anorg. Allgem. Chem., **285**, 29–48 (1956).

[307] Paukov, I. E., Tonkov, E. Yu., Mirinskii, D. S., Dokl. Chem., **164**, 914–915 (1965); Engl. Transl. of Dokl. Akad. Nauk SSSR, **164**, 588–589 (1965).

[308] Paukov, I. E., Tonkov, E. Yu., Mirinskii, D. S., Russ. J. Phys. Chem., **41**, 995–997 (1967); Engl. Transl. of Zh. Fiz. Khim., **41**, 1857–1860 (1967).

[309] Pavlovskii, M. N., Sov. Phys. Solid State, **9**, 2514–2518 (1968); Engl. Transl. of Fiz. Tverd. Tela, **9**, 3192–3197 (1967).

[310] Pearson, W. B., "Handbook of Lattice Spacings and Structures of Metals," Vol. II, Pergamon Press, Oxford, 1967, pp. 79–91.

[311] Perez-Albuerne, E. A., Clendenen, R. L., Lynch, R. W., Drickamer, H. G., Phys. Rev., **142**, 392–399 (1966).

[312] Piermarini, G. J., Weir, C. E., J. Res. Nat. Bur. Stand. Sect. A, **66**, 325–331 (1962).

[313] Piermarini, G. J., Weir, C. E., Science, **144**, 69–71 (1964).

[314] Poniatovskii, E. G., Sov. Phys. Crystallogr., **3**, 512 (1958); Engl. Transl. of Kristallografiya, **3**, 508 (1958).

[315] Ponyatovskii, E. G., Sov. Phys. Dokl., **3**, 498–500 (1958); Engl. Transl. of Dokl. Akad. Nauk SSSR, **120**, 1021 (1958).

[316] Ponyatovskii, E. G., Sov. Phys. Crystallogr., **4**, 237–238 (1960); Engl. Transl. of Kristallografiya, **4**, 257 (1959).

[317] Ponyatovskii, E. G., Sov. Phys. Crystallogr., **5**, 147–149 (1960); Engl. Transl. of Kristallografiya, **5**, 154–156 (1960).

[318] Ponyatovskii, Ye. G., Phys. Metals Metallogr., **11**, 146–147 (1961); Engl. Transl. of Fiz. Metal. Metalloved., **11**, 476–477 (1961).

[319] Ponyatovskii, E. G., Sov. Phys. Crystallogr., **8**, 221–223 (1963); Engl. Transl. of Kristallografiya, **8**, 287–290 (1963).

[320] Pospelov, Yu. A., Sov. Phys. Solid State, **12**, 1695–1696 (1971); Engl. Transl. of Fiz. Tverd. Tela, **12**, 2135–2136 (1970).

[321] Rapoport, E., Kennedy, G. C., J. Phys. Chem. Solids, **27**, 93–98 (1966).

[322] Rieux, M., Jerome, D., Solid State Commun., **9**, 1179–1181 (1971).

[323] Riggleman, B. M., Drickamer, H. G., J. Chem. Phys., **38**, 2721–2724 (1963).

[324] Robinson, L. B., Milstein, F., Jayaraman, A., Phys. Rev. A, **134**, 187–192 (1964).

[325] Roof, R. B., Aust. J. Phys., **25**, 335–336 (1972).

[326] Rose, H., Mugge, D., Nach. Ges. Wiss. Goettingen Math Phys. Kl., **1922**, 110–120 (1922); Chem. Abstr., **17**, 3632 (1923).

[327] Rose, H., Mugge, D., Neues Jahrb. Mineral. Geol. Palaeontol., **48**, 250–256 (1923); Chem. Abstr., **18**, 3575 (1924).

[328] Roux, C., Andreani, M., Rapin, M., in "Les Proprietes Physiques des Solids Sous Pression," R. Georges and R. Maury, Eds., Centre National de la Recherche Scientifique, Paris, 1970, pp. 447–452.

[329] Roux, C., LeRoux, P., Rapin, M., J. Nuclear Mater., **40**, 305–310 (1971).

[330] Roy, N. N., Steward, E. G., Nature, **224**, 905 (1969).

[331] Schaufelberger, Ph., Merx, H., Contre, M., High Temp.—High Pressures, **4**, 111 (1972).

[332] Schirber, J. E., Swenson, C. A., Acta Met., **10**, 511–513 (1962).

[333] Schoessow, G. J., Phys. Rev. Lett., **21**, 738–741 (1968).

[334] Schock, R. N., Johnson, Q., Engl. Transl. of Fiz. Metal. Metalloved., **31**, 1100 (1971).

[335] Sclar, C. B., Carrison, L. C., Gager, W. B., Stewart, O. M., J. Phys. Chem. Solids, **27**, 1339–1343 (1966).

[336] Slykhouse, T. E., Drickamer, H. G., J. Phys. Chem. Solids, **7**, 275 (1958).

[337] Smith, T. F., Gardner, W. E., Phys. Rev., **146**, 291–294 (1966).

[338] Sorgato, I., Guarise, G. B., Marani, A., High Temp. High Pressures, **2**, 105–111 (1970).

[339] Souers, P. C., Jura, G., Science, **140**, 481–483 (1963).

[340] Souers, P. C., Jura, G., Science, **145**, 575–577 (1964).

[341] Stager, R. A., Balchan, A. S., Drickamer, H. G., J. Chem. Phys., **37**, 1154 (1962).

[342] Stager, R. A., Drickamer, H. G., Science, **139**, 1284 (1963).

[343] Stager, R. A., Drickamer, H. G., Phys. Rev., **131**, 2524–2527 (1963).

[344] Stager, R. A., Drickamer, H. G., Phys. Rev., **132**, 124–127 (1963).

[345] Stager, R. A., Drickamer, H. G., Phys. Rev. A, **133**, 830–835 (1964).

[346] Stager, R. A., Drickamer, H. G., Phys. Rev. Lett., **12**, 19–20 (1964).

[347] Stark, W., Jura, G., ASME Publication 64–WA/PT-28, 4 pp., 1964.

[348] Stephens, D. R., J. Phys. Chem. Solids, **24**, 1197–1202 (1963).

[349] Stephens, D. R., J. Phys. Chem. Solids, **25**, 423–429 (1964).

[350] Stephens, D. R., J. Phys. Chem. Solids, **26**, 943–948 (1965).

[351] Stephens, D. R., J. Phys. Chem. Solids, **27**, 1201–1204 (1966).

[352] Stephens, D. R., Stromberg, H. D., Lilley, E. M., J. Phys. Chem. Solids, **29**, 815–821 (1968).

[353] Stephens, D. R., Johnson, Q., J. Less-Common Metals, **17**, 243–246 (1969).

[354] Sterrett, K. F., Klement, W., Kennedy, G. C., J. Geophys. Res. **70**, 1979–1984 (1965).

[355] Stishov, S. M., Tikhomirova, N. A., Sov. Phys. JETP, **21**, 810–811 (1965); Engl. Transl. of Zh. Eksp. Teor. Fiz., **48**, 1215–1216 (1965).

[356] Stishov, S. M., Tikhomirova, N. A., Sov. Phys. JETP, **22**, 429–430 (1966); Engl. Transl. of Zh. Eksp. Teor. Fiz., **49**, 618–620 (1965).

[367] Stishov, S. M., Tikhomirova, N. A., Tonkov, E. Yu., JETP Lett., **4**, 111–113 (1966); Engl. Transl. of Zh. Eksp. Teor. Fiz. Pis'ma Red., **4**, 161–164 (1966).

[358] Stishov, S. M., Makarenko, I. N., Sov. Phys. JETP, **27**, 378–380 (1968); Engl. Transl. of Zh. Eksp. Teor. Fiz., **54**, 708–713 (1968).

[359] Stolin, O., Pokroky Prask. Met. VUPM, **1968** (4), 41–57 (1968).

[360] Stromberg, H. D., Stephens, D. R., J. Phys. Chem. Solids, **25**, 1015–1022 (1964).

[361] Stromberg, H. D., Stephens, D. R., ASME Publication 64–WA/PT-13, 4 pp. (1964).

[362] Stromberg, H. D., Stephens, D. R., Private Communication.

[363] Strong, H. M., Nature, **183**, 1381–1382 (1959).

[364] Strong, H. M., J. Geophys. Res., **64**, 653–659 (1959).

[365] Strong, H. M., Bundy, F. P., Phys. Rev., **115**, 278–284 (1959).

[366] Strong, H. M., in "Progress in Very High Pressure Research," F. P. Bundy, W. R. Hibbard and H. M. Strong, Eds., John Wiley and Sons, New York, 1961, pp. 182–194.

[367] Strong, H. M., Tuft, R. E., Hanneman, R. E., General Electric Report No. 73CRD017, 6 pp. (1973). Also to be published in Metall. Trans.

[368] Suchan, H. L., Wiederhorn, S., Drickamer, H. G., J. Chem. Phys., **31**, 355–357 (1959).
[369] Susse, C., Epain, R., Vodar, B., C. R. Acad. Sci., **258**, 4513–4516 (1964).
[370] Susse, C., Epain, R., C. R. Acad. Sci., **259**, 3756–3759 (1964).
[371] Susse, C., Epain, R., Vodar, B., J. Chim. Phys., **1966**, 1502–1506 (1966).
[372] Susse. C., Epain, R., C. R. Acad. Sci. Ser. C, **263**, 613–615 (1966).
[373] Susse, C., Epain, R., J. Chim. Phys., **1966**, 1580–1581 (1966).
[374] Swenson, C. A., Phys. Rev., **111**, 82–91 (1958).
[375] Takahashi, T., Bassett, W. A., Science, **145**, 483–486 (1964).
[376] Takahashi, T., Bassett, W. A., Mao, H., J. Geophys. Res., **73**, 4717–4725 (1968).
[377] Takahashi, T., Mao, H. K., Bassett, W. A., Science, **165**, 1352–1353 (1969).
[378] Tamayama, M., Andersen, T. N., Eyring, H., Proc. Nat. Acad. Sci., **57**, 554–561 (1967).
[379] Tammann, G., Z. Anorg. Allgem. Chem., **40**, 54–60 (1904).
[380] Tammann, G., "The States of Aggregation," D. Van Nostrand Co., New York, abt. 1925, pp. 177–178; Engl. Transl. of "Aggregatzustande," 2nd ed., Leopold Voss, Leipzig, abt. 1923.
[381] Tikhomirova, N. A., Stishov, S. M., Sov. Phys. JETP, **16**, 1639–1640 (1963); Engl. Transl. of Zh. Eksp. Teor. Fiz., **43**, 2321 (1962).
[382] Tikhomirova, N. A., Tonkov, E. Yu., Stishov, S. M., JETP Lett., **3**, 60–62 (1966); Engl. Transl. of Zh. Eksp. Teor. Fiz. Pis'ma Red., **3**, 96–98 (1966).
[383] Tonkov, E. Yu., Paukov, I. E., Dokl. Chem., **160**, 111–112 (1965); Engl. Transl. of Dokl. Akad. Nauk SSSR, **160**, 619–620 (1965).
[384] Vaidya, S. N., Akella, J., Kennedy, G. C., J. Phys. Chem. Solids, **30**, 1411–1416 (1969).
[385] Vaidya, S. N., Kennedy, G. C., J. Phys. Chem. Solids, **31**, 2329–2345 (1970).
[386] Vaidya, S. N., Kennedy, G. C., J. Phys. Chem. Solids, **33**, 1377–1389 (1972).
[387] Vaughan, R. W., Drickamer, H. G., J. Phys. Chem. Solids, **26**, 1549–1553 (1965).
[388] Venttsel', V. A., Rakhmanina, A. V., Sov. Phys. Solid State, **14**, 2325–2327 (1973); Engl. Transl. of Fiz. Tverd. Tela, **14**, 2693–2696 (1972).
[389] Vereshchagin, L. F., Semerchan, A. A., Popova, S. V., Sov. Phys. Dokl., **6**, 488–489 (1961); Engl. Transl. of Dokl. Akad. Nauk SSSR, **138**, 1059–1061 (1961).
[390] Vereshchagin, L. F., Semerchan, A. A., Kuzin, N. N., Popova, S. V., Sov. Phys. Dokl., **6**, 41–42 (1961); Engl. Transl. of Dokl. Akad. Nauk SSSR, **136**, 320–321 (1961).
[391] Vereshchagin, L. F., Zubova, E. V., Sov. Phys. Solid State, **2**, 2473 (1961); Engl. Transl. of Fiz. Tverd. Tela, **2**, 2776–2777 (1960).
[392] Vereshchagin, L. F., Semerchan, A. A., Popova, S. V., Sov. Phys. Dokl., **6**, 609–610 (1962); Engl. Transl. of Dokl. Akad. Nauk SSSR, **139**, 585–586 (1961).
[393] Vereshchagin, L. F., Semerchan, A. A., Popova, S. V., Kuzin, N. N., Sov. Phys. Dokl., **7**, 692–694 (1963); Engl. Transl. of Dokl. Akad. Nauk SSSR, **145**, 757–760 (1962).
[394] Vereshchagin, L. F., Kabalkina, S. S., Troitskaya, Z. V., Sov. Phys. Dokl., **9**, 894–896 (1965); Engl. Transl. of Dokl. Akad. Nauk SSSR, **158**, 1061–1063 (1964).
[395] Vereshchagin, L. F., Kabalkina, S. S., Sov. Phys. JETP, **20**, 274–277 (1965); Engl. Transl. of Zh. Eksp. Teor. Fiz., **47**, 414–418 (1964).
[396] Vereshchagin, L. F., Zubova, E. V., Burdina, K. P., Sov. Phys. Dokl., **11**, 422 (1966); Engl. Transl. of Dokl. Akad. Nauk SSSR, **168**, 314–315 (1966).
[397] Vereshchagin, L. F., Semerchan, A. A., Kuzin, N. N., Sadlov, Yu. A., Sov. Phys. Dokl., **14**, 557–559 (1969); Engl. Transl. of Dokl. Akad. Nauk SSSR, **186**, 1045–1047 (1969).
[398] Vereshchagin, L. F., Semerchan, A. A., Kuzin, N. N., Sadlov, Yu. A., Sov. Phys. Dokl., **14**, 340–342 (1969); Engl. Transl. of Dokl. Akad. Nauk SSSR, **185**, 785–787 (1969).
[399] Vereshchagin, L. F., Fateeva, N. S., Sov. Phys. JETP, **28**, 597–600 (1969); Engl. Transl. of Zh. Eksp. Teor. Fiz., **55**, 1145–1152 (1968).
[400] Vereshchagin, L. F., Il'ina, M. A., Itskevich, E. S., Instrum. Exp. Tech., **1969**, 237–239 (1969) and Cryogenics, **9**, 477–478 (1969); Engl. Transl. of Prib. Tekh. Eksp., **1969**, 219–221 (1969).
[401] Vereshchagin, L. F., Semerchan, A. A., Kuzin, N. N., Sadlov, Yu. A., Sov. Phys. Dokl., **15**, 292–295 (1970); Engl. Transl. of Dokl. Akad. Nauk SSSR, **191**, 557–560 (1970).
[402] Vezzoli, G. C., Dachille, F., Roy, R., J. Polym. Sci. Part A–1, **7**, 1557–1566 (1969).
[402] Vezzoli, G. C., Dachille, F., Roy, R., Science, **166**, 218–221 (1969).
[404] Vezzoli, G. C., Dachille, F., Roy, R., Inorg. Chem., **8**, 2658–2661 (1969).
[405] Vezzoli, G. C., Dachille, F., Inorg. Chem., **9**, 1973–1975 (1970).
[406] Vezzoli, G. C., Zeto, R. J., Inorg. Chem., **9**, 2478–2484 (1970).
[407] Vezzoli, G. C., Z. Kristallogr., **134**, 305–307 (1971).
[408] Voronov, F. F., Vereshchagin, L. F., Goncharova, V. A., Sov. Phys. Dokl., **135**, 1280–1283 (1960); Engl. Transl. of Dokl. Akad. Nauk SSSR, **135**, 1104–1107 (1960).
[409] Voronov, F. F., Stal'gorova, O. V., Sov. Phys. JETP, **22**, 524–527 (1966); Engl. Transl. of Zh. Eksp. Teor. Fiz., **49**, 755–759 (1965).
[410] Wakabayashi, I., Kobayashi, H., Nagasaki, H., Minomura, S., J. Phys. Soc. Jap., **25**, 227–233 (1968).
[411] Ward, K. B., Deaton, B. C., Phys. Rev., **153**, 947–951 (1967).
[412] Warnes, R. H., J. Appl. Phys., **38**, 4629–4631 (1967).
[413] Weir, C. E., Piermarini, G. J., Block, S., J. Chem. Phys., **54**, 2768–70 (1971).
[414] Wentorf, R. H., Kasper, J. S., Science, **139**, 338–339 (1963).
[415] Wentorf, R. H., Science, **147**, 49–50 (1965).
[416] Wentorf, R. H., Nat. Bur. Stand (U.S.) Spec. Publ. 326, pp. 81–89 (1971).
[417] Whittaker, A. G., Kintner, P., Science, **165**, 589–591 (1969).
[418] Wittig, J., Phys. Rev. Lett., **15**, 159 (1965).
[419] Wittig, J., Matthias, B. T., Science, **160**, 994–995 (1968).
[420] Wittig, J., J. Phys. Chem. Solids, **30**, 1407–1410 (1969).
[421] Wittig, J., Matthias, B. T., Phys. Rev. Lett., **22**, 634–636 (1969).
[422] Wittig, J., Phys. Rev. Lett., **24**, 812–815 (1970).
[423] Wittig, J., J. Chem. Phys., **58**, 2220–2222 (1973).
[424] Wittig, J., Private Communication.
[425] Wyckoff, R. W. G., *"Crystal Structures," 2nd ed., Vol. I, Interscience*, New York, 1965.
[426] Yomo, S., Mori, N., Mitsui, T., J. Phys. Soc. Japan, **32**, 667–676 (1972).
[427] Zarubina, O. A., Sov. Phys. Solid State, **14**, 2497–2499 (1973); Engl. Transl. of Fiz. Tverd. Tela, **14**, 2890–2893 (1972).
[428] Zeitlin, A., Brayman, J., in "High-Pressure Measurement," A. A. Giardini and E. C. Lloyd, Eds., Butterworths, Washington, D.C., 1963, pp. 301–320.
[429] Zil'bershteyn, V. A., Estrin, E. I., Phys. Metals Metallogr., **28**, 189–191 (1969); Engl. Transl. of Fiz. Metal. Metalloved., **28**, 369–370 (1969).
[430] Zhokhovskii, M. K., Engl. Transl. of Izmer. Tekh., **1955**, 3–6 (1955).
[431] Zhokhovskii, M. K., Razuminkhin, V. N., Zolotykh, E. V., Burova, L. L., Meas. Tech. (USSR), **1959**, 865–868 (1959); Engl. Transl. of Izmer. Tekh., **1959**, 26–29 (1959).